PRE-THESIS SUBMISSION COLLOQUIUM SYNOPSIS

Submitted to Mangalore University for the Ph.D. thesis entitled

PROTEOMIC ANALYSIS OF *CAPSICUM FRUTESCENS* L. IN RESPONSE TO PLANT HORMONAL STRESS AND *POLYPHAGOTARSONEMUS LATUS* INFESTATION

In Partial fulfilment of the requirements of the degree of

DOCTOR OF PHILOSOPHY IN BIOTECHNOLOGY

BY

Mr. SACHIN S. PATAVARDHAN

Registration No: MU/EXB/Ph.D/CR-47/Biotech./2019-20/E.13

Research Guide

Dr. Shashi Kiran Nivas

Associate Professor

DEPARTMENT OF POSTGRADUATE STUDIES AND RESEARCH IN BIOTECHNOLOGY

ST. ALOYSIUS COLLEGE (AUTONOMOUS)

MANGALURU 575003.

AFFILIATED TO MANGALORE UNIVERSITY

OCTOBER 2023

TABLE OF CONTENTS

1 CHAPTER 1: INTRODUCTION 1

1.1 CHILLI: 1

1.2 BROAD MITE 1

1.3 PLANT HORMONES 2

1.4 ROLE OF PLANT HORMONES IN PLANT PATHOLOGY 3

2 CHAPTER 2: REVIEW OF LITERATURE 3

2.1 BROAD MITE INFESTATION 3

2.2 MASS SPECTROMETRY-BASED PROTEOMICS OF CAPSICUM: 4

2.3 COMMON WORKFLOW OF BOTTOM-UP PROTEOMICS EXPERIMENTS: 5

2.4 TANDEM MASS TAG (TMT) MULTIPLEXING: 6

2.5 DATA ANALYSIS 7

3 CHAPTER 3: MORPHOLOGICAL, HISTOLOGICAL, AND BIOCHEMICAL STUDIES OF *CAPSICUM FRUTESCENS* SEEDLINGS UPON ABIOTIC STRESS CAUSED BY PLANT HORMONES 7

3.1 INTRODUCTION 7

3.2 MATERIALS AND METHODS 8

3.2.1 Seed sterilization 8

3.2.2 Preparation of Plant materials for biochemical analysis: 8

3.2.3 Malondialdehyde assay (MDA) 9

3.2.4 Photographic documentation: 9

3.2.5 Selection of seedlings for biochemical, histological studies: 9

3.2.6 Analysis of total carbohydrate content (TCC) by Anthrone method: 9

3.2.7 Estimation of Total soluble sugars (TSS) by Anthrone method: 9

3.2.8 Total lipid content (TL) by gravimetry Bligh and Dyer method: 9

3.2.9 Total phenolic content (TPC) by Folin-Ciocalteu method (FC method): 10

3.2.10 Analysis of Antioxidant activity using the DPPH method: 10

3.2.11 Statistics for biochemical analysis: 10

3.2.12 Histology 10

3.3 RESULTS AND DISCUSSION 12

3.3.1 MDA analysis 12

3.3.2 Morphological changes of chilli seedlings upon abiotic stress caused by plant hormones 12

3.3.2.1 Effect on the Anatomy of shoot apical meristem 14

3.3.2.2 Effect on cell proliferation and callus formation: 17

3.3.2.3 Effect on the anatomy of leaf: 18

3.3.2.4 Effect on the anatomy of stem: 21

3.3.2.5 Effect on the anatomy of root: 23

3.3.3 Biochemical investigation of abiotic stress caused by plant hormones 26
3.3.3.1 Soluble reducing sugars 26
3.3.3.2 Total carbohydrate content 27
3.3.3.3 DPPH-free radicle scavenging assay 28
3.3.3.4 Total phenolic content 28
3.3.3.5 Total lipid content 29
3.4 CONCLUSION: 30
4 CHAPTER 4: PROTEOMIC INVESTIGATION OF ABIOTIC STRESS CAUSED BY PLANT HORMONES 30
4.1 INTRODUCTION 30
4.2 MATERIALS AND METHODS 31
4.2.1 Sample collection 31
4.2.2 Protein extraction 31
4.2.3 Trypsin digestion 31
4.2.4 Mass Spectrometry Analysis 31
4.2.5 Data analysis 31
4.2.6 Data availability 31
4.3 RESULTS: 32
4.3.1 Dysregulated proteins: 32
4.3.2 Effect of BAP photosynthetic pathway 33
4.3.3 Effect of IAA on chilli seedlings 36
4.3.4 Effect of ABA on chilli seedlings 38
4.3.5 Effect of GA3 on chilli seedlings 40
4.3.6 Effect of ethylene on chilli seedlings 43
4.3.7 Effect of 2,4D on chilli seedlings 48
4.3.8 Effect of DICAMBA on chilli seedlings 52
4.3.9 Effect of PICLORAM on chilli seedlings 56
4.3.10 Effect of TIBA on chilli seedlings 58
4.4 CONCLUSION: 61
5 CHAPTER 5: MORPHOLOGICAL, HISTOLOGICAL AND BIOCHEMICAL STUDIES OF *CAPSICUM FRUTESCENS* (BIRDS EYE CHILLI) SEEDLINGS UPON BIOTIC STRESS INDUCED BY *POLYPHAGOTARSONEMUS LATUS* (BROAD MITE) 61
5.1 INTRODUCTION 61
5.2 MATERIALS AND METHODS 62
5.2.1 Sample processing for microscopy 62
5.2.2 Pathogenicity test: 62
5.2.3 Molecular identification : DNA Extraction and polymerase chain reaction 62
5.2.4 Effective miticides against broad mite 63

5.2.5 Preparation of Plant materials for biochemical analysis: *63*
5.2.6 Malondialdehyde assay (MDA) *63*
5.2.7 Selection of seedlings for biochemical, histological studies: *63*
5.2.8 Analysis of total carbohydrate content (TCC) by Anthrone method: *63*
5.2.9 Estimation of Total soluble sugars (TSS) by Anthrone method: *64*
5.2.10 Total lipid content (TL) by gravimetry Bligh and Dyer method: *64*
5.2.11 Total phenolic content (TPC) by Folin-Ciocalteu method (FC method): *64*
5.2.12 Analysis of Antioxidant activity using the DPPH method: *64*
5.2.13 Statistics for biochemical analysis: *64*
5.2.14 Histology *64*
5.3 RESULTS AND DISCUSSION 64
5.3.1 Morphological observations of broad mite infection in chilli plants *64*
5.3.2 Light microscopic observations *65*
5.3.3 Scanning electron microscopic observations *65*
5.3.4 Molecular identification *66*
5.3.5 Pathogenicity test *66*
5.3.6 Efficacy of miticides to control broad mite infestation on chilli plant *66*
5.3.7 Variation of the Malondialdehyde content of biotic stress caused by broad mite infestation in chilli plant *67*
5.3.8 Histological observations *68*
5.3.9 Biochemical investigation of biotic stress caused by broad mite infestation in chilli plant *69*
5.3.9.1 Soluble sugar content 69
5.3.9.2 Total carbohydrate content 70
5.3.9.3 DPPH free radicle assay 71
5.3.9.4 Total phenolic content 72
5.3.9.5 Total lipid content 73
5.4 CONCLUSION 73
6 CHAPTER 6: PROTEOMIC INVESTIGATION OF BIOTIC STRESS CAUSED BY BROAD MITE (*POLYPHAGOTARSONEMUS LATUS*) INFESTATION ON CHILLI PLANT 74
6.1 INTRODUCTION 74
6.2 MATERIALS AND METHODS 75
6.2.1 Sample collection *75*
6.2.2 Protein extraction *75*
6.2.3 Trypsin digestion *75*
6.2.4 Mass spectrometry analysis *76*
6.2.5 Data analysis *76*
6.2.6 Data availability *77*
6.3 RESULTS AND DISCUSSION 78

6.3.1 Proteins and peptides identified *78*
6.3.2 Gene Ontology and protein interactions *83*
6.3.3 Proteins associated with the plant-pathogen response *85*
6.3.4 Proteins associated with the MAPK pathway *86*
6.3.5 Proteins associated with plant hormone regulation *87*
6.3.6 Proteins associated with alpha-linolenic acid metabolism and jasmonate synthesis *88*
6.3.7 Proteins associated with the phenylpropanoid pathway: *91*
6.4 CONCLUSIONS 91

7 CHAPTER 7: COMMON PATHWAYS DYSREGULATED UPON ABIOTIC AND BIOTIC STRESS CAUSED BY PLANT HORMONES AND BROAD MITE INFESTATION IN CHILLI PLANT 92

7.1 INTRODUCTION 92
7.2 MATERIALS AND METHODS 92
7.3 RESULTS AND DISCUSSION 93
7.3.1 Role of ubiquitin-mediated proteolysis in biotic and abiotic stress in chilli caused by hormonal stress and broad mite infestation *93*
7.3.2 Role of mitogen-activated protein kinases (MAPKs) in biotic and abiotic stress in chilli caused by hormonal stress and broad mite infestation *96*
7.3.3 Role of Plant hormone signal transduction in biotic and abiotic stress in chilli caused by hormonal stress and broad mite infestation *97*
7.4 CONCLUSIONS: 101

8 REFERENCES 101

9 PUBLICATIONS 122

9.1 PUBLICATIONS IN JOURNALS 122
9.2 SCIENTIFIC PRESENTATIONS IN CONFERENCES: 122

10 ATTACHMENTS 122

10.1 PAPER 1: PLANT-PATHOGEN INTERACTIONS: BROAD MITE (*POLYPHAGOTARSONEMUS LATUS*)-INDUCED PROTEOMIC CHANGES IN CHILLI PEPPER PLANT (*CAPSICUM FRUTESCENS*) 122
10.2 PAPER 2: PROTEOME DATASET OF CHILLI PEPPER PLANT (*CAPSICUM FRUTESCENS*) INFESTED BY BROAD MITE (*POLYPHAGOTARSONEMUS LATUS*) 134

CHAPTER 1

Introduction

1 Introduction

1.1 Chilli:

Chilli cultivation plays a significant role in the Indian economy, contributing to both agricultural output and socio-economic development. India is one of the largest producers, consumers, and exporters of chilli peppers in the world. Various states in India, with regions like Andhra Pradesh, Karnataka, Rajasthan, and Maharashtra are major contributors to the country's chilli production. The favourable climatic conditions, fertile soil, and skilled farming practices have made India an ideal location for chilli cultivation. It not only generates significant employment opportunities, especially in rural areas. Farmers, labourers, and various ancillary industries involved in chilli production, such as packaging, transportation, and processing, benefit from the sector. The income generated through chilli cultivation helps improve the livelihoods of numerous individuals and families, alleviating poverty and contributing to rural development. India's abundant chilli production not only caters to domestic consumption but also allows for substantial exports to international markets. Chilli cultivation also promotes crop diversification and crop rotation practices, enhancing soil fertility and reducing the risk of pests and diseases. This has a positive impact on the sustainability and resilience of agricultural systems, ensuring long-term productivity and food security. The Bird's Eye chilli (*Capsicum frutescens*), also known as Thai chilli, Gandhari menasu, or Jeerige menasu, is a small, fiery pepper widely used in Southeast Asian and African cuisines. These peppers are usually green or red and have a distinctively pungent and spicy flavour that can range from mildly spicy to extremely hot, depending on the variety and how it is used.

1.2 Broad Mite

Broad mite infestation poses a significant threat to Indian agriculture, impacting various crops and causing substantial economic losses. Broad mites (*Polyphagotarsonemus latus*) are small pests that can infect a wide range of plants, including vegetables, fruits, and ornamental crops. They can quickly develop resistance to chemical pesticides. The impact of broad mite infestation on Indian agriculture is a matter of concern and requires attention from farmers, researchers, and policymakers alike. Cash crops such as chilli peppers, tomatoes, cucumbers, and roses are particularly vulnerable, as they play a significant role in India's agricultural economy and the livelihoods of farmers. Controlling broad mite infestations is a complex task that requires an integrated approach, including cultural practices such as regular scouting, and optimizing growing conditions. The use of biological control agents, like predatory mites, can also be effective and environmentally friendly in managing broad mites. Some preventative measures include ensuring the usage of certified disease-free planting materials, maintaining good

sanitation practices, and minimizing stress factors. Monitoring the crop regularly for early infestation detection is also essential for effective control (McMurtry et al., 1984).

The damage caused by broad mites can also render the crop unsuitable for sale, leading to additional expenses for disposal and clean-up (Brust & Gotoh, 2018). Growers may need to invest in control agents, such as pesticides or biological control agents, but their efficacy may be limited due to the mites' ability to develop resistance The use of pesticides can also increase production costs and affect the marketability of the crop if residues exceed legal limits (Kupferschmied et al., 2013). If the infestation is uncontrolled, the mites can spread to other crops and neighbouring farms, causing further losses and increasing the risk of trade restrictions (Peña, 1990). Research is needed to identify resistant crop varieties, study the mite's biology and behaviour, and evaluate alternative control methods. Raising awareness among farmers about identifying, preventing, and managing broad mites is crucial to minimize their impact on Indian agriculture.

1.3 Plant hormones

Plant hormones, also called phytohormones or plant growth regulators, play crucial roles in regulating physiological and developmental processes in plants. They act as signalling molecules, enabling plants to respond to internal and external cues, influencing growth, development, and responses to environmental stimuli, including defence against pathogens. From germination to flowering, fruiting, and senescence, plant hormones govern the balance of growth and differentiation. They are synthesized in specific tissues and transported to target sites, eliciting responses such as cell division, elongation, tissue differentiation, metabolic modulation, and coordination of environmental responses. The major classes of plant hormones include auxins, cytokinins, gibberellins, abscisic acid, ethylene, and brassinosteroids. Auxins regulate cell elongation, differentiation, apical dominance, and tropic responses. Cytokinins promote cell division, and differentiation, delay senescence, and regulate nutrient allocation. Gibberellins participate in stem elongation, seed germination, and flowering. Abscisic acid modulates plant responses to environmental stresses like seed dormancy, stomatal closure, and drought tolerance. Ethylene acts as a ripening hormone in fruits promotes senescence, and influences responses to biotic and abiotic stresses.

Synthetic analogues of plant hormones like 2,4-D (2,4-Dichlorophenoxyacetic acid), DICAMBA (3,6-Dichloro-o-anisic acid), PICLORAM (4-Amino-3,5,6-trichloropyridine-2-carboxylic acid), and TIBA (2,3,5-Triiodobenzoic Acid) disrupt the growth and development of weeds while minimizing effects on desired crops. 2,4-D mimics the natural plant hormone indole-3-acetic acid (IAA) and in higher quantities, primarily affects broadleaf weeds, leading to uncontrolled growth and eventual death. DICAMBA and PICLORAM also mimic auxin activity, selectively targeting broadleaf weeds without harming grasses, these agents are known to be used to manipulate plant tissues in *in vitro* conditions. TIBA acts as a synthetic cytokinin, inhibiting cell division and inducing abnormal growth patterns in weeds. However, the use of plant hormone-based weedicides carries potential risks. Residual effects in soil or water can impact non-target plants, aquatic organisms, and soil microorganisms. The development of herbicide-resistant weeds poses a long-term challenge to the effectiveness of these weed control methods.

Comprehensive scientific investigations such as proteomics are crucial to assess efficacy, environmental impacts, and the sustainable use of plant hormone-based weedicides.

1.4 Role of plant hormones in plant pathology

In vitro culture has enabled the identification of new plant cultivars and helped researchers understand the mechanisms of resistance to plant pathogens (Brettell & Ingram, 1979). One of the major advantages of plant tissue culture is that it allows for the production of genetically identical plants, making it easier to study the interaction between the pathogen and the plant at the molecular level. Tissue culture also provides a sterile environment, which reduces the chance of contamination and allows for precise control of the environmental conditions. Plant physiology and biochemical investigations have been used to shed light on the mechanisms underlying these interactions and to develop strategies for controlling plant diseases (Conrath et al., 2002). Changes in hormone levels and signalling pathways in response to infection and defence mechanisms can be used to study the plant-pathogen interaction. Another strategy is to alter hormone levels in the media or exogenous applications of plant hormones to study the signalling pathways and compare them with pathways involved in host-pathogen interactions, thereby elucidating the relationship between them via data analytical tools (William Allwood et al., 2010). A different approach would involve using genetic engineering to alter the expression of genes involved in hormone biosynthesis or signalling (Mourgues et al., 1998). However, this method of investigating each gene is costly and time-consuming.

CHAPTER 2

Review of Literature

2 Review of Literature

2.1 Broad mite infestation

Polyphagotarsonemus latus (Broad mite) infestation in chilli is the frequently observed mite infestation accounting for the highest loss. broad mite infestation results in downward curved leaves and stunted growth. Mites usually feed on apical meristems and young leaves leading to coppery or dark purple leaves. Fruits are curled and discolouration occurs with greyish dried spots on the fruits. Blooming is aborted if infestation sets in young plants (Fan & Petitt, 1994). Mites feed on the fluids inside plant cells, causing leaves to become discoloured, curled, and

stunted. This feeding damage can lead to a reduction in the overall leaf area and can weaken the plant, making it more susceptible to other stress factors such as drought or disease (Grinberg et al., 2005). Mite infestations can affect the plant's ability to photosynthesize effectively, reducing its growth and overall health (LeFors et al., 2017). In severe cases, mite infestations can cause complete defoliation, leading to serious harm to the plant. It is important to monitor for mite infestations and take action to prevent or control them to maintain the health of the plant and its leaves (Gerson, 1992)

Broad Higher survival rates were observed between 17-30^{0}C when broad mite was infested on *Rhododendron simsii* (Luypaert et al., 2014) Jasmonic Acid and Salicylic Acid Levels play a crucial role in the Defense Response of Azalea (*Rhododendron simsii Hybrid*) against Broad Mites (*Polyphagotarsonemus latus*) (Leus et al., 2022). Upregulation of several enzymes of the phenylpropanoid, carotenoid biosynthetic pathways, jasmonic acid synthesis, and Plant hormone signal transduction pathways dysregulated upon broad mite infestation in birds eye chilli. This study provides the first in-depth proteomic analysis that correlates broad mite infestation in chilli and dysregulation of various pathways that take part in plant defence (Patavardhan et al., 2020). Extracellular and subcellular proteins localized to mitochondria, chloroplast, Golgi complex, nuclear, etc. were altered upon broad mite infestation on *Capsicum frutescens* (Patavardhan et al., 2021).

2.2 Mass spectrometry-based proteomics of capsicum:

In recent years, There are several reports of mass spectrometry based proteomic analysis on chilli plant, such as, To study the effects of *Sclerotium rolfsii* infection on mitochondria and chloroplast (Liao et al., 2022), to study the effects of Xiangcaoliusuobingmi (B1), a candidate plant immune activator drug on capsicum (Shi et al., 2018), to study the role of abscisic acid-responsive 1 (ABR1), which is involved in cell death and defense signalling in capsicum (Choi & Hwang, 2011), Transcriptomic and Proteomic Analysis to study the complex network regulating pollen abortion in GMS (msc-1) capsicum variety (Q. Cheng et al., 2019), to study the chloroplast differentiation in capsicum (Rödiger et al., 2021), to study the effects of Lysine Acetylation and its role in cold resistance (Z. Liu et al., 2021), to study the sterile and fertile lines (Pei et al., 2022), to study the fruit development (Pei et al., 2022), to study the effect of supplementation of silicon to resist the salinity stress (Manivannan et al., 2016) to study the cytoplasmic male sterility (Z. Wu et al., 2013), to study the role of tyrosine nitration while ripening of fruit (Chaki et al., 2015), to study the effects of vanisulphane – a defence inducing molecule on defense mechanism of capsicum against pepper mild mottle virus (Shi et al., 2022) Peroxisomal proteome of ripening fruit (González-Gordo et al., 2022) to identify fruit quantitative trait locus of capsicum (Z. Liu et al., 2022) to study selenium stress (C. Zhang et al., 2019) to study the effect of green peach aphid (*Myzus persicae Sulzer*) (Florencio-Ortiz et al., 2021), phospho proteomic analysis of fruit development (Z. Liu et al., 2020), to study mitochondrial carbonylated proteins (Camejo et al., 2015), to study the chilling injury (Sánchez-Bel et al., 2012), to study the effects of ghost pepper on human renal carcinoma (Perla et al., 2018) Apoplast proteomic analysis to study drought stress-responsive proteins (Jaswanthi et al., 2019) low-temperature plasma ionization mass spectrometry imaging (LTP-MSI) to study the histology of capsicum (Maldonado-Torres et al., 2014).

2.3 Common workflow of bottom-up proteomics experiments:

- **Mass spectrometer-friendly protein extraction**: The combination of chemical and mechanical lysis, along with protease inhibitors, ensures a high yield of intact proteins. This is especially important in plant proteomics, where the goal is often to identify novel proteins or post-translational modifications that could be easily overlooked if degradation occurs. Which requires the elimination of the high concentration of urea, and polymers such as SDS during the extraction protocol. These molecules are difficult to remove during the sample clean-up procedures and contribute to the noise during mass spectrometry analysis (E. I. Chen et al., 2007). The use of protease inhibitors like PMSF and EDTA based buffer is crucial to ensure the integrity of proteins during and after the extraction process.
- **Sample digestion:** Proteolytic digestion is performed using suitable enzymes such as trypsin and chymotrypsin to convert all the proteins into respective peptides, Trypsin cleaves proteins at specific amino acid residues (lysine and arginine), generating peptides that are suitable for mass spectrometry analysis. Factors like pH, temperature, and enzyme-to-substrate ratio must be meticulously controlled to ensure complete digestion, thereby enabling a comprehensive analysis of the plant proteome (Tsiatsiani & Heck, 2015).
- **Reduction by DTT:** Disulfide bonds within and between protein molecules can hinder enzymatic digestion. Dithiothreitol (DTT) is commonly used to reduce these bonds, effectively denaturing the proteins and making them more accessible to trypsin. The process usually takes place at elevated temperatures to facilitate the breaking of disulfide bonds (Lukesh et al., 2012).
- **Alkylation:** Following reduction, alkylation is performed to prevent the reformation of disulfide bonds, usually using agents like iodoacetamide. This ensures that the proteins remain in a denatured state, making them more susceptible to enzymatic digestion (Boja & Fales, 2001).
- **Isobaric labelling:** To increase the efficiency of the analysis, multiple samples can be pooled. So that in a single mass spectrometry run, data from multiple samples can be captured. This greatly reduces the sample analysis time, consumables such as solvents, and column life (Dancy et al., 2015; Gant-Branum et al., 2009).
- **Fractionation:** Basic reverse phase liquid chromatography (bRPLC) is used to separate the pool of peptides into different fractions. This helps to reduce the sample complexity during Nano LC separation followed by mass spectrometry (S. R. Wilson et al., 2015). This step is crucial for enhancing the depth of proteome coverage by separating peptides based on their hydrophobicity
- **Sample clean-up:** Sample clean-up steps are usually performed to remove debris and undigested protein matrix which could be present in the sample during protein extraction (Tubaon et al., 2017). Desalting can be performed using the C-18 packed stage tips or ion exchange resins (Y. Yu et al., 2014).
- **Concatenation:** Concatenation involves the pooling of different peptide fractions after their separation. This strategy aims to simplify the mass spectrometry workflow and increase throughput. By combining less complex fractions, The number of mass spectrometer runs can be reduced without sacrificing the depth of proteome coverage.

- **Nano LC – HRMS**: labelled, Fractionated, and cleaned samples are further separated using the Nano LC column. Later this sample was ionized and the amino acid sequencing was performed using high-resolution mass analyzers such as orbitrap or time of flight technologies (K. A. Jones et al., 2013).
- **Data analysis**: Post mass spectrometry data analysis to identify the peptides, proteins can be identified using software platforms such as proteome discoverer using the Mascot or SEQUEST Algorithms (Russell et al., 2004)
- **Bioinformatics:** After primary data analysis, bioinformatic analysis can be performed such as pathway analysis, gene ontology analysis, enrichment analysis, differential expression profiles, etc. (Colangelo et al., 2015)

2.4 Tandem Mass Tag (TMT) multiplexing:

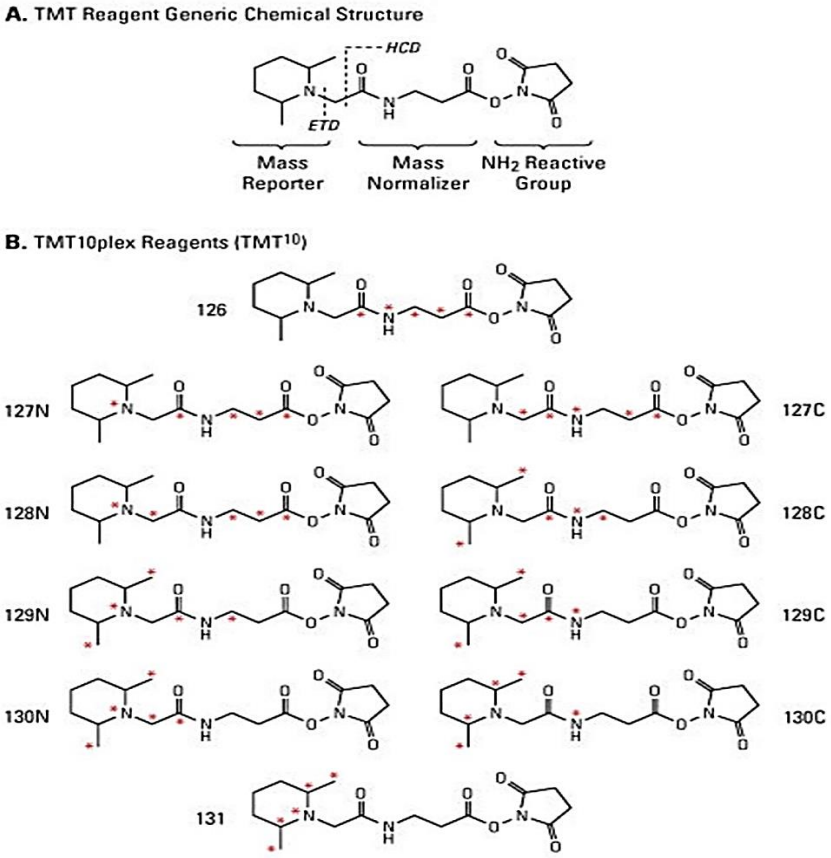

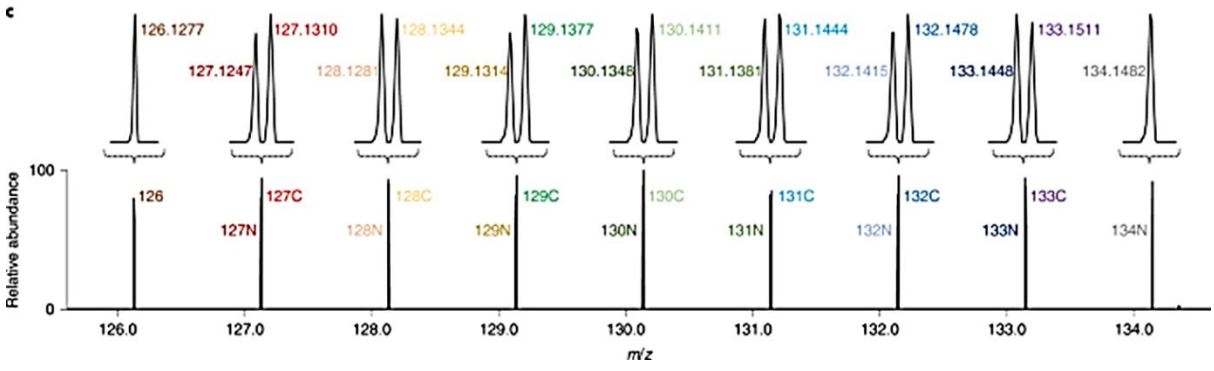

Figure 1: Structure of TMT labels featuring A: MS/MS fragmentation locations induced by Higher-energy Collisional Dissociation (HCD) and Electron Transfer Dissociation (ETD). B: Structures of TMT10plex reagents highlighting positions of heavy isotopes 13C and 15N, denoted by red asterisks. C: Depiction of the MS2 spectrum for the TMT label, showing the relative abundance of the corresponding peptide. Courtesy: (TMT10plexTM Isobaric Label Reagents and Kits, 2018)

2.5 Data analysis

Data analysis involves comparing the experimental peptide sequence with *In Silico* fragmented peptides and identification of the peptides by database search against existing protein databases using Mascot (*Matrix Science - Mascot - Peptide Mass Fingerprint*, 2015), SEQUEST (Eng et al., 1994), X!! tandem (Bjornson et al., 2008) or any other algorithms. If protein databases are not readily available, proteome databases have to be created via 6- a frame translation of existing genome sequences (Blakeley et al., 2012). However instruments, algorithm software, and other parameters can contribute to the false discovery thus it is necessary to set stringent FDR(false discovery rates) (Jeong et al., 2012). Statistical validation of MS/MS database matching can be done using tools such as Peptide Prophet, and MS-GF. Spectral counting or isotope labelling strategy also helps to understand the relative protein abundance across the samples(Milac et al., 2012). Relative protein abundance can be used to compare different molecular dynamics and physiological statuses between the samples. Protein identification and further bioinformatic analysis such as gene ontology, pathway analysis, and network analysis can be done using bioinformatic tools such as DAVID and Bioconductor.

CHAPTER 3

Morphological, Histological, and Biochemical Studies of *Capsicum Frutescens* Seedlings Upon Abiotic Stress Caused by Plant Hormones

3 Morphological, Histological, and Biochemical Studies of *Capsicum Frutescens* Seedlings Upon Abiotic Stress Caused by Plant Hormones

3.1 Introduction

Studying the effects of plant growth regulators in chilli plants through histological, biochemical and proteomic approaches is crucial for understanding how these plants respond

to abiotic stress conditions caused by external applications of compounds, and plant hormones in general. Histological studies can reveal how growth regulators affect cell division, elongation, and differentiation, thereby providing insights into their role in stress adaptation. Monitoring malondialdehyde content can indicate the level of lipid peroxidation and oxidative stress in the plant. This is crucial due to oxidative stress is often a byproduct of abiotic stress conditions. Traditionally considered a byproduct of lipid peroxidation, MDA has been shown to function as a signalling molecule in stress responses. MDA can activate various defence-related genes, modulate the expression of stress-responsive transcription factors, and regulate the synthesis of other signalling molecules. Accumulation of MDA under drought, salinity, biotic and abiotic stress has been well documented (Morales & Munné-Bosch, 2019). Similarly, analyzing reducing free sugars and total carbohydrate content can provide information on how growth regulators affect the plant's energy storage and utilization under stress. Carbohydrates are not just energy reserves but also act as an osmotic agent, helping the plant cells to maintain their structure and function under stress conditions (Sumaryono et al., 2012). DPPH (2,2-diphenyl-1-picrylhydrazyl) free radical scavenging analysis is another important analysis to monitor the antioxidant capacity of the plant, which is vital for combating the reactive oxygen species generated under stress conditions (Iwaniuk & Lozowicka, 2022). Total phenolic content is also a significant parameter, as phenolic compounds have been shown to have various roles including as antioxidants, signalling molecules, and as part of the plant's defence mechanisms (Chowdhary et al., 2021). Total lipids can indicate membrane integrity or damage. The lipid composition of cell membranes can change under stress conditions, affecting their permeability (Y. Wang et al., 2020)

3.2 Materials and Methods

3.2.1 Seed sterilization

Seeds of *Capsicum frutescens* were soaked in distilled water for 24 hours. Treated with fungicide solution for 20 minutes (carbendazim: tricyclazole – 2:1), washed with distilled water 3-4 times, treated with sodium hypochlorite for 10 minutes (NaOCl: H_2O – 1:1), treated with 70% alcohol for 30 seconds. To remove traces of sterilizing agents, washed in autoclaved distilled water 3-4 times and then soaked in potassium nitrate (1% in water) and sodium peroxide (6%) (1:1) solution for 2 hours, proceeded with inoculation. Germinated seedlings (30 days old) were inoculated onto MS medium containing various plant growth regulators at concentrations of 0, 0.5, 1.0, 3.0, and 6.0mg/L. Ethylene was supplied at a volume of 0, 0.5, 1.0, 3.0, 6.0cc (cm^3) with the help of sterile injection via rubber stop cork. Ethylene was supplied to an air-tight conical flask fitted with a rubber stop cork. The plants were grown under controlled environmental conditions, which included a temperature of 27°C, a humidity range of 50-70% and a light-dark cycle of 16:8 hours. The light was provided by cool white fluorescent tubes, emitting approximately 270 μmol photons per square meter per second

3.2.2 Preparation of Plant materials for biochemical analysis:

Plants for biochemical analysis were harvested. seedlings were finely ground into powder using mortar and pestle and liquid nitrogen. The ground powder was stored at -80^0C until further analysis. Subsequent biochemical analysis was carried out using this sample.

3.2.3 Malondialdehyde assay (MDA)

MDA analysis was carried out using Himedia EZAssayTM TBARS Estimation Kit for Lipid Peroxidation, Product Code: CCK023. Procedure was followed as per the manufacturer's instructions.

3.2.4 Photographic documentation:

Photographs were taken using Fujifilm X-T100 24.2 MP Mirrorless Camera attached to XC 15-45 mm Lens, Illumination was achieved by Gossen GKL 315 Fiber Optic Lamp. Microscopic images were obtained using Light microscopy images taken using an Olympus BX41 microscope fitted with a DP73 CCD camera connected to the Olympus CellSens standard software.

3.2.5 Selection of seedlings for biochemical, histological studies:

On the 40^{th} day, after inoculation on MS media supplemented with various growth regulators, at 3mg/L concentration, seedlings were chosen for experiments. This selection was based on, an analysis of MDA content as described in section 3.2.3 and 3.3.1 which aimed to assess the biotic stress levels of the seedlings. To ensure consistency across all experiments, seedlings treated with 3mg/L of plant growth regulators on MS medium were selected. In the case of ethylene, seedlings grown on MS medium and supplemented with 3cc of gaseous ethylene were chosen.

3.2.6 Analysis of total carbohydrate content (TCC) by Anthrone method:

Total carbohydrates were analyzed according to a modified method as described by (Yemm & Willis, 1954). Briefly, 500µL of Anthrone reagent (0.2g of anthrone in 100ml of cold 98% sulphuric acid) was added to 100mg of powdered plant sample in a microcentrifuge tube. The mixture was vortexed using a cyclomixer and heated to 90^0C in a water bath for 15 min. To this mixture, 400µL water was added and vortexed. Centrifuged at 2000 G for 10 minutes to settle the suspended particles. 100µL of supernatant was transferred to a microplate, 100 µL water was added and absorbance was recorded at 630nm using a Microplate reader (Multiskan SkyHigh Microplate Spectrophotometer). A standard curve was obtained using a standard glucose solution (20-100µg/ml). The concentration of total carbohydrates was estimated using $y = 0.0057x - 0.0043$, $R^2 = 0.9969$ equation.

3.2.7 Estimation of Total soluble sugars (TSS) by Anthrone method:

To analyze soluble sugars, 100mg of powdered plant sample was taken in 1000µL of hot 85% ethyl alcohol. This mixture was heated to 50^0C in a water bath for 20 min. Centrifuged at 2000 G for 10 minutes to settle the suspended particles. The supernatant was dried using a freeze-drier. The freeze-dried pellet was analyzed for total carbohydrates as described in the earlier section (Irigoyen et al., 1992; Yemm & Willis, 1954).

3.2.8 Total lipid content (TL) by gravimetry Bligh and Dyer method:

To the 1000mg of powdered plant sample taken in a microcentrifuge tube, 3750 µL of 1:2 Chloroform: methanol was added, and the mixture was vortexed for 1 min. 1250 µL chloroform was added and vortex. To this 1250 µL water was added and vortex. Centrifuged at 80G for 5 min. The lower phase was taken in a pre-weighed fresh microcentrifuge tube. Dried at 50^0C for

1 hour and freeze-dried. Care was taken to prevent water condensation during these processing steps. Dried tubes were weighed and the weight of the extracted lipids was noted (Bligh & Dyer, 1959).

3.2.9 Total phenolic content (TPC) by Folin-Ciocalteu method (FC method):

Total phenolic content was measured with a modified protocol as described by (Ainsworth & Gillespie, 2007). 200µL methanol was added to 100mg of the powdered plant and vortexed for 5 min. and centrifuged at 2000 G for 5 min at 0^0C. The supernatant was collected in a fresh microcentrifuge tube. Similarly, extraction was carried out 3 more times. The pooled supernatant portion was dried over a constant flow of dried nitrogen gas. Care was taken to maintain the sample at cold temperatures and from exposure to the air to reduce the oxidation of phenols. To the vial containing residue, 100 µL methanol was added to re-suspend the residue. 200µL FC reagent was added and vortexed, and 700 µL of 700mM of Na_2CO_3 was added and incubated at 50^0C for 30 min to develop a blue colour. 200 µL of this solution was transferred to the microplate to record the absorbance at 765nm. The amount of phenolic content was calculated using the equation $y = 0.0041x + 0.0116$, $R^2 = 0.9993$. Gallic acid 5-50 µg/mL was used to construct the standard curve.

3.2.10 Analysis of Antioxidant activity using the DPPH method:

The free radicle scavenging capacity of samples was analyzed using the modified DPPH method as described by (Kedare & Singh, 2011; Rajurkar & Hande, 2011). 100µL of 4:1 methanol: water mixture was added 100mg of powdered fresh plant sample, vortexed for 5 min., centrifuged and the supernatant was collected. Similarly, extraction was carried out 4 times. The pooled supernatant was dried using a constant flow of nitrogen. To the residue, 500µL of methanol was added and re-suspended prior to the analysis this solution was transferred to an microplate. 500 µL of DPPH solution (0.1mM solution in methanol) was added to the sample. This mixture was incubated at 30^0C at dark conditions. 200µL of the sample was taken in a microplate and absorbance was recorded at 517nm. Vitamin C was used as a positive control. Percentage Scavenging activity was calculated using the following equation.

$$Percentage\ scavenging\ activity\ = 100 - \left[\frac{(Abs\ control - Abs\ sample\ ) \times 100}{Abs\ control}\right]$$

3.2.11 Statistics for biochemical analysis:

All experiments were carried out in triplicates. The data was presented in the format of mean ± Standard deviation. Minitab ver. 17.0, Jamovi ver. 1.3.23 and Microsoft Excel were used to analyze the data. GraphPad Prism ver. 6 was used for plotting the data. One way Analysis of variance (ANOVA) was conducted, followed by post hoc Tukey's test. The levels of significance were considered at $p<0.05$, $p<0.01$ and $p<0.001$.

3.2.12 Histology

Histological analysis was carried as described by (T.-K. Chen et al., 2016) with slight modifications.

- **Fixation:** Fresh plant samples or tissues were collected and cut into small pieces (about 1 cm× 2cm). Samples were fixed in an FAA fixative. Plant tissue was fixed in FAA fixative overnight at room temperature.
- **Dehydration:** Samples were rinsed in 80% alcohol. Samples were dehydrated using a series of graded alcohols, such as 70%, 95%, and 100% ethanol. Samples were kept in each solution for 60 minutes to equilibrate before being transferred to the next alcohol concentration. Similarly, xylene is infiltrated to replace alcohol. 25%, 50%, 70%, 95%, and 100% xylene were used. Samples were kept in each solution for 60 minutes to equilibrate before being transferred to the next xylene concentration.
- **Wax infiltration and preparation of wax blocks:** Finally, samples were transferred to liquid wax maintained at 58^0C and allowed to equilibrate for 24 hours. The infiltrated tissue is then placed in a mould with molten wax and allowed to cool and solidify. Embedded wax blocks were cut accordingly to affix the blocks on a stage.
- **Sectioning:** The wax block was then sectioned using a microtome (RMT-30 from Radical instruments) to produce thin sections (10 μm). Such that, sections result in a uniform ribbon form. Longitudinal sections were obtained from the apical meristem, while transverse sections were collected from the leaves, stems, and roots. opting for a stem segment situated 1 cm above the root-shoot junction, and selecting a root segment located 1 cm below the junction for the sectioning.
- **Processing of sections:** Sections were collected from the blade using a fine brush and floated and flattened on a water bath maintained at 52^0C, using a hydrophilic slide, sections were collected. Slides were kept in an incubator (58^0C) overnight so that sections could be fixed on the surface of the slide.
- **Dewaxing and rehydration:** The sections were then dewaxed by immersing them in 90% xylene in ethyl alcohol for 5 min. Slides were later transferred to 100% alcohol, and immersed in a series of graded alcohols (100%, 95%, 70%, 50%, and 30%) for 5 min each to allow the tissue to reabsorb water.
- **Staining:** Alcian blue stain was prepared by dissolving 100mg of the Alcian blue powder in 3% acetic acid (pH 2.5) or distilled water. The solution was stirred well until the stain was completely dissolved. The solution was filtered through a filter paper to remove any undissolved particles; the solution was in a dark bottle to protect it from light. The solution can be stored at room temperature for up to 6 months.

  Alcian blue staining: The rehydrated sections were then stained with Alcian blue solution. The sections were stained for 2 minutes, and washed with distilled water twice to remove the traces of unbound stain solution. Safranin staining was also done.
- **Dehydration and clearing:** The sections were then dehydrated and cleared using xylene to prepare them for mounting with a coverslip.
- **Mounting:** Finally, the sections were mounted with a coverslip and a mounting medium, using DPX, and allowed to dry before examination under the microscope.

3.3 Results and Discussion

3.3.1 MDA analysis

The MDA analysis of chilli seedlings was conducted over 80 days using various concentrations of plant growth regulators (BAP, IAA, ABA, GA3, 2,4-D, DICAMBA, TIBA, PICLORAM) ranging from 0 to 6.0 mg/L. The gaseous ethylene was also tested in a range of 0 to 6cc within a sealed 250 ml conical flask at atmospheric pressure. The study revealed varying levels of MDA, indicating different stress statuses. Based on the results, samples were selected at 3 mg/L on the 40^{th} day for the plant growth regulators and 3cc on the 40^{th} day for ethylene.

3.3.2 Morphological changes of chilli seedlings upon abiotic stress caused by plant hormones

Figure *2*A: Control: Chilli seedlings inoculated onto plain MS medium showed normal growth. The control group serves as the baseline for evaluating the effects of different growth regulators.

Figure *2*B: BAP: Growth was stunted due to the inactive apical meristem. Shoots, leaves and roots did not grow. BAP affects root development and apical meristem activity, leading to altered leaf formation as observed in potatoes (Z. Zhang et al., 2005). However BAP along with IAA induced callus chilli (Ashrafuzzaman et al., 2009)

Figure *2*C (a): IAA: The apical meristem was actively producing leaves, as evidenced by a higher number of leaves observed compared to the control. The vitrification of leaves was observed.

Figure *2*C (b): IAA: Rooting was active, as evidenced by the presence of many hairy roots with an actively proliferating rooting system indicated by the observation of multiple branched roots. IAA-induced rooting in chilli at a concentration of 5.71-11.42µM (Orantes-Bonilla & Chen, 2015) which supports the observation.

Figure *2*D: ABA: Internodal elongation was suppressed; leaves turned yellow and curled downward after the 20th day, and root development halted. These observations are consistent with the report that ABA generally inhibits growth and can induce leaf yellowing and senescence (Zhao et al., 2016). There was an increased amount of ABA accumulation in potato plants infected with tomato yellow leaf curl Sardinia virus (TYLCSV), which results in the curling of leaves (Sacco Botto et al., 2023).

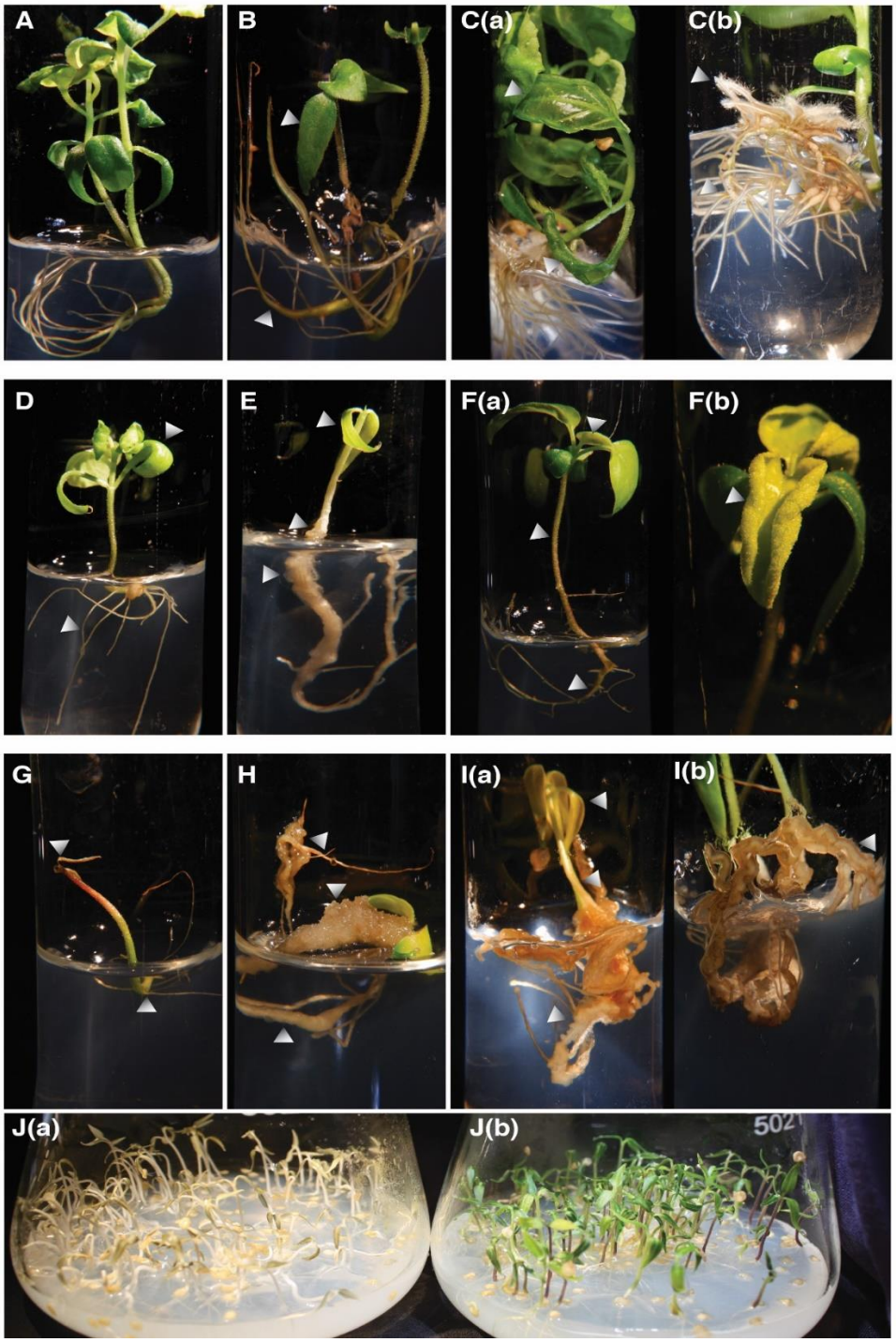

Figure 2: Morphological changes of chilli seedlings on the 40th day upon abiotic stress caused by plant hormones at a concentration of 3mg/L. (A) Control, (B) BAP, (C.a) IAA, (C.b) rooting in IAA, (D) ABA, (E) DICAMBA, (F.a) internodal elongation in GA3, (F.b) curling of leaves in GA3, (G) TIBA, (H) 2,4D (I.a) PICLORAM, (I.b) callus formation in PICLORAM, (J.a) 3 cc of Ethylene (J.b) control for ethylene

Figure *2*E: DICAMBA: Plant parts which are in contact with media, developed callus, apical meristem was not active, roots did not grow, and extensive callusing was observed in roots, leaves turned yellow after 5th day of inoculation. DICAMBA is known to induce callus in wheat (Ren

et al., 2010). Low doses of DICAMBA and 2,4D induced foliar injuries in Cucurbitaceae and Solanaceae families including *Capsicum annuum* (Hynes, 2012).

Figure *2*F(a): GA3: Internodal elongation was observed, but rooting was not active. The elongation aligns with studies that have shown GA3 to promote stem elongation while inhibiting root growth in *Lemna minor* (Inada et al., 2000). However, in adult jalapeño pepper, GA3 treatment increased the yield (Pichardo-González et al., 2018).

Figure *2*F(b): Yellowing and inward curling of leaves were observed, as seen in the *Hibiscus cannabinus* (Muniandi et al., 2018).

Figure *2*G: TIBA: Apical meristem started to die off after day 5; leaves and roots did not grow. These effects are consistent with studies that report TIBA as an inhibitor of apical dominance, leading to malformation of the regenerated shoot tips in certain cultivars (Dreger & Szalata, 2022).

Figure *2*H: 2,4D: No further growth was observed; callusing was seen in roots, stems, and leaves. The callusing and growth inhibition are reported in Chilli (Kim & Lim, 2019) and other plants.

Figure *2*I(a): PICLORAM: Leaves yellowed, and loosely-bound callus was observed. This phenomenon is also observed in onion tissue culture (Phillips & Luteyn, 1983).

Figure *2*I(b): Callusing was observed in roots upon supplementation of PICLORAM as reported in Gerbera (Gantait & Mahanta, 2021).

Figure *2*J (a): Ethylene: Seedlings turned yellow, and no further growth was observed after supplying 5cc of ethylene. Ethylene can act as a stress inducer in plants and can affect the growth of the plants as seen in the Arabidopsis (Vaseva et al., 2018). Unlike other fruits of Solanaceae, like tomato, which ripens post-harvest, chillies usually do not ripe further after harvesting. This is attributed to the fact that ethylene signalling in chilli plants was superseded due to lowering the ethylene-mediated gene expression and subsequent breakdown of the cell wall and carotenoid biosynthesis (Hou et al., 2018; Osorio et al., 2012). However, the study is limited to the ripening of the fruits.

Figure *2*J(b): Control for ethylene experiment showing normal growth of the plants.

Histological observation of abiotic stress caused by the supplementation of plant hormones to the seedlings of *Capsicum frutescens*

3.3.2.1 Effect on the Anatomy of shoot apical meristem

Figure *3*A: Control: Darkfield microscopic picture of the apical meristem of a seedling inoculated on plain MS medium (control). Observations: defined tunica, corpus, axillary bud, new leaf initial, procambium, ground meristem, and ground tissue were observed.

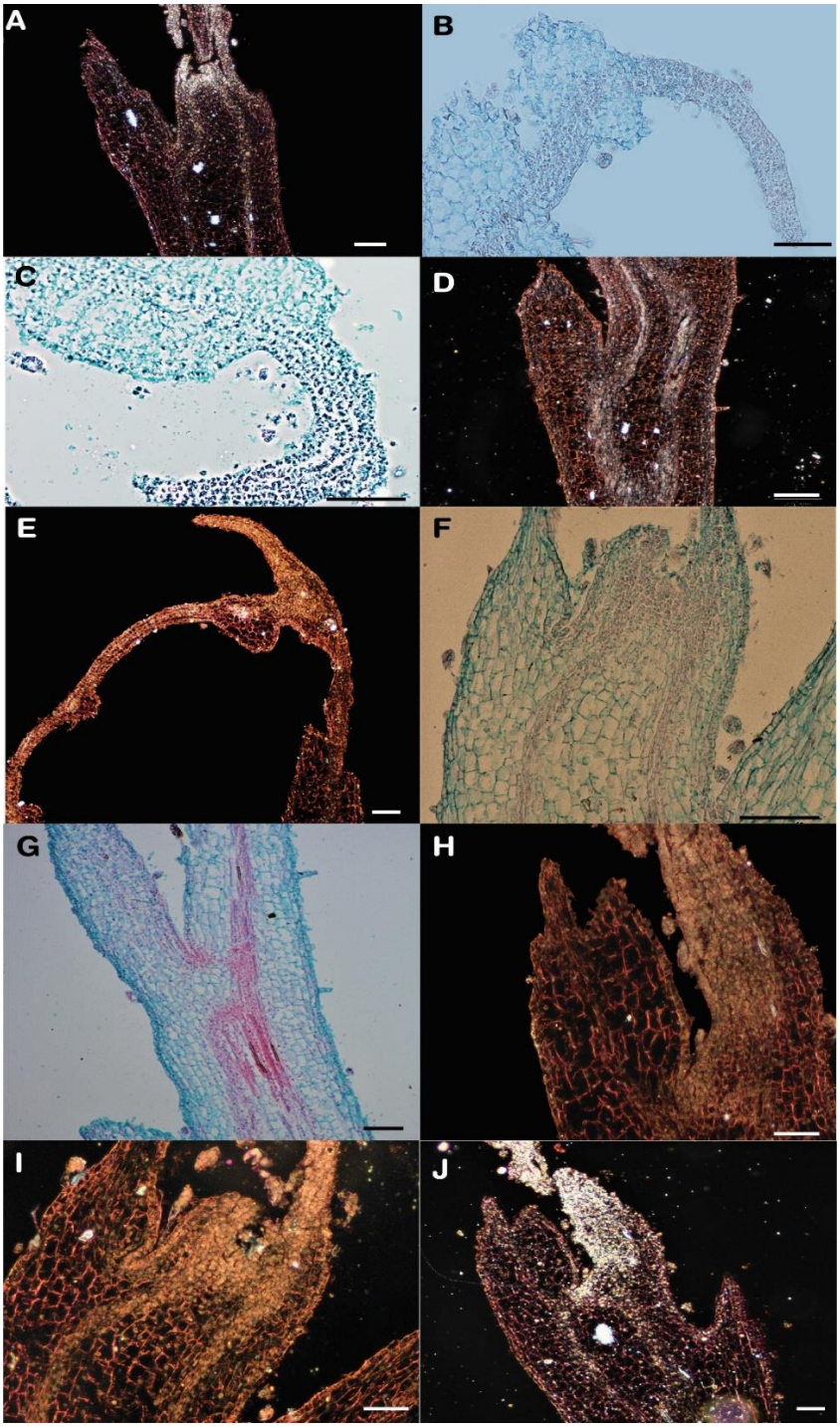

Figure 3: Histological Observations were made on the shoot apical meristem of chilli seedlings cultured in MS medium supplemented with growth regulators. (A) Control, (B) DICAMBA, (c) 2,4D, (D) TIBA, (E) BAP, (F) Ethylene(3 cc), (G) ABA, (H) IAA, (I) GA3, (J) PICLORAM at 3mg/L on the 40th day of application. (Scale: 20µm).

Figure *3*B: DICAMBA: Upon supplementing DICAMBA at a concentration of 3mg/mL, an increase in meristematic activity was observed, characterized by enlarged cells that appeared fragile. This resulted in the formation of callus tissue. The periblem region displayed meristematic characteristics, as indicated by the presence of a prominent nucleus in the cells.

There is no previous documentation on how DICAMBA affects the anatomy of shoot apical meristem.

Figure *3*C: 2,4D: When exposed to a 3mg/mL concentration, the apical meristem exhibited irregular meristematic activity. The typical structures of the Shoot Apical Meristem (SAM) were indistinguishable, this indicates an alteration in cellular differentiation and development. New leaf primordia appeared meristematic, and cells were fragile, leading to the formation of a friable callus. This was particularly evident in plant parts in contact with the agar medium indicating contact stress response. This phenomenon can also indicate the inability of 2,4D to translocate in the plant system. This deferential translocation of 2,4D is also documented in cotton plants (Perez et al., 2022). In general, 2,4D is known to affect the anatomy of SAM, as observed in *Phaseolus vulgaris* (Pereira & Dale, 1982).

Figure *3*D: TIBA: Application of TIBA at a concentration of 3mg/L led to the death of the apical meristem. Consequently, observations were made on samples treated with 0.5mg/L. Compared to the control, these samples exhibited well-defined structures such as tunica, corpus, axillary bud, new leaf initial, procambium, ground meristem, and ground tissue. However, increasing the concentration of the TIBA to 1mg/L resulted in the death of the seedling. This indicates the concentration-dependent toxic effect of TIBA on plant development. At 0.5mg/L, the apical meristem displayed normal anatomical features, suggesting that this concentration is non-lethal. However, a slight increase was found to be fatal to the seedlings. TIBA is known to affect the structure of SAM in tomatoes (Reinhardt et al., 2000).

Figure *3*E: BAP: Though new leaf primordial did not form after the supplementation of BAP, a prominent nucleus in the existing leaf primordial was observed as indicated by the absorption of safranin dye, this can be correlated to observations made in *in vitro* regenerated lily bulblets (Langens-Gerrits et al., 2003). A more defined midrib structure was observed compared to the control. The application of BAP at 3mg/mL appears to stimulate cellular activity in leaf initials. The more defined midrib suggests enhanced vascular development. These observations align with the known roles of cytokinins like BAP in promoting cell differentiation (Z. Chen et al., 2021).

Figure *3*F: Ethylene: Upon exposure to 3cc of ethylene at atmospheric pressure, seedlings exhibited yellowing by the 40^{th} day. Despite this, histological analysis revealed structures comparable to the control, including well-defined tunica, corpus, axillary bud, procambium, ground meristem, and ground tissue; implying that ethylene's impact may be more physiological than structural. The yellowing of seedlings could suggest a stress response, possibly due to ethylene exposure(Iqbal et al., 2017).

Figure *3*G: ABA: Treatment with 3mg/mL ABA led to increased activity in the Plerome region, prominent nucleus was observed indicated by enhanced safranin dye absorption. well-defined structures such as tunica, corpus, axillary bud, new leaf initial, procambium, ground meristem, and ground tissue were observed. This suggests that ABA may play a role in modulating cellular activity in this area. As observed in Arabidopsis, ABA promotes the formation of a band-like

structure near the procambium region, absence of ABA, this band differentiated into vascular elements (Paulraj et al., 2015).

Figure *3*H: IAA: Dark field microscopy revealed that leaf initials treated with 3mg/mL IAA exhibited elevated meristematic activity in the periblem when compared to the control. Auxins like IAA are known to promote cell elongation and division (Reinhardt et al., 2000).

Figure *3*I: GA3: Dark field microscopy showed that 3mg/mL GA3 treatment led to increased meristematic activity in leaf initials, especially in the periblem. Cells in the ground tissue appeared slightly enlarged compared to the control. Gibberellins like GA3 are known to affect the expression of genes related to cell cycle regulation and cell wall elongation (R. L. Jones & Kaufman, 1983).

Figure *3*J: Dark field microscopy of the apical meristem treated with 3mg/mL PICLORAM showed well-defined tunica, corpus, procambium, ground meristem, and ground tissue. However, axillary buds were absent. The meristematic activity was elevated compared to the control, and no friable tissues or callusing were observed in the apical meristem. Contrary to this observation, PICLORAM is known to induce cell proliferation in axillary buds as observed in white yam (Manoharan et al., 2016). The increased meristematic activity could be attributed to this.

3.3.2.2 Effect on cell proliferation and callus formation:

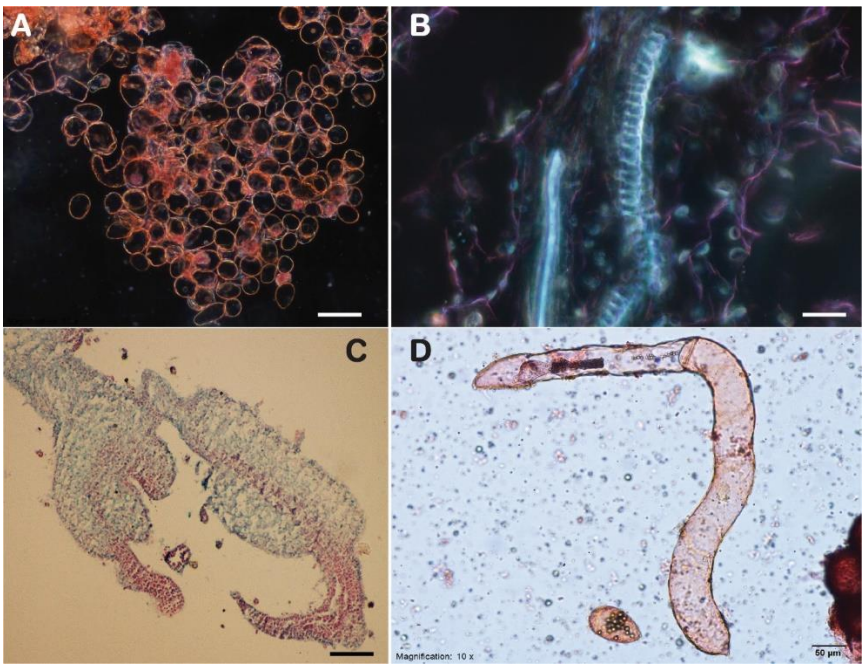

Figure 4: Effects of plant growth regulators on chilli seedlings - Histology of friable tissues and callus, (A and C) 2,4D, (B) DICAMBA, (D) PICLORAM. (Scale: 50µm).

Figure *4*A and C: 2,4D: Dark field microscopy revealed two distinct types of callus tissue in seedlings treated with 3mg/mL of 2,4D. In the callus obtained from roots, the tissue was friable and cells were not adherent to the base. In contrast, the callus from the leaf and apical meristem callus were compact, and xylogenesis was observed. This is due to the type of callus formation

in chilli upon exposure to 2,4D depends upon the co-presence of the other plant growth regulators (Yunita et al., 2021).

Figure *4*B: Dark field microscopy of seedling callus tissue grown on MS media with 3mg/mL DICAMBA showed compact tissue, and xylogenesis was evident. This suggests that DICAMBA may promote organized cell structure and differentiation in seedling callus (Akoyi et al., 2013; Hanus-Fajerska, 2006).

Figure *4*D: Callus from root tissue from seedlings grown on MS media with 3mg/mL PICLORAM revealed friable tissue with elongated, actively dividing cells. Xylogenesis was not observed. PICLORAM is known to alter the morphology of callus in *Sophora flavescens* (Park et al., 2020) and to induce callus and aid in plant regeneration in Gerbera (Gantait & Mahanta, 2021).

3.3.2.3 Effect on the anatomy of leaf:

Figure *5*A: Control: Microscopic examination of chilli seedling leaves grown on MS media without any growth regulators revealed well-defined vascular bundles, epidermis, bundle sheath, xylem tissue, mesophyll, palisade parenchyma, and spongy parenchyma; Indicative of normal growth.

Figure *5*B: Ethylene: leaves of chilli seedlings exposed to 3 cc of gaseous ethylene at atmospheric pressure revealed significant changes. The leaves turned yellowish-brown, and the texture became soft. The mesophyll was collapsed, and the distinction between palisade and spongy parenchyma was unclear. The yellowish-brown colouration and soft texture suggest ethylene-induced senescence or stress response. The collapsed mesophyll and indistinct parenchyma layers indicate altered cellular structure, possibly due to ethylene exposure and cell senescence (Jing et al., 2005). Ethylene is known to modulate gene expression related to senescence and stress responses. The observed changes could be due to the upregulation of genes promoting cell death (Trobacher, 2009) and the downregulation of genes involved in maintaining cell structure and function. Ethylene exposure to peaches resulted in softening of the tissues, indicative of upregulation of xylosidase and galactosidase (Zhu et al., 2019).

Figure *5*C: BAP: Chilli seedlings grown on MS medium with 3mg/mL BAP showed significant anatomical changes in the leaf. A thickened wax layer on the epidermis, compactly packed spongy parenchyma, and shrunken, small vascular bundles were observed. The thickened wax layer and compact spongy parenchyma suggest that BAP may influence leaf cuticle formation (Jenks et al., 2002) and cellular packing (Skalák et al., 2019) as observed in Arabidopsis. The shrunken vascular bundles could indicate reduced vascular development, possibly affecting nutrient and water transport within the leaf.

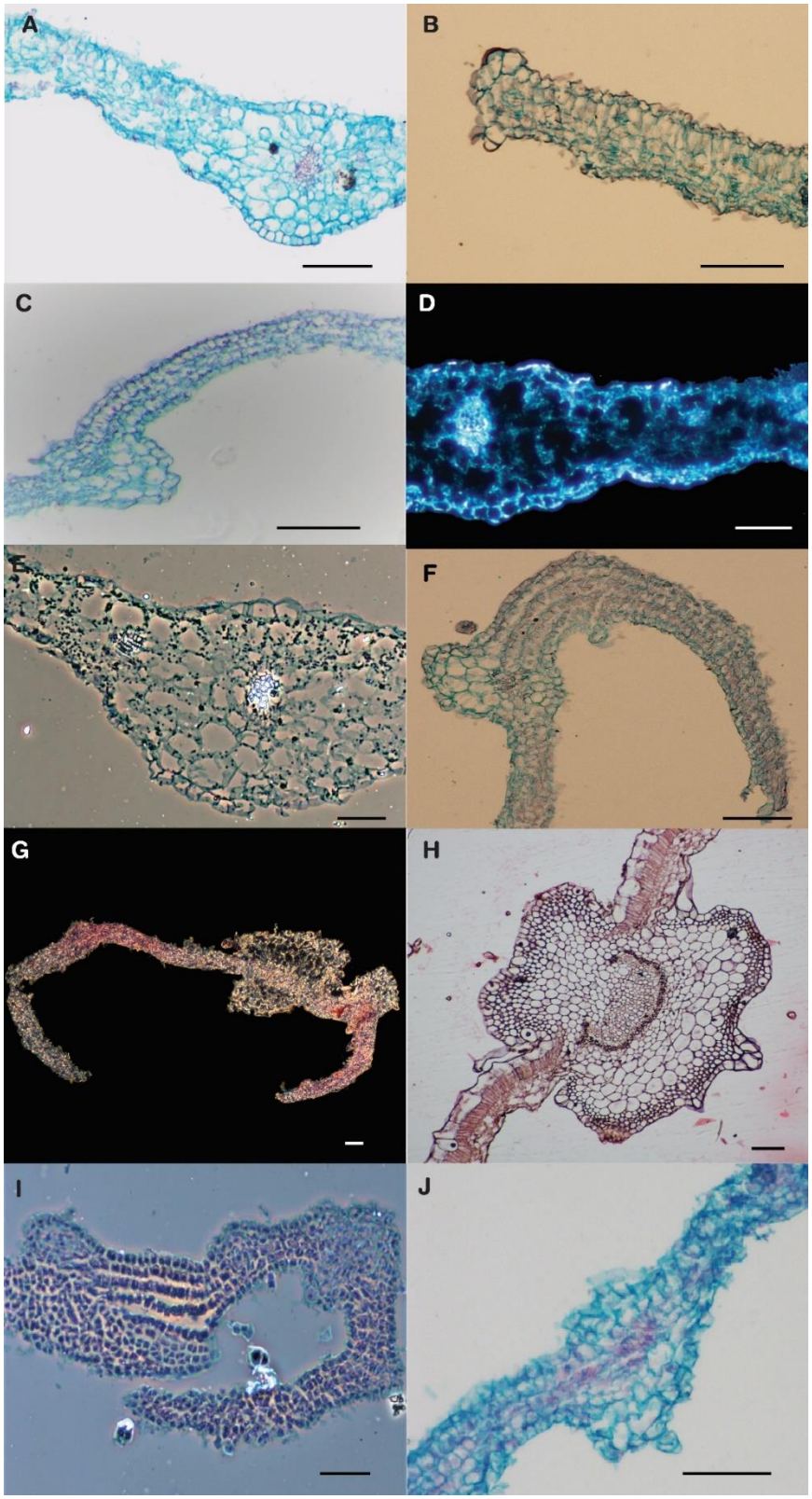

Figure 5: Effects of plant growth regulators on the anatomy of chilli leaf (A) Control, (B) Ethylene (3cc), (C) BAP, (D) TIBA, (E) GA3, (F) ABA, (G) 2,4D, (H) IAA, (I) PICLORAM, (J) DICAMBA. (Scale: 20µm).

Figure 5D: TIBA: Dark field microscopy of chilli seedling growth on MS media supplemented with 3mg/mL TIBA revealed changes in the leaf, indicating indistinct epidermis, clearly visible vascular bundles with thickened bundle sheaths, and enlarged, actively dividing parenchymatous cells in the mesophyll. Due to the friable nature of the cells, microtomy images were unclear. The enlarged, actively dividing mesophyll cells indicate increased cellular activity, possibly affecting leaf structure and function. TIBA, an auxin transport inhibitor (Karabaghli-Degron et al., 1998), could affect gene expression related to cell division, differentiation, and vascular development (Ghorashy et al., 1969).

Figure 5E: ABA: Microscopic image of a leaf of chilli seedling inoculated on MS media supplemented with ABA at 3mg/mL concentration indicates indifferentiable spongy and palisade parenchyma, with a shrunken vascular bundle. This suggests altered cellular differentiation in the mesophyll as ABA is known to be synthesized in mesophyll cells and affects transpiration and stomatal activity (McAdam & Brodribb, 2018). The shrunken vascular bundles could indicate reduced vascular development, potentially affecting nutrient and water transport within the leaf.

Figure 5F: GA3: Darkfield Microscopic image of a leaf of a seedling grown on MS media supplemented with 3mg/mL GA3 revealed distinct vascular bundles with only xylem tissue visible, suggesting altered vascular development (Gray, 1957). The distinction between palisade and spongy parenchyma was unclear, and parenchymatous tissues were tightly compacted compared to the control suggesting changes in cellular organization in the leaf (Binenbaum et al., 2018). Both the upper and lower epidermis were visible, curling of the leaf indicates the influence of GA3 on leaf shape as observed in *Hibiscus cannabinus* (Muniandi et al., 2018).

Figure 5G: 2,4D: Chilli seedlings treated with 3mg/mL 2,4D showed changes in foliar anatomical features with unclear epidermis and mesophyll tissues. Cells were small, and meristematic activity was observed at the vascular bundle, which was either shrunken or not visible. Random meristematic activity in the mesophyll led to callus formation. This is the indicative feature of the effects of 2,4D on cellular differentiation as observed in *Aspilia africana* (Okello et al., 2021).

Figure 5H: IAA: IAA supplementation to the MS media changed anatomical features compared to the control, it revealed clear, large vascular bundles with distinct xylem and phloem tissues. The upper epidermis consisted of large cells covered by a wax layer. The mesophyll featured tightly packed palisade parenchyma and loosely arranged spongy parenchyma. The leaves were larger. This is an indicative feature of enhanced vascular and epidermal development. Auxins such as IAA are known to participate in the optimization of the photosynthetic efficiency of the leaf by changing the cellular arrangement (Esteban et al., 2016).

Figure 5I: PICLORAM: PICLORAM showed highly meristematic spongy and palisade parenchyma, leading to callus formation suggestive feature of undifferentiated growth as observed in Gerbera (Gantait & Mahanta, 2021). The vascular bundle was indistinct, and leaf parts in contact with the media also gave rise to callus. The prominence of the nucleus was indicated by the absorption of safranin dye.

Figure 5J: DICAMBA: 3mg/L DICAMBA in MS medium affected the leaf anatomy of the chilli seedlings, which revealed indistinguishable spongy and palisade parenchyma. DICAMBA, a synthetic auxin is known to induce irregular meristematic activity, e.g. wheat (Ren et al., 2010). Parenchymatous cells exhibited thick cell walls, as indicated by the absorption of alcian blue dye. The vascular bundle was indistinct. DICAMBA is also known to disrupt membrane permeability and oxygen uptake in *Cyprus rotundus* (Magalhaes & Ashton, 1969).

3.3.2.4 Effect on the anatomy of stem:

Figure *6*A: Control: epidermis, hypodermis, xylem, and pith are observed indicating normal development.

Figure *6*B: 2,4D: Seedling grown on MS media supplemented with 3mg/mL 2,4D showed abnormal stem structure with meristematic cells with prominent nuclei. The absence of typical stem structures like epidermis, xylem, and pith suggests that 2,4D disrupts normal stem development. The presence of meristematic, dividing cells indicates that 2,4D induces undifferentiated growth as observed in *Cassia tora* (Kamble, 2013).

Figure *6*C: Seedlings grown on MS media supplemented with 3mg/mL IAA revealed a more prominent epidermis compared to the control. Increased xylogenesis was observed, and the cells in the pith region were smaller than those in the control. In flax plants, IAA increased cortex, xylem and phloem fibers indicating increased xylogenesis (El-Shourbagy et al., 1995).

Figure *6*D: DICAMBA: 3mg/mL DICAMBA showed abnormal anatomical features in the stem, Epidermis was not intact. Endodermis exhibited meristematic activity indicating DICAMBA may induce undifferentiated growth in this tissue. Limited publications report the effects of DICAMBA on plant stems.

Figure *6*E: TIBA: 3mg/mL TIBA significantly affected the anatomy of the stem. Enlarged epidermal and hypodermal cells were observed compared to the control. The xylem in the vascular bundle was prominent, and irregular meristematic activity was observed, which did not lead to callus formation. However, on supplementation of TIBA, cambial cells preferentially became xylem parenchyma, which supports this finding, indicating preferential maturation of xylem tissues.

Figure *6*F: Supplementation of PICLORAM showed unclear epidermis and irregular meristematic activity. This could indicate that PICLORAM affects cellular differentiation and induction of undifferentiated growth. In *Phaseolus vulgaris* supplementation of PICLORAM affected the structure of the stem, and stems became swollen and bent (Fisher et al., 1968).

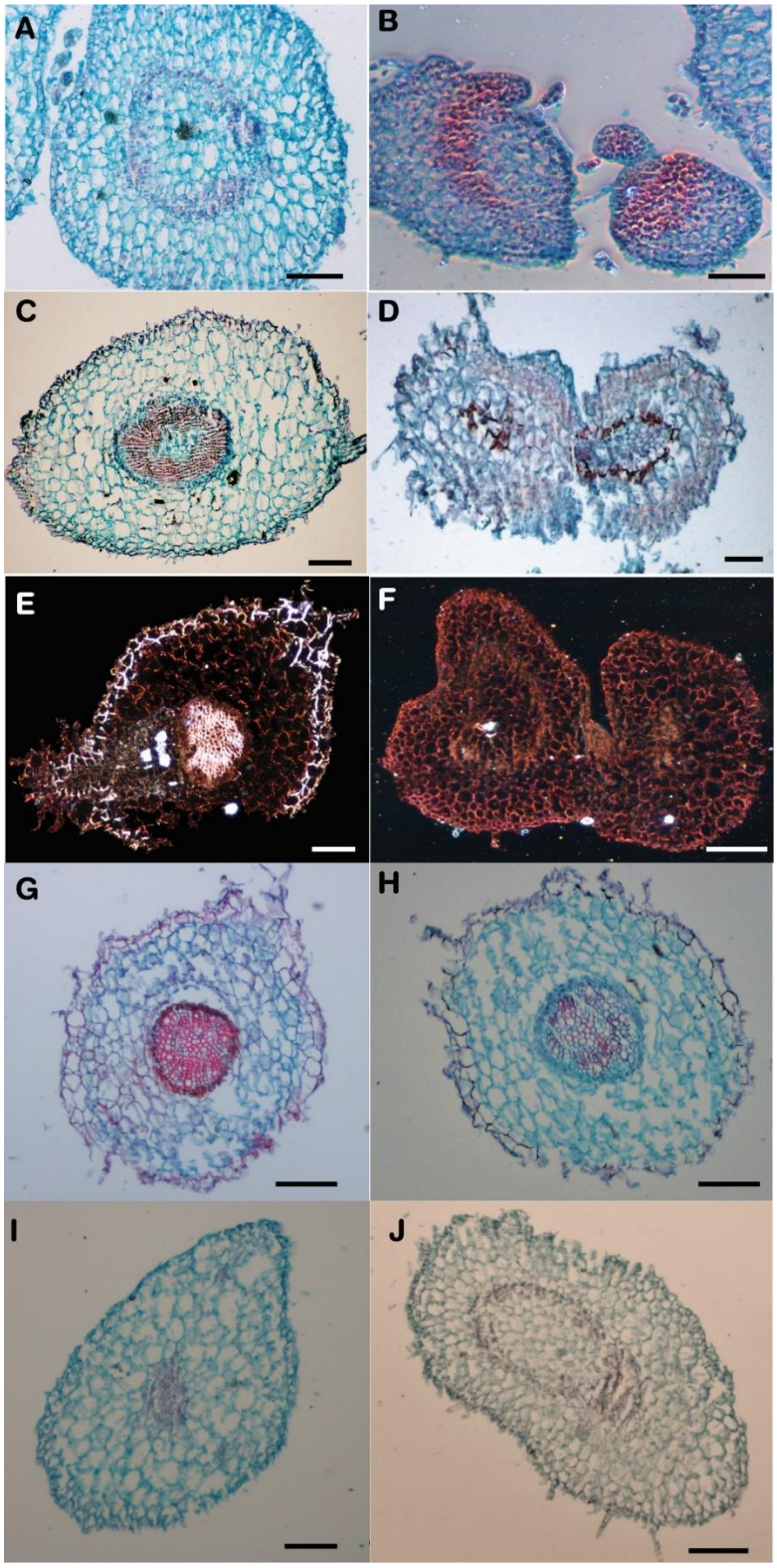

Figure 6: Effects of plant growth regulators on the anatomy of seedlings of chilli stem. (Scale: 20µm). (A) Control, (B) 2,4D, (C) IAA, (D) DICAMBA, (E) TIBA, (F) PICLORAM, (G) ABA, (H) Ethylene (3 cc), (I) GA3, (J) BAP.

Figure *6*G: ABA: 3mg/L ABA supplementation to the MS medium and anatomical features of the stem. A layer of cuticular deposition outside the epidermis was observed. Parenchymatous

hypodermal cells were slightly enlarged compared to the control. The endodermis was visible, and the xylem in the vascular bundle was prominent, as indicated by strong safranin dye absorption. The pith was absent. Popularly known as stress hormones, ABA is known to induce anatomical changes in xylem tissue. As xylem tissue actively participates and controls the translocation of ABA (Hartung et al., 2002).

Figure *6*H: Ethylene: Supplementation of 3cc of gaseous ethylene at atmospheric pressure changed the texture and anatomy of the stem. A cuticular layer outside the epidermis was observed. Parenchymatous hypodermal cells were slightly enlarged compared to the control. The endodermis was prominently visible, and the xylem in the vascular bundle was notably prominent, as indicated by strong safranin dye absorption. The pith was absent. The diameter of the stem was reduced. Ethylene is known to stimulate cell division in the cambial meristem and soften the cell walls (Love et al., 2009; Trobacher, 2009). Degradation of the cell wall or increased permeability exerts pressure on the cuticle (Lara et al., 2019).

Figure *6*I: GA3: In GA3 seedlings, stems with normal epidermis and parenchymatous hypodermis with enlarged cells were observed compared to the control. The diameter of the stem was reduced. Both the endodermis and vascular bundles appeared shrunken, and the xylem and phloem tissues were not visible. The pith was absent. This could indicate inhibited vascular growth. Smaller stem diameter and elongated stems were observed in *Xanthium strumarium* upon supplementation of GA3.

Figure *6*J: BAP: 3mg/L BAP supplementation to the MS medium altered the anatomy of the stem of the chilli seedlings. The epidermis was observed with epidermal hairs. The cells of the parenchymatous hypodermis were slightly smaller than those in the control. The endodermis was visible and absorbed safranin dye, while xylem tissues in the vascular bundles were observed along with a prominent parenchymatous pith. Cytokinins in general are known to control xylem differentiation (Alabdallah et al., 2017).

3.3.2.5 Effect on the anatomy of root:

Figure *7*A: Control: Root anatomy of chilli seedlings inoculated onto MS media had a defined anatomical structure. The observed layers include the epiblema, cortex, endodermis, xylem, and conjunctive tissues. Each layer exhibits distinct characteristics, indicative of a healthy growth pattern.

Figure *7*B: IAA: Microscopic examination of the seedling stem, inoculated on MS media with a 3mg/mL IAA concentration, indicates anatomical changes compared to the control. A thin sheath envelops the epiblema, and the cortex cells are enlarged with thicker walls. Secretory and starch storage cells are present in the cortex. The endodermis and pericycle show a sheath-like structure, lacking clear cellular demarcation. The vascular bundle is dominated by xylem tissue, and the pith region is notably replaced by xylem, indicating enhanced xylogenesis, as documented in carrots when indole butyric acid was supplemented exogenously cambial division gave rise to xylogenesis (Khadr et al., 2020). Since multiple lateral roots originate from the pericycle, the cells are active and, could be the reason for the thickening of the layer.

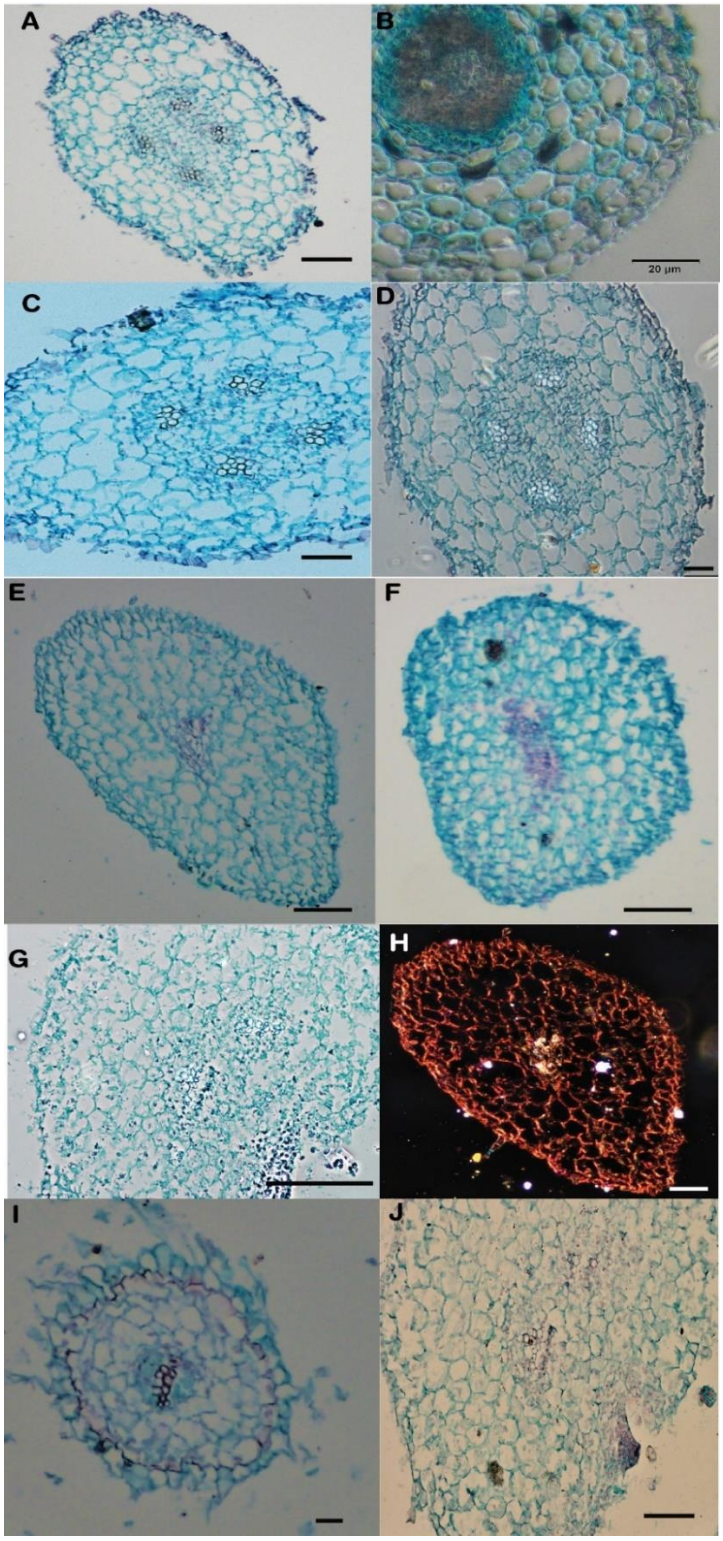

Figure 7: Effects of plant growth regulators on the anatomy of seedlings of chilli root. (Scale: 20µm). (A) Control, (B) IAA, (C) BAP, (D) ABA, (E) Ethylene, (F) GA3, (G) DICAMBA, (H) TIBA, (I) PICLORAM, (J) 2,4D.

Figure *7*C: BAP: exogenous application of BAP in MS medium at 3mg/L, root anatomical variations were noted. The epiblema displayed weakened cell walls, while the endodermis exhibited slightly enlarged cells. Both xylem and pith tissues were present with no remarkable changes. BAP or cytokinins in general known to inhibit the growth of the roots (De Vries & Dubois, 1988).

Figure *7*D: ABA: Application of ABA at 3mg/L in MS medium revealed specific anatomical changes in roots. The epiblema was present, and the cortex displayed enlarged cells. The endodermis exhibited cells with thickened walls, while the organization of the xylem tissue was unclear. The pith region was predominantly parenchymatous. ABA is known to regulate the thickness of the cell wall in Arabidopsis (C. Liu et al., 2021) and to alter the cell wall to influence the phosphorus deficiency in rice (Fang Zhu et al., 2018).

Figure *7*E: Ethylene: Microscopic Exogenous gaseous ethylene application changed anatomical features in the roots. The epiblema was observed, Cortex cells were similar to the control. The endodermis was notably absent, and the vascular tissues appeared shrunken. Xylem tissues were visible, but conjunctive tissue was not observed. Ethylene is reported to inhibit root formation and increase the diameter (Pierik et al., 1999), the reason for the shrinkage of the vascular bundle is unknown.

Figure *7*F: GA3: Supplementation of gibberellic acid thickened epiblema. The cell walls of the cortex cells were also thickened, as evidenced by the absorption of alcian blue dye. Gibberellic acid enhanced the production of secondary metabolites in the airy roots of *Echinacea purpurea* (Abbasi et al., 2012) and *Artemisia annua* (Smith et al., 1997). Gibberelic acid also plays a pivotal role in microtubule orientation thereby influencing the cell growth polarity in maize (Baluška et al., 1993).

Figure *7*G: DICAMBA: Supplementation of DICAMBA resulted in friable callus formation. Similar observations were made in *Oryza sativa* (Zimny & Lörz, 1986). The parenchymatous cells were enlarged and featured prominent nuclei, as evidenced by the absorption of safranin dye.

Figure *7*H: TIBA: Observable epiblema and slightly enlarged cortex cells were observed when supplemented with TIBA at 3mg/L to the MS medium. The vascular tissues appeared shrunken, and conjunctive tissues were absent. Xylem tissues were visible. Application of TIBA decreased root length and lateral root development in rice seedlings (Malheiros et al., 2019).

Figure *7*I: PICLORAM: Supplementation of PICLORAM resulted in irregular meristematic activity in the cortex region of the roots. This led to the formation of a friable callus, consisting of fragile cells, which disintegrated while performing sectioning. Both the epiblema and cortex cells were disintegrated. The vascular region was intact and there was no irregular meristematic activity. Pacific effects of PICLORAM on roots remain unknown. PICLORAM is known to be readily absorbed in the roots of Oats and Soybeans (Isensee et al., 1971).

Figure 7J: 2,4D: friable callus was formed upon the application of 2,4D in MS media. There were no distinguishable regions in the anatomy of the roots. Cells were meristematic. 2,4D induced callus in the roots of the rice (Na Ayudhaya et al., 2022).

3.3.3 Biochemical investigation of abiotic stress caused by plant hormones

3.3.3.1 Soluble reducing sugars

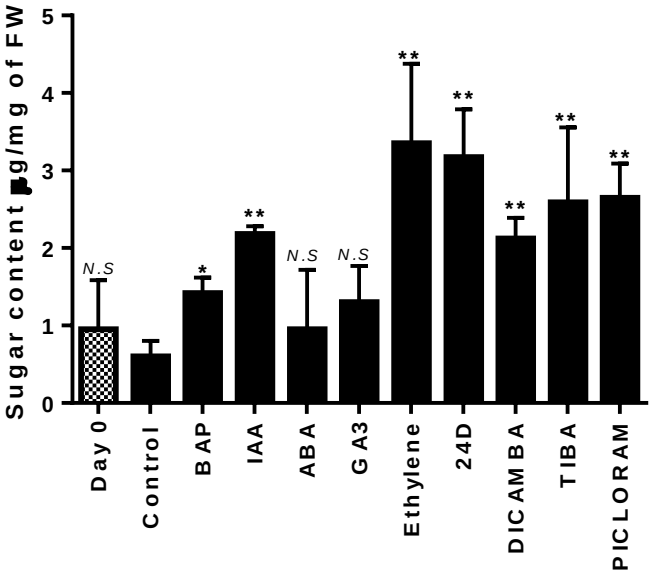

Figure 8: Variation of soluble reducing sugar content upon abiotic stress caused by supplementation of plant growth hormones at a concentration of 3mg/L to MS medium Data shown are means ± standard deviations of the means (SD). Analysis was carried out on the 40th day after the supplementation of growth regulators, with control being plain MS media without any growth regulators. The sample at day 0 is also analyzed for comparison. N.S: not significant, * $p < 0.05$, ** $p < 0.01$, *** $p < 0.001$, N=3.

Soluble sugars are important metabolites in plants that play a crucial role in energy storage, osmotic adjustment, and signalling. The effects of hormonal stress on soluble sugars have been studied in several plant species. Abscisic acid and ethylene induce the accumulation of soluble sugars in response to various stress conditions such as drought, salinity, and cold. This accumulation of soluble sugars is thought to be a mechanism for osmotic adjustment and protection against dehydration (Tonini et al., 2010). Cytokinins and gibberellins also alter the soluble sugar contents in plants (M. Wang et al., 2021). Weedicide treatment is also known to affect the soluble sugar content and related hormonal pathways in plants, accumulation of carbohydrates and sugars are one of the markers to study the herbicide toxicity in plants. Higher levels in leaf after herbicide treatment are attributed to the arrest of the physiological response towards the toxicity. Glyphosate an inhibitor of the shikimate pathway is known to alter soluble sugar content in several plant species (Fernández-Escalada et al., 2019).

3.3.3.2 Total carbohydrate content

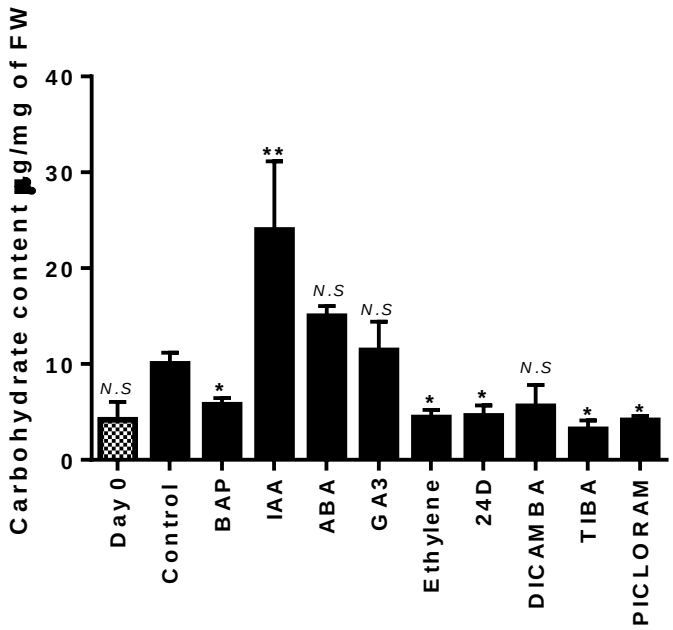

Figure 9: Variation of total carbohydrate content upon abiotic stress caused by supplementation of plant growth hormones at a concentration of 3mg/L to MS medium. Data shown are means ± standard deviations of the means (SD). Analysis was carried out on the 40th day after the supplementation of growth regulators, with control being plain MS media without any growth regulators. The sample at day 0 is also analyzed for comparison. N.S: not significant, * $p < 0.05$, ** $p < 0.01$, *** $p < 0.001$, N=3.

Similar to the effect of plant hormones on soluble sugar content, hormonal stress also alters the carbohydrate content of the plant upon exposure to various plant growth regulators. Variation is generally attributed to the various enzymes such as glycosidases, participating in the sugar and carbohydrate-related pathways, since free sugars actively participate in the signal transductions, the availability of free sugars as a result of glycosidases activity can have various physiological alterations in the plant. ABA induces the expression of genes involved in carbohydrate metabolism, such as sucrose synthase and invertase, which are responsible for the synthesis and breakdown of sucrose (Finkelstein & Gibson, 2002). ABA also can modulate the activity of enzymes involved in the regulation of starch metabolism, leading to an increase in total carbohydrate content (Kempa et al., 2008). Similarly, Ethylene regulates the expression of genes involved in carbohydrate metabolism, such as starch synthase and amylase, which are responsible for the synthesis and breakdown of starch in banana (Xia et al., 2020). Ethylene can regulate the activity of enzymes involved in the regulation of sucrose metabolism, leading to an increase in total carbohydrate content (Z. Chen et al., 2019). Weedicides such as glyphosate, 2,4D, and DICAMBA are known to alter the carbohydrate content upon exposure (Fernández-Escalada et al., 2019; R. G. Wilson & Michiels, 2003).

3.3.3.3 DPPH-free radicle scavenging assay

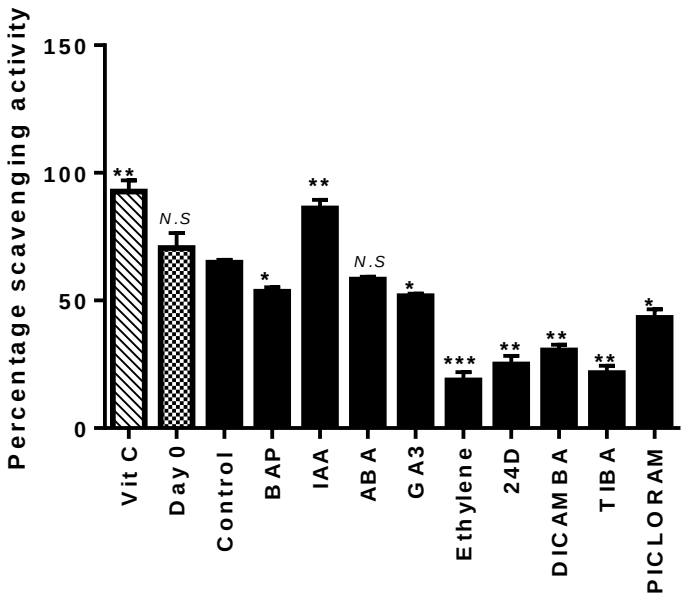

Figure 10: Variation of free radicle scavenging capacity of chilli seedlings upon abiotic stress caused by supplementation of plant growth hormones at a concentration of 3mg/L to MS medium. Analysis was carried out on the 40th day after the supplementation of growth regulators, with control being plain MS media without any growth regulators. The sample at day 0 is also analyzed for comparison. Data shown are means ± standard deviations of the means (SD). N.S: not significant, * $p < 0.05$, ** $p < 0.01$, *** $p < 0.001$, N=3.

Hormonal stress can affect the DPPH scavenging capacity of plants. Application of exogenous auxin (indole-3-acetic acid) to tomato plants increased the DPPH scavenging capacity of the leaves (Lobo et al., 2022). Treatment with other plant hormones such as Kinetin and IAA was noted to alter the free radicle scavenging capacity of the seedlings, which was attributed to altered pathways that are responsible for the production of plant secondary metabolites such as polyphenols, ascorbate, vitamins and other strong free radicle scavengers (Meza et al., 2020; Nadiveedhi et al., 2021). Such variations can also be correlated to dysregulated gene expression or enzymes that directly participate in the mitigation of free radicles (U. Kumar et al., 2012).

3.3.3.4 Total phenolic content

Cytokinins such as benzyl adenine and auxins such as indole acetic acid (IAA) have been shown to increase the total phenolic content in plants. Treatment of *Arabidopsis thaliana* plants with BAP increased the TPC of leaves (Hönig et al., 2018). Variations in plant metabolic pathways, and metabolic pathways of aromatic amino acids, which are responsible for the synthesis of phenolic compounds (Kisa et al., 2021). Synthetic herbicides plant growth regulators are also known to alter the total phenolic content (Zarzecka et al., 2019).

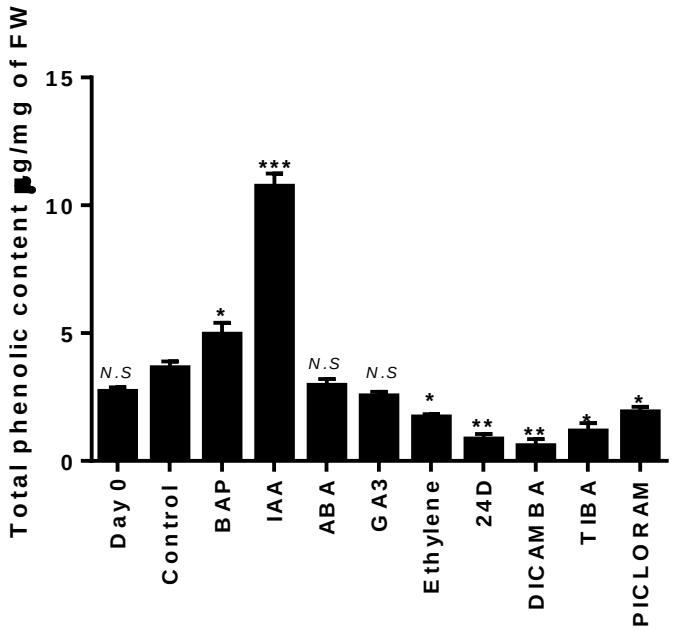

Figure 11: Variation of total phenolic content upon abiotic stress caused by supplementation of plant growth hormones at a concentration of 3mg/L to MS medium. Analysis was carried out on the 40th day after the supplementation of growth regulators, with control being plain MS media without any growth regulators. The sample at day 0 is also analyzed for comparison. Data shown are means ± standard deviations of the means (SD). N.S: not significant, * $p < 0.05$, ** $p < 0.01$, *** $p < 0.001$, N=3.

3.3.3.5 Total lipid content

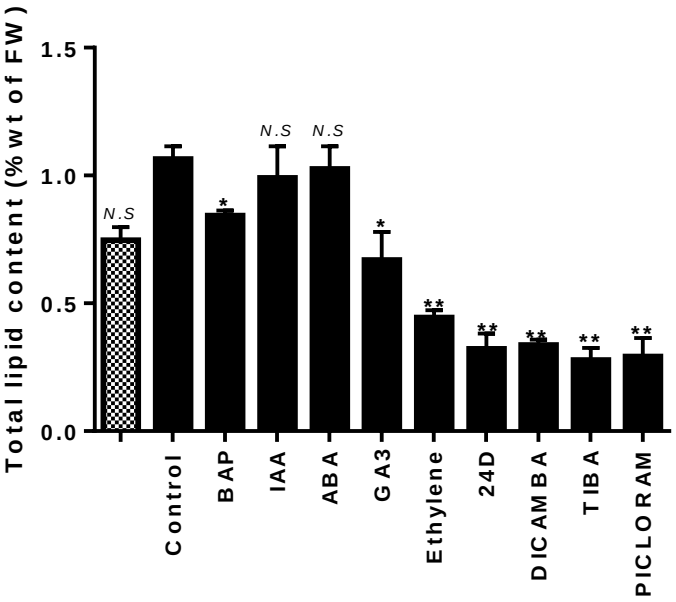

Figure 12: Variation of the total lipid content of chilli seedlings upon abiotic stress caused by supplementation of plant growth hormones at a concentration of 3mg/L to MS medium. Analysis was carried out on the 40th day after the supplementation of growth regulators, with control being plain MS media without any growth regulators. The sample at day 0 is also analyzed for comparison. Data shown are means ± standard deviations of the means (SD). N.S: not significant, * $p < 0.05$, ** $p < 0.01$, *** $p < 0.001$, N=3.

Total lipid content may be affected by altered expression of the genes or dysregulated levels of proteins or enzymes that participate in lipid biosynthetic pathways, such as the acetyl-CoA carboxylase pathway (Guschina et al., 2014), fatty acid synthase, and acyl-CoA synthase (ACS) genes (Schnurr et al., 2002).

3.4 Conclusion:

The study revealed that different PGRs had distinct effects on the growth and development of chilli seedlings. BAP led to stunted growth, while IAA promoted leaf and root proliferation. ABA and DICAMBA had growth inhibitory and callusing effects, Ethylene also led to yellowing and halted growth, indicating stress induction in plants, leading to cellular changes. IAA led to elevated meristematic activity, while ABA and GA3 treatments resulted in well-defined but altered structures. Ethylene exposure led to compromised vascular bundles and mesophyll structures, indicating its detrimental effects at the cellular level. Supporting this, Biochemical assays revealed that most PGRs led to an increase in soluble reducing sugar content, with IAA and Ethylene showing the most significant elevations. The DPPH free radical scavenging capacity was notably increased by IAA treatment, suggesting its potential to enhance the plant's stress tolerance due to significant elevation in total phenolic content.

CHAPTER 4

Proteomic Investigation of Abiotic Stress Caused by Plant Hormones

4 Proteomic investigation of abiotic stress caused by plant hormones

4.1 Introduction

Along with other OMICS, mass spectrometry-based proteomics is an indispensable tool for understanding the complexities of biological systems. Proteomics has been particularly impactful in elucidating the molecular mechanisms that underpin responses to environmental and hormonal

stressors. Plant life is a balancing act of growth, development, and response to environmental conditions. This balancing act is largely influenced by plant hormones such as Benzyl Amino Purine (BAP), Indole-3-Acetic Acid (IAA), Abscisic Acid (ABA), Gibberellic Acid (GA3), Ethylene other plant hormones. These hormones serve as pivotal signalling molecules, influencing a wide array of cellular pathways that dictate plant responses to stress conditions. One of the most significant contributions of proteomics to plant science is the ability to identify key biochemical pathways affected by various stimuli. Understanding these pathways is critical for deciphering how plants respond to hormonal and abiotic stress at the molecular level. By employing gel free proteomic techniques, this study aims to shed light on the pathways influenced by plant hormones and weedicides in *Capsicum frutescens*.

Capsicum frutescens, popularly known as Bird's eye chilli, is not only an economically valuable crop but also a model system for studying stress responses. This study specifically explores the proteomic alterations in *Capsicum frutescens* seedlings under the influence of different hormonal treatments, mapping these changes to specific biochemical pathways. In agriculture, weedicides such as 2,4-D, DICAMBA, TIBA, and PICLORAM are frequently used for controlling invasive plant species. However, their impact extends beyond target plants, affecting various biochemical pathways in non-target species as well. This study delves into these less-understood aspects, contributing to our knowledge about weedicide-induced stress at the proteomic level.

The objective of this study is to elucidate the specific pathways modulated by hormonal and chemical stressors in *Capsicum frutescens*. By employing state-of-the-art global proteomic techniques, the study offers a holistic view of how stress conditions affect protein expression and cellular pathways.

4.2 Materials and methods

Includes following steps, kindly refer sections from 6.2.1 to 6.2.6

4.2.1 Sample collection

4.2.2 Protein extraction

4.2.3 Trypsin digestion

4.2.4 Mass Spectrometry Analysis

4.2.5 Data analysis

4.2.6 Data availability

The mass spectrometry raw data and the Proteome Discoverer output MSF files obtained from this study have been uploaded to the ProteomeXchange Consortium (http://proteomecentral.proteomexchange.org) through the PRIDE partner repository with Project accession: PXD025082; DOI: 10.6019/PXD025082 (privet project), PXD024834; DOI: 10.6019/PXD024834 (privet project, phospho proteomic data, not discussed in this thesis)

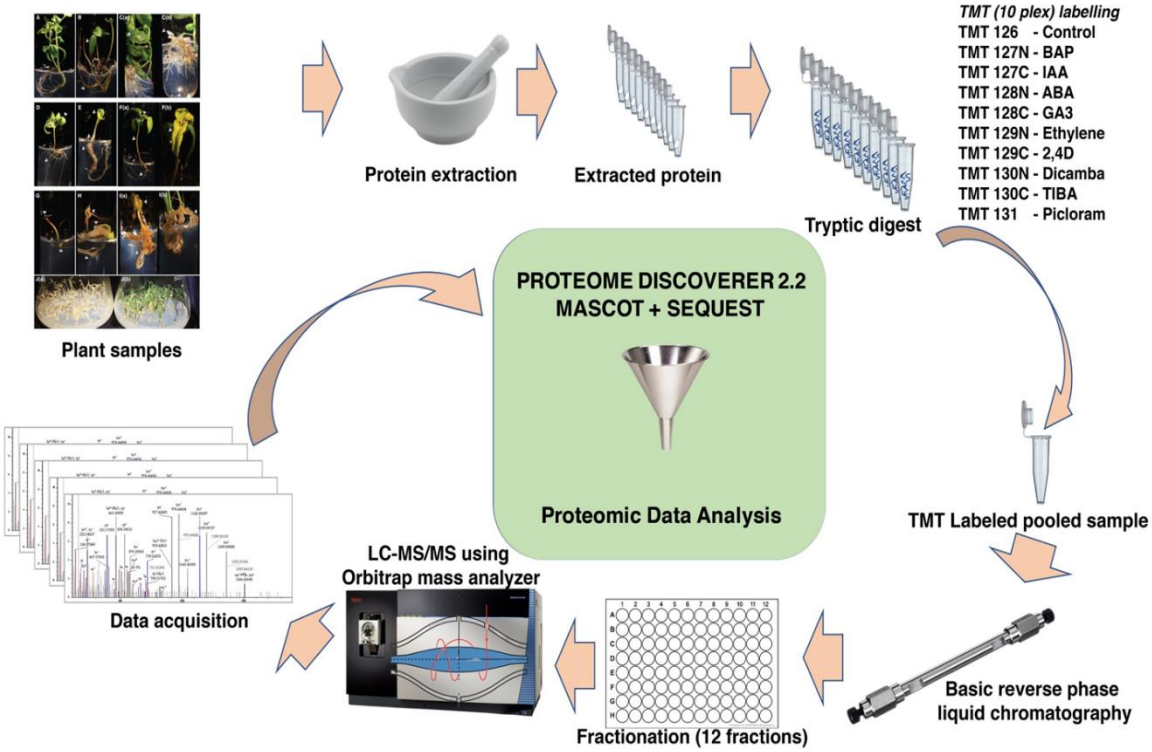

Figure 13: Schematic representation of the experimental plan for the proteomic analysis of broad mite infestation in Chilli: a workflow showing the steps involved in the proteomic analysis of capsicum seedlings supplemented with plant growth regulators. Proteins were extracted from the tissues and estimated using BCA. The proteins were then digested with trypsin and labelled with Tandem Mass Tags (TMT). Labelled peptides were analyzed on the Orbitrap Fusion Tribrid mass spectrometer. The acquired data from the mass spectrometer were searched against the *Capsicum annuum* (Pepper Zunla 1 Ref_v1.0) database using both Sequest HT and Mascot.

4.3 Results:

4.3.1 Dysregulated proteins:

In the proteomic study examining the impact of various plant growth regulators on protein expression, significant changes were observed in both overexpression and downregulation of proteins across different treatments. Upon supplementation with BAP, 266 proteins were overexpressed while 164 were downregulated. For IAA, 59 proteins showed overexpression and 44 were downregulated. In the case of ABA, there were 40 overexpressed and 33 downregulated proteins. GA3 exhibited overexpression in 15 proteins and downregulation in 18. Ethylene was associated with the overexpression of 119 proteins and downregulation of 106. The 2,4-D treatment resulted in the overexpression of 241 proteins and downregulation of a notably higher 299 proteins. DICAMBA and TIBA treatments led to the overexpression of 108 and 147 proteins, and downregulation of 94 and 93 proteins, respectively. Lastly, PICLORAM had the most pronounced effect, with 278 proteins overexpressed and 335 downregulated.

4.3.2 Effect of BAP photosynthetic pathway

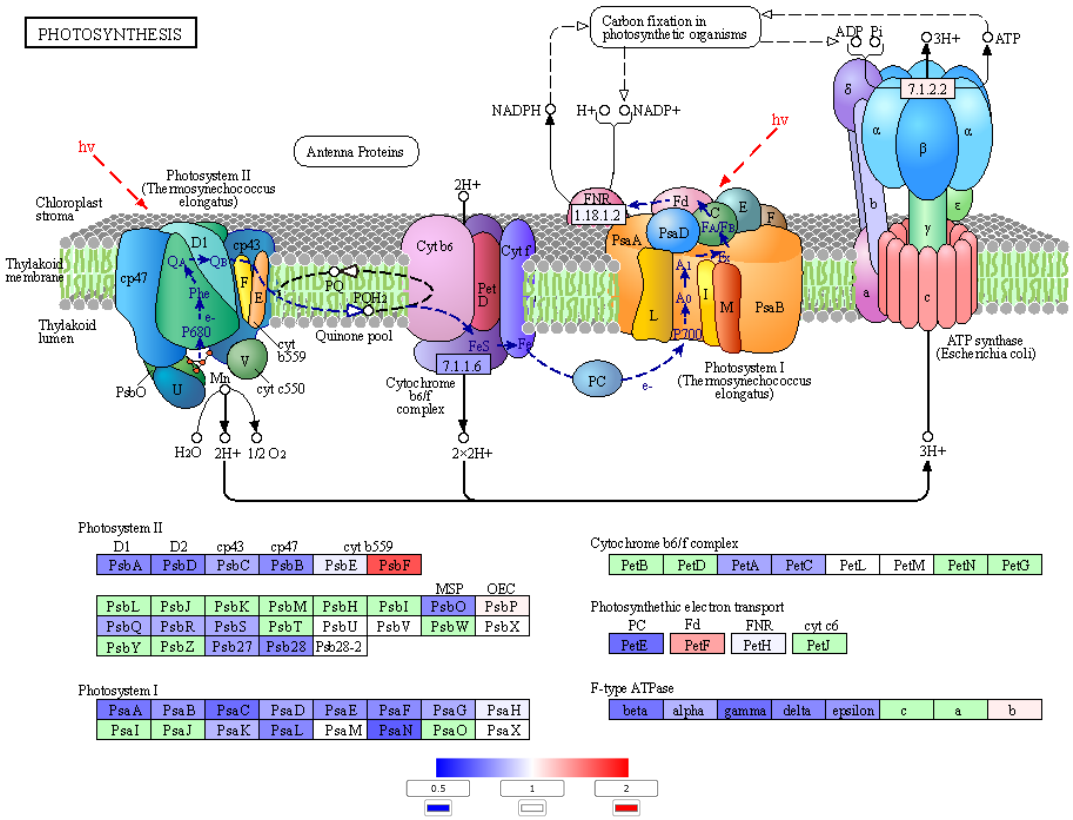

Figure 14: Effect of BAP photosynthetic pathway. Multiple proteins of photosystem I and II, cytochrome b6/f complex, electron transport system is dysregulated. The colour scale is used to illustrate the extent of dysregulation in relation to the fold change of the identified protein, where a deep red hue signifies the degree of overexpression, and a deep blue hue signifies the degree of downregulation.

Cytokinines, in general, are known to be involved in the repair process of photosystems. They increase the levels of subunits of photosystems (Gururani et al., 2015). Cytokinines also affect the electron transportation rates on photosystems (Shao et al., 2010). The current study indicates the downregulation of multiple subunits of the photosystem (PsbA, PsbD, PsbC, PsbB and PsbE) however PsbF is unregulated. The B6/F complex is a key component of the electron transport chain in photosynthesis, responsible for transferring electrons from photosystem I to photosystem II. Benzylaminopurine (BAP) is a synthetic cytokinin that has been shown to affect the functioning of the B6/F complex. BAP has been shown to upregulate the expression of genes involved in the synthesis of B6/F complex subunits, such as petD, petL and petG (Zubo et al., 2008). BAP has also been shown to enhance the repair of the B6/F complex in response to photodamage.

Table 1: List of dysregulated proteins in *Capsicum frutescens* seedlings upon the addition of BAP 3mg/mL to the MS medium. These proteins are known to participate in the photosynthesis pathway (cann00195)

Accession	Description	Fold change	Percentage variation	P-Value	Score (Mascot)	Score (Sequest HT)	Coverage [%]
YP_006666037.1	ATP synthase CF1 beta subunit (chloroplast)	0.459	0.3	0.016	8575	1433.03	75
XP_016561169.1	oxygen-evolving enhancer protein 1, chloroplastic	0.619	1.9	0.021	5923	1275.61	62
XP_016558935.1	oxygen-evolving enhancer protein 1, chloroplastic	0.547	0.49	0.021	5288	1196	65
YP_006666015.1	ATP synthase CF1 alpha subunit (chloroplast)	0.707	1.73	0.021	4182	830.32	46
XP_016556969.1	oxygen-evolving enhancer protein 2, chloroplastic	0.595	5.36	0.043	3760	942.78	56
XP_016559008.1	cytochrome f-like	0.653	2.24	0.044	1458	295.24	16
XP_016560066.1	oxygen-evolving enhancer protein 3-2, chloroplastic	1.229	1.67	0.023	935	235.33	45
XP_016560123.1	ATP synthase gamma chain, chloroplastic	0.435	0.26	0.014	597	168.33	30
XP_016568374.1	photosystem I reaction center subunit IV B, chloroplastic	0.664	0.75	0.015	1176	274.22	58
XP_016577466.1	photosystem I reaction center subunit IV A, chloroplastic	0.587	1.47	0.021	1139	278.98	43
XP_016543391.1	oxygen-evolving enhancer protein 2, chloroplastic-like	0.854	6.52	0.100	832	281.45	48
XP_016575286.1	photosystem I reaction center subunit II, chloroplastic	0.658	0.1	0.014	710	190.91	43
YP_006666036.1	ATP synthase CF1 epsilon subunit (chloroplast)	0.599	0.49	0.021	1088	135.71	51
XP_016559311.1	photosystem I reaction center subunit III, chloroplastic-like	0.548	1.93	0.021	1800	288.39	38
XP_016574951.1	ATP synthase subunit b', chloroplastic	0.565	0.84	0.034	539	133.74	25
YP_006666056.1	photosystem II CP47 chlorophyll apoprotein (chloroplast)	0.554	2.66	0.039	758	195.83	24
YP_006666029.1	photosystem I P700 apoprotein A2 (chloroplast)	0.604	0.93	0.133	754	157.58	13
YP_009049725.1	hypothetical protein (mitochondrion)	0.683	0.95	0.034	460	130.1	18
YP_006666016.1	ATP synthase CF0 subunit I (chloroplast)	0.73	2.11	0.061	502	109.17	49
XP_016563377.1	psbP-like protein 1, chloroplastic	1.046	3	0.236	541	122.5	30
YP_006666010.1	photosystem II protein D1 (chloroplast)	0.542	3.34	0.029	620	168.47	20
YP_006666081.1	photosystem I subunit VII (chloroplast)	0.426	3.16	0.037	1241	234.66	53

XP_016552487.1	photosystem I reaction center subunit N, chloroplastic	0.368	1.66	0.022	632	113.49	34
XP_016568322.1	plastocyanin, chloroplastic	0.431	0.56	0.022	476	115.61	28
XP_016551634.1	ATP synthase delta chain, chloroplastic	0.538	0.08	0.023	444	144.82	33
XP_016559391.1	ferredoxin--NADP reductase, root-type isozyme, chloroplastic	0.957	7.65	0.665	257	95.83	24
YP_006666030.1	photosystem I P700 apoprotein A1 (chloroplast)	0.465	0.6	0.024	507	159.88	11
XP_016575162.1	photosystem II 22 kDa protein, chloroplastic	0.666	3.15	0.031	185	51.82	21
XP_016564625.1	cytochrome b6-f complex iron-sulfur subunit, chloroplastic	0.656	6.37	0.054	473	102.08	22
XP_016541900.1	photosystem II reaction center Psb28 protein	0.546	0.43	0.015	342	52.25	22
XP_016562688.1	photosystem I reaction center subunit VI, chloroplastic-like	0.943	8.87	0.829	46	37.03	37
XP_016581568.1	photosystem II 10 kDa polypeptide, chloroplastic	0.684	6.47	0.096	272	44.96	22
YP_006666025.1	photosystem II protein D2 (chloroplast)	0.513	1.6	0.020	440	79.37	14
XP_016555469.1	photosystem II repair protein PSB27-H1, chloroplastic	0.64	3.48	0.053	286	58.73	10
XP_016577558.1	photosystem I reaction center subunit XI, chloroplastic-like	0.533	3.3	0.032	209	32.74	10
XP_016552228.1	ferredoxin, root R-B2-like	0.926	30.81	0.749	36	14.22	13
YP_006666047.1	photosystem II cytochrome b559 alpha subunit (chloroplast)	0.934	4.9	0.305	234	34.76	23
XP_016548442.1	photosystem I reaction center subunit psaK, chloroplastic	0.716	6.87	0.100	80	25.59	8
XP_016546595.1	photosynthetic NDH subunit of lumenal location 2, chloroplastic isoform X1	0.676	14.83		103	9.47	13
YP_009049738.1	hypothetical protein (mitochondrion)	1.066	7.4	0.375	37	10.49	8
XP_016581512.1	photosystem I reaction center subunit V, chloroplastic	0.677	0		36	2.51	5
YP_006666046.1	photosystem II cytochrome b559 beta subunit (chloroplast)	1.678	11.4	0.065	36	9.1	21
XP_016577945.1	ferredoxin, root R-B1-like isoform X1	1.355	0		0	0	13

4.3.3 Effect of IAA on chilli seedlings

4.3.3 Effect of IAA on chilli seedlings

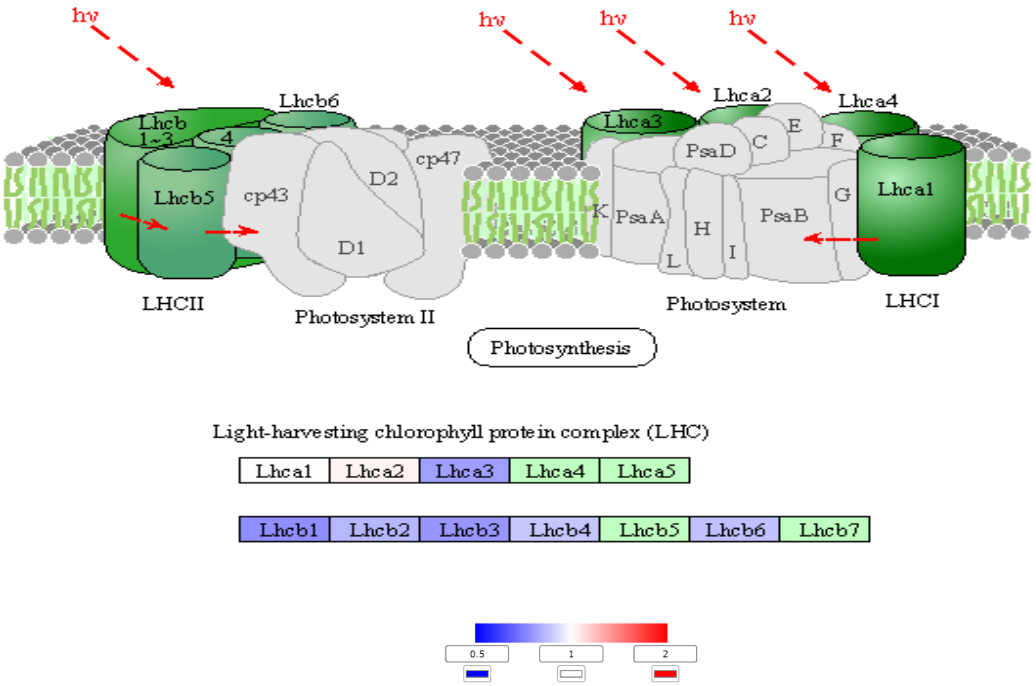

Figure 15: Effect of IAA on the light harvesting complex of the photosynthetic pathway. Multiple proteins of LHC are unregulated. The colour scale is used to illustrate the extent of dysregulation in relation to the fold change of the identified protein, where a deep red hue signifies the degree of overexpression, and a deep blue hue signifies the degree of downregulation.

Light harvesting complexes (LHCs) are responsible for capturing light energy during photosynthesis. One of the effects of auxins on LHCs is the modulation of their synthesis and accumulation. Studies have shown that auxins (Indole acetic acid) along with strigolactones can increase the expression of LHC genes and promote the accumulation of LHC complexes in tomatoes (Mayzlish-Gati et al., 2010). This effect is believed to be due to the ability of auxins to alter the photosynthetic pigments as seen in the algae *Desmodesmus* (Chung et al., 2018). Another effect of auxins on LHCs is the stimulation of their energy transfer efficiency. Studies have shown that auxins and light regimens affect the uptake of urea and ammonium ions, and levels of indole acetic acids were correlated with the photosynthetic efficiency in terms of quantum yields (Esteban et al., 2016). Since auxins are known to be synthesized at chloroplast via tryptophan metabolism, they play an important role in chloroplast development (Salazar-Iribe & De-la-Peña, 2020).

Table 2: List of dysregulated proteins in *Capsicum frutescens* seedlings upon the addition of IAA 3mg/mL to the MS medium. These proteins are known to participate in the Photosynthesis - antenna proteins(cann00196)

Accession	Description	Fold change	Percentage variation	P-Value	Score (Mascot)	Score (Sequest HT)	Coverage [%]
XP_016556256.1	chlorophyll a-b binding protein 21, chloroplastic-like	0.59	0.34	0.019	592	259.6	49
XP_016556253.1	chlorophyll a-b binding protein 1B, chloroplastic-like	0.661	1.13	0.034	726	298.78	33
XP_016556254.1	chlorophyll a-b binding protein 21, chloroplastic-like	0.561	0.22	0.105	665	274.55	33
XP_016580520.1	chlorophyll a-b binding protein 5, chloroplastic-like	0.717	0.87	0.029	1031	349.35	25
XP_016539209.1	chlorophyll a-b binding protein CP24 10A, chloroplastic	0.755	1.72	0.041	845	156.71	23
XP_016542199.1	chlorophyll a-b binding protein CP29.1, chloroplastic-like	0.775	2.35	0.043	508	137.45	16
XP_016545107.1	chlorophyll a-b binding protein 8, chloroplastic	0.622	0.32	0.034	54	40.36	16
XP_016573908.1	chlorophyll a-b binding protein 6A, chloroplastic	1.009	14.8		0	6.84	10
XP_016565396.1	chlorophyll a-b binding protein 13, chloroplastic	0.593	1.27	0.029	0	13.57	18
XP_016537571.1	chlorophyll a-b binding protein 7, chloroplastic	1.045	39.2	0.971	58	14.43	4

4.3.4 Effect of ABA on chilli seedlings

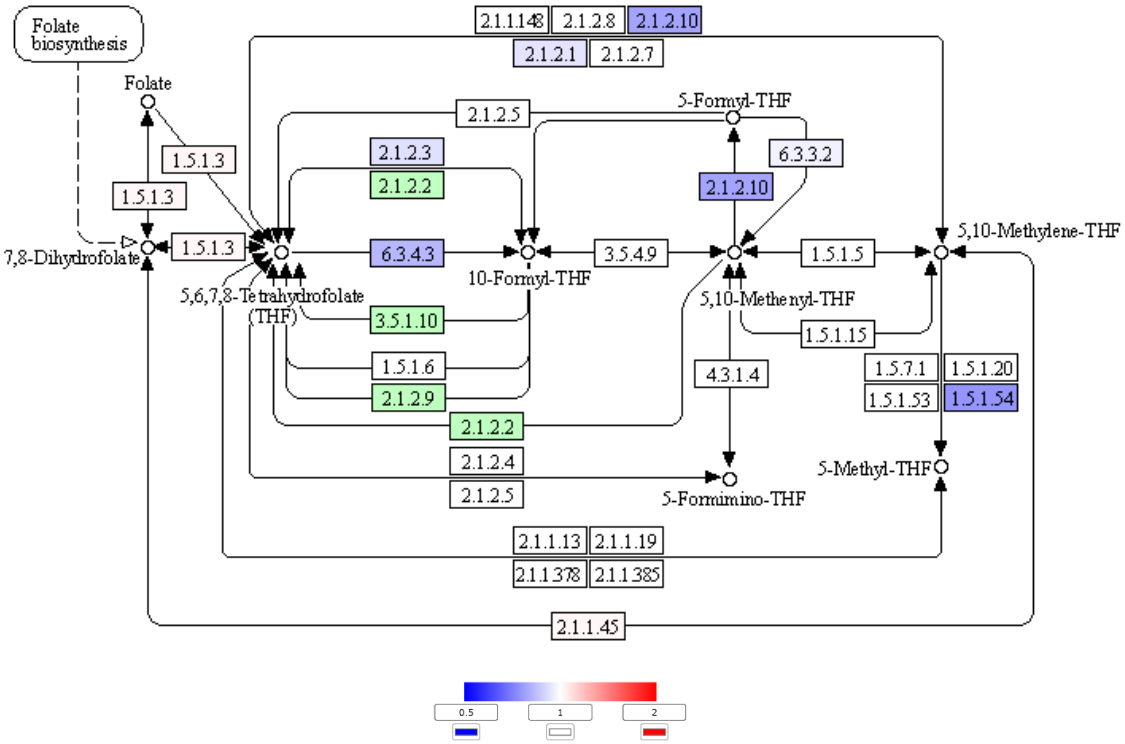

Figure 16: Altered folate one carbon pool pathway in chilli seedlings when supplemented at a concentration of 3mg/L ABA to MS medium. The colour scale is used to illustrate the extent of dysregulation in relation to the fold change of the identified protein, where a deep red hue signifies the degree of overexpression, and a deep blue hue signifies the degree of downregulation.

Under stress conditions such as drought, high salinity, or oxidative stress, plants experience an increase in reactive oxygen species (ROS) production, hence there will be an imbalance in redox homeostasis in the plants, which results in ROS induced damage in the cell. Dihydrofolate and related enzymes such as dihydrofolate reductase are known to control folate status in the cell, thereby playing a crucial role in the redox balance of the cell (Gorelova et al., 2017). Amino Acid Metabolism: One-carbon metabolism, including tetrahydrofolate, is essential for the synthesis of amino acids such as glycine, histidine, and tryptophan (Tjong et al., 2023). These amino acids are involved in the synthesis of defence-related compounds, such as ethylene and polyamines, which play roles in plant stress responses. Changes in tetrahydrofolate availability can impact the levels of these amino acids and subsequent defence responses (Hildebrandt et al., 2015).Nucleotide Biosynthesis: Tetrahydrofolate is required for the de novo synthesis of purine and pyrimidine nucleotides, which are essential for DNA and RNA synthesis (Moffatt & Ashihara, 2002).

Table 3: List of dysregulated proteins in *Capsicum frutescens* seedlings upon the addition of ABA 3mg/mL to the MS medium. These protein are known to participate in the One-carbon pool by folate (cann00670)

Accession	Description	Fold change	Percentage variation	Score (Mascot)	Score (Sequest HT)	P-Value	Coverage [%]
XP_016560855.1	serine hydroxymethyltransferase, mitochondrial	1.078	1.41	1957	399.72	0.34	36
XP_016573654.1	serine hydroxymethyltransferase 4	0.92	1.6	680	217.96	0.89	22
XP_016560143.1	aminomethyltransferase, mitochondrial	0.842	0.2	934	199.3	0.04	32
XP_016568990.1	serine hydroxymethyltransferase, mitochondrial-like	1.108	4.78	1099	200.31	0.25	21
XP_016551170.1	methylenetetrahydrofolate reductase 2-like	0.736	8.22	124	60.45	0.14	16
XP_016576447.1	formate--tetrahydrofolate ligase	0.813	1.6	74	25.23	0.11	12
XP_016550104.1	serine hydroxymethyltransferase 3, chloroplastic-like isoform X1	0.982	9.07	162	39.64	0.73	13
XP_016537710.1	serine hydroxymethyltransferase 3, chloroplastic-like	0.724	0	188	28.96		9
XP_016572328.1	bifunctional purine biosynthesis protein PurH	1.007	6.54	56	21.57	0.81	5
XP_016563545.1	5-formyltetrahydrofolate cyclo-ligase, mitochondrial isoform X1	1.179	0	0	4.22		4
XP_016539767.1	bifunctional dihydrofolate reductase-thymidylate synthase-like	1.252	1.82	16	4.62	0.05	1

4.3.5 Effect of GA3 on chilli seedlings

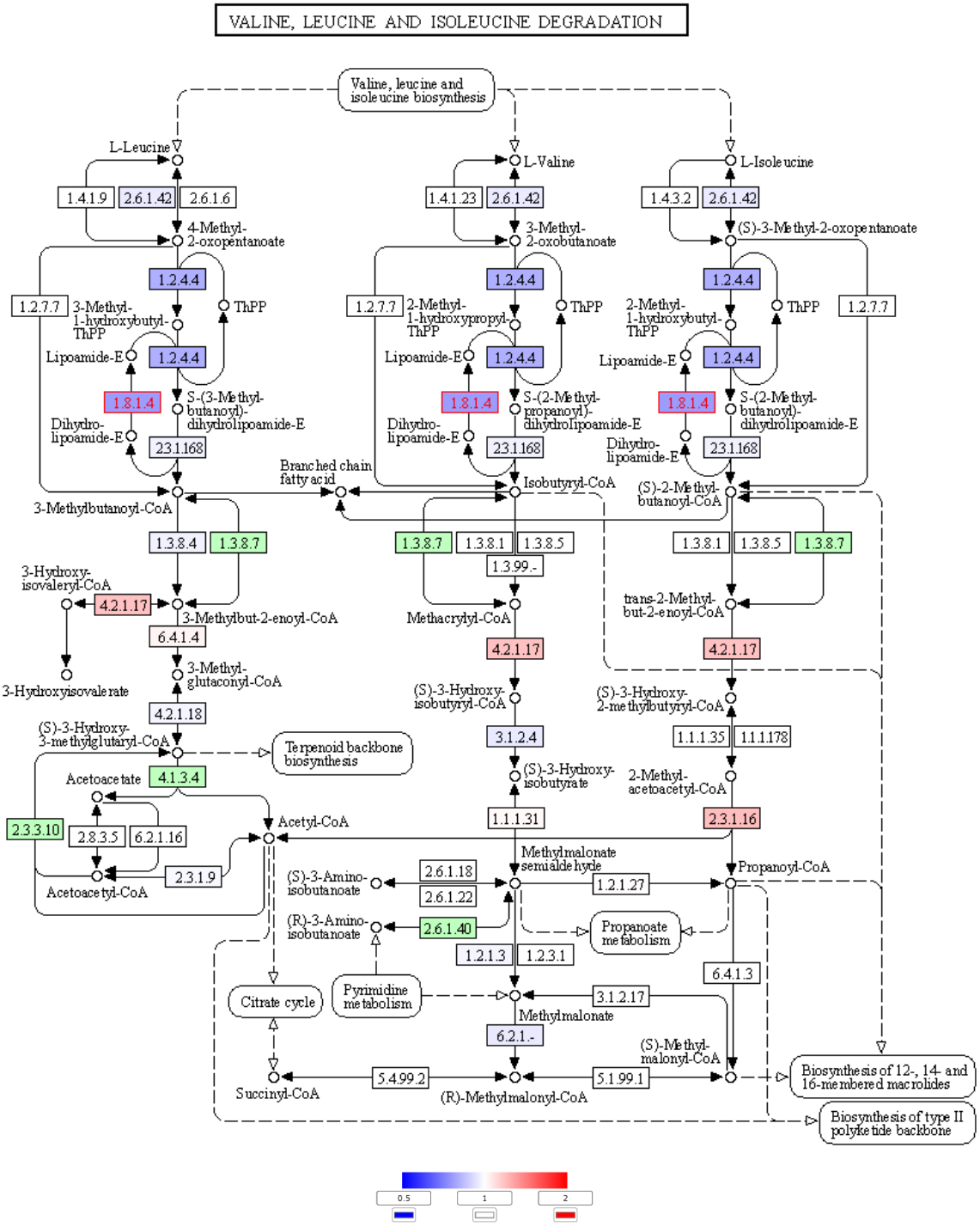

Figure 17: Effect of GA3 (3mg/L in MS medium) on valine leucine degradation pathway in chilli seedlings. The colour scale is used to illustrate the extent of dysregulation in relation to the fold change of the identified protein, where a deep red hue signifies the degree of overexpression, and a deep blue hue signifies the degree of downregulation.

Table 4: List of dysregulated proteins in *Capsicum frutescens* seedlings upon the addition of GA3 3mg/mL to the MS medium. These proteins are known to participate in valine, leucine and isoleucine degradation (cann00280)

Accession	Description	Fold change	Percentage variation	P-Value	Score (Mascot)	Score (Sequest HT)	Coverage [%]
XP_016550118.1	dihydrolipoyl dehydrogenase, mitochondrial	1.118	0.91	0.169	1230	277.58	33
XP_016563469.1	aldehyde dehydrogenase family 2 member B4, mitochondrial-like	1.086	0.76	0.114	1432	288.36	30
XP_016566389.1	3-ketoacyl-CoA thiolase 2, peroxisomal	0.876	1.46	0.202	605	192.25	35
XP_016580453.1	acetyl-CoA acetyltransferase, cytosolic 1	0.973	1.92	0.347	425	140.84	33
XP_016539331.1	methylmalonate-semialdehyde dehydrogenase [acylating], mitochondrial	1.006	9.84	0.899	380	85.5	18
XP_016538607.1	probable 3-hydroxyisobutyrate dehydrogenase-like 1, mitochondrial	0.918	4.2	0.419	269	63.22	18
XP_016538757.1	dihydrolipoyl dehydrogenase 2, chloroplastic-like	1.01	1.27	0.769	382	79.11	11
XP_016562466.1	aldehyde dehydrogenase family 7 member A1	1.086	7.31	0.463	210	55.39	17
XP_016547869.1	isovaleryl-CoA dehydrogenase, mitochondrial isoform X1	0.948	2.41	0.433	68	31.76	16
XP_016560903.1	branched-chain-amino-acid aminotransferase 3, chloroplastic-like	0.923	9.34	0.541	100	27.12	11
XP_016551169.1	2-oxoisovalerate dehydrogenase subunit alpha 2, mitochondrial-like	0.783	10.64	0.292	194	36.57	9
XP_016573538.1	dihydrolipoyl dehydrogenase 2, chloroplastic-like isoform X2	0.611	0.29	0.148	262	34.1	5
XP_016561534.1	aldehyde dehydrogenase family 2 member B7, mitochondrial-like	1.115	15.06		129	30.73	5
XP_016553804.1	probable 3-hydroxyisobutyrate dehydrogenase, mitochondrial	1.022	15.99	0.922	75	23.45	10
XP_016544139.1	3-hydroxyisobutyryl-CoA hydrolase 1-like	0.827	3.07	0.113	39	21.2	8

XP_016541790.1	3-ketoacyl-CoA thiolase 2, peroxisomal-like isoform X1	1.253	2.24	0.513	26	7.51	13
XP_016575178.1	aldehyde dehydrogenase-like	0.959	4.95	0.346	63	16.72	8
XP_016582236.1	lipoamide acyltransferase component of branched-chain alpha-keto acid dehydrogenase complex, mitochondrial	0.95	2.53	0.769	59	14.45	7
XP_016579265.1	2-oxoisovalerate dehydrogenase subunit beta 1, mitochondrial-like	0.685	5.21	0.267	122	12.7	4
XP_016541586.1	3-hydroxyisobutyryl-CoA hydrolase-like protein 5	0.914	34.24		16	4.41	5
XP_016540772.1	methylcrotonoyl-CoA carboxylase subunit alpha, mitochondrial	1.044	19.78		31	5.95	3
XP_016581765.1	probable enoyl-CoA hydratase 1, peroxisomal	1.243	0		0	2.2	3
XP_016550418.1	malonate--CoA ligase-like isoform X1	0.919	0		0	2.67	3
XP_016570339.1	probable enoyl-CoA hydratase 2, mitochondrial isoform X1	0.959	0		0	1.9	4

Gibberellic acid (GA) is a plant hormone that plays a key role in promoting plant growth and development. While GA does not directly affect the degradation of amino acids such as valine, leucine, and isoleucine, it can indirectly impact the rate at which these amino acids are broken down when treated with PAC, a known antagonist of GA3 (Ribeiro et al., 2012). GA has been shown to stimulate the production of enzymes involved in protein synthesis and degradation in plants. This can lead to an increase in the rate at which proteins are broken down, which in turn can release amino acids such as valine, leucine, and isoleucine into the plant cell. Once these amino acids are released, their degradation is primarily controlled by enzymes such as branched-chain amino acid transaminase (BCAT) and branched-chain alpha-keto acid dehydrogenase (BCKD) (Hutson, 2001). However, the activity of these enzymes can be influenced by the availability of co-factors such as thiamine pyrophosphate, which are necessary for their proper function (Hutson, 2001).

4.3.6 Effect of ethylene on chilli seedlings

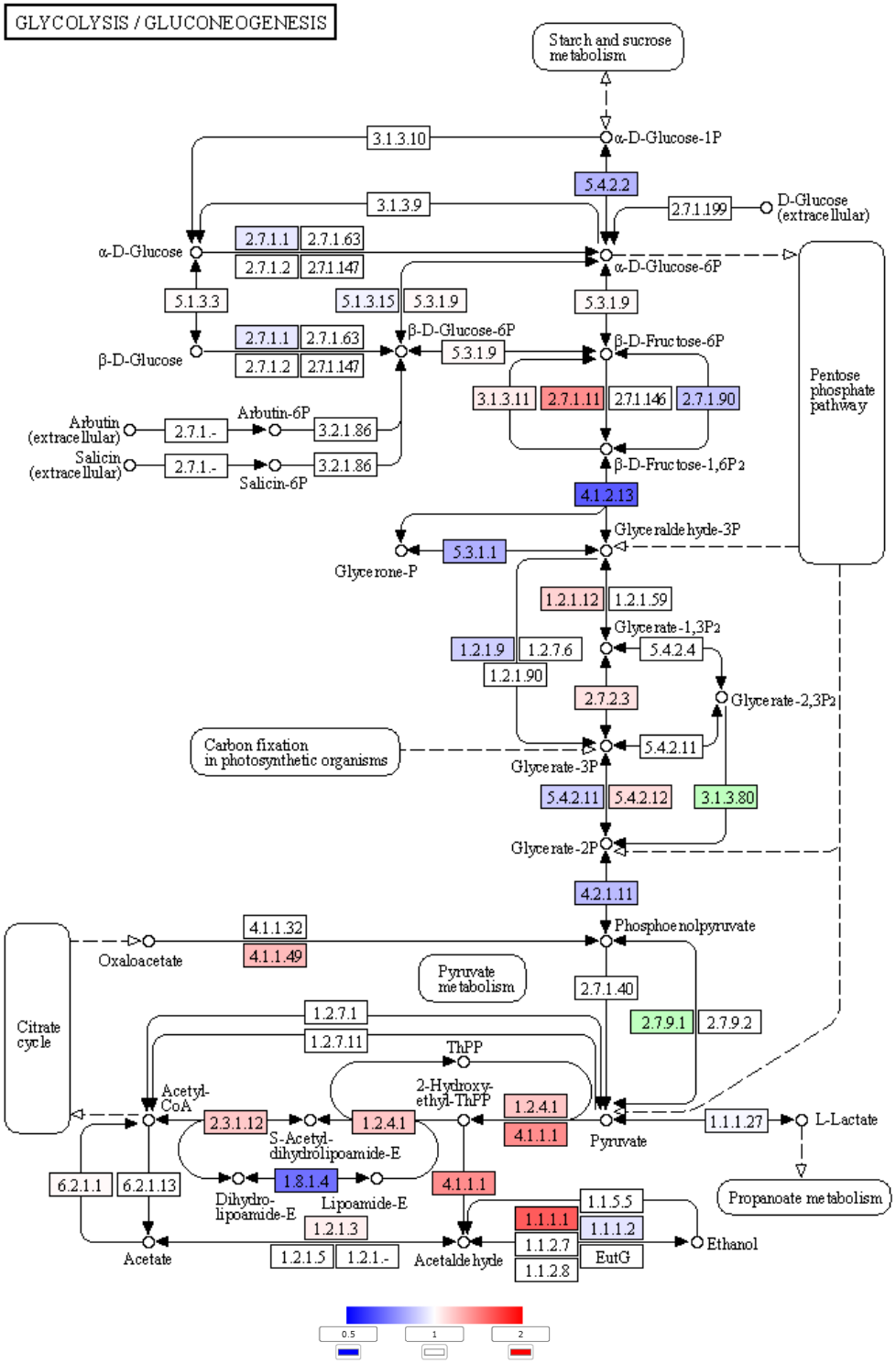

Figure 18: Effect of ethylene on glycolysis pathway. The colour scale is used to illustrate the extent of dysregulation in relation to the fold change of the identified protein, where a deep red hue signifies the degree of overexpression, and a deep blue hue signifies the degree of downregulation.

Table 5: List of dysregulated proteins in *Capsicum frutescens* seedlings upon the addition of Ethylene 5cc to the MS medium. These proteins are known to participate in the Glycolysis / Gluconeogenesis (cann 00010)

Accession	Description	Fold change	Percentage variation	P-Value	Score (Mascot)	Score (Sequest HT)	Coverage [%]
XP_016542903.1	enolase	0.947	3.31	0.148	4552	1319.99	53
XP_016581535.1	phosphoglycerate kinase, chloroplastic	0.665	0.17	0.037	5273	817.38	51
XP_016553860.1	fructose-bisphosphate aldolase cytoplasmic isozyme	1.117	1.31	0.084	3926	828.02	46
XP_016581536.1	phosphoglycerate kinase, cytosolic	1.111	6.32	0.153	3359	620	53
XP_016578224.1	glyceraldehyde-3-phosphate dehydrogenase, cytosolic	1.146	2.84	0.067	8322	1640.74	59
XP_016558766.1	fructose-bisphosphate aldolase 1, chloroplastic-like	0.557	0.26	0.023	3591	579.2	56
XP_016542801.1	phosphoglucomutase, cytoplasmic	0.989	3.86	0.867	1785	376.83	34
XP_016543474.1	fructose-bisphosphate aldolase cytoplasmic isozyme-like	1.066	9.49	0.342	2042	449.1	35
XP_016550118.1	dihydrolipoyl dehydrogenase, mitochondrial	1.087	1.76	0.113	1230	277.58	33
XP_016539907.1	triosephosphate isomerase, chloroplastic	0.793	1.44	0.199	1462	355.9	69
XP_016563829.1	glyceraldehyde-3-phosphate dehydrogenase, cytosolic-like	1.401	14.23	0.159	5850	1097.02	48
XP_016547571.1	probable fructose-bisphosphate aldolase 3, chloroplastic	1.19	1.18	0.074	1872	389.41	40
XP_016563469.1	aldehyde dehydrogenase family 2 member B4, mitochondrial-like	1.326	4.92	0.045	1432	288.36	30
XP_016560542.1	fructose-bisphosphate aldolase 1, chloroplastic-like	0.686	0.65	0.033	2727	439.99	51
XP_016575214.1	alcohol dehydrogenase 1	0.895	11.54	0.308	1539	352.66	43
XP_016572139.1	triosephosphate isomerase, cytosolic	0.846	3.57	0.108	2312	485.87	60
XP_016553268.1	glyceraldehyde-3-phosphate dehydrogenase, cytosolic	1.031	10.03	0.617	6911	1348.17	39
XP_016580396.1	2,3-bisphosphoglycerate-independent phosphoglycerate mutase	1.135	3.27	0.080	1115	287.39	28
XP_016539832.1	fructose-bisphosphate aldolase 1, chloroplastic	0.36	0.11	0.023	2245	354.46	38
XP_016543426.1	pyruvate kinase 1, cytosolic	1.215	3.63	0.086	671	156.23	24
XP_016581480.1	fructose-bisphosphate aldolase, cytoplasmic isozyme 1 isoform X2	0.353	0.77	0.030	781	211.48	30

XP_016568194.1	pyrophosphate--fructose 6-phosphate 1-phosphotransferase subunit alpha	1.061	1.73	0.072	441	144.6	30
XP_016559762.1	pyruvate decarboxylase 1	1.455	7.09	0.163	414	144.78	26
XP_016569113.1	phosphoglucomutase, cytoplasmic-like	0.783	0		795	179.77	17
XP_016568983.1	phosphoenolpyruvate carboxykinase [ATP]-like	1.266	5.23	0.078	467	150.23	21
XP_016572427.1	pyruvate kinase, cytosolic isozyme	1.023	5.67	0.729	781	128.38	23
XP_016579643.1	dihydrolipoyllysine-residue acetyltransferase component 3 of pyruvate dehydrogenase complex, mitochondrial-like	1.069	2.22	0.918	672	108.35	21
XP_016564733.1	phosphoglucomutase, chloroplastic	0.71	0.05	0.037	466	58.44	16
XP_016544999.1	glyceraldehyde-3-phosphate dehydrogenase GAPCP1, chloroplastic	1.172	5.6	0.209	624	121.78	28
XP_016569084.1	glucose-6-phosphate isomerase 1, chloroplastic	1.375	2.15	0.248	180	68.79	14
XP_016578148.1	pyruvate dehydrogenase E1 component subunit beta-1, mitochondrial	0.935	2.71	0.176	741	145.83	17
XP_016569230.1	L-lactate dehydrogenase B-like	0.967	7.15	0.977	1098	182.58	24
XP_016550706.1	pyruvate kinase 1, cytosolic-like	1.003	24.14	0.866	354	78.92	21
XP_016550244.1	ATP-dependent 6-phosphofructokinase 6-like isoform X1	1.097	17.05	0.424	142	47.45	18
XP_016538757.1	dihydrolipoyl dehydrogenase 2, chloroplastic-like	0.922	2.28	0.759	382	79.11	11
XP_016575862.1	triosephosphate isomerase, cytosolic-like	0.69	0		993	187.9	18
XP_016563413.1	enolase 1, chloroplastic	1.159	11.91	0.190	296	81.99	18
XP_016562466.1	aldehyde dehydrogenase family 7 member A1	1.314	2.69	0.052	210	55.39	17
XP_016550998.1	dihydrolipoyllysine-residue acetyltransferase component 1 of pyruvate dehydrogenase complex, mitochondrial isoform X1	1.316	2.04	0.037	303	71.03	10
XP_016542355.1	aldo-keto reductase family 4 member C9-like	1.011	5.03	0.592	109	64.95	33
XP_016564062.1	pyruvate dehydrogenase E1 component subunit beta-1, mitochondrial	1	9.43	0.835	657	117.16	12
XP_016562641.1	hexokinase-1	1.614	2.52	0.149	202	35.68	9
XP_016546988.1	dihydrolipoyllysine-residue acetyltransferase component 4 of pyruvate dehydrogenase complex, chloroplastic	0.928	2.1	0.125	199	45.2	8
XP_016561420.1	aldose 1-epimerase-like	1	4.61	0.633	266	65.68	11

XP_016551550.1	pyrophosphate--fructose 6-phosphate 1-phosphotransferase subunit alpha-like	1.05	28.19	0.770	305	72.67	10
XP_016560660.1	putative glucose-6-phosphate 1-epimerase	0.89	1.99	0.696	199	29.46	7
XP_016547479.1	pyruvate dehydrogenase E1 component subunit alpha, mitochondrial	1.104	5.88	0.157	232	81.01	14
XP_016560175.1	pyrophosphate--fructose 6-phosphate 1-phosphotransferase subunit beta	0.767	8.5	0.149	150	63.21	10
XP_016557107.1	pyruvate dehydrogenase E1 component subunit alpha-3, chloroplastic-like	0.804	0.56	0.101	242	54.39	13
XP_016541792.1	alcohol dehydrogenase class-3	0.864	2.04	0.449	190	44.62	10
XP_016579812.1	NADP-dependent glyceraldehyde-3-phosphate dehydrogenase	0.811	3.91	0.114	239	54.3	11
XP_016569491.1	fructose-1,6-bisphosphatase, cytosolic	0.683	5.63	0.078	114	32.51	15
XP_016572851.1	pyruvate dehydrogenase E1 component subunit alpha, mitochondrial-like isoform X1	0.839	0.57	0.045	125	64.51	12
XP_016557965.1	pyruvate kinase, cytosolic isozyme-like	0.994	22.27	0.685	223	34.13	15
XP_016561419.1	aldose 1-epimerase-like	1.129	36.46	0.632	130	31.97	9
XP_016546005.1	pyruvate decarboxylase 1	1.448	7.03	0.189	232	55.4	5
XP_016561423.1	aldose 1-epimerase-like isoform X2	2.029	4.67	0.083	175	47.57	11
XP_016569565.1	alcohol dehydrogenase 1	1.644	8.41	0.067	185	31.96	7
XP_016550847.1	fructose-1,6-bisphosphatase, cytosolic-like	1.727	0		77	25	11
XP_016573538.1	dihydrolipoyl dehydrogenase 2, chloroplastic-like isoform X2	0.439	4.26	0.086	262	34.1	5
XP_016578594.1	hexokinase-2	0.968	2.63		114	21.73	5
XP_016564461.1	Plastidial pyruvate kinase 2	0.808	10.23	0.261	68	14.05	6
XP_016561534.1	aldehyde dehydrogenase family 2 member B7, mitochondrial-like	1.283	8.41		129	30.73	5
XP_016566588.1	pyruvate kinase isozyme A, chloroplastic	0.896	2.33	0.104	195	31.95	6
XP_016545995.1	fructose-1,6-bisphosphatase, chloroplastic-like	0.721	0.7	0.035	139	22.55	8
XP_016561421.1	aldose 1-epimerase-like	0.984	31.5	0.855	62	23.52	7

XP_016564979.1	ATP-dependent 6-phosphofructokinase 4, chloroplastic-like isoform X1	1.771	0		35	15.04	8
XP_016575178.1	aldehyde dehydrogenase-like	1.061	6.77	0.354	63	16.72	8
XP_016559097.1	putative glucose-6-phosphate 1-epimerase	0.77	4.43	0.167	120	17.16	10
XP_016551551.1	ATP-dependent 6-phosphofructokinase 5, chloroplastic-like isoform X1	1.443	55.63		16	6.32	3
XP_016543252.1	aldo-keto reductase family 4 member C9-like	0.896	0		79	10.9	6
XP_016563209.1	aldose 1-epimerase	0.913	8.25		32	5.81	6
XP_016561758.1	acetyl-coenzyme A synthetase, chloroplastic/glyoxysomal isoform X1	1.024	0		0	3.27	2
XP_016571358.1	pyruvate kinase isozyme G, chloroplastic	1.001	11.98		44	5.92	4
XP_016568397.1	hexokinase-2, chloroplastic	0.902	0		0	4.63	5
XP_016564880.1	glucose-6-phosphate isomerase, cytosolic isoform X1	1.022	0		30	8.46	2
XP_016563608.1	aldose 1-epimerase	1.016	23.22		33	7.81	3
XP_016580265.1	putative glucose-6-phosphate 1-epimerase	0.95	0		17	2.84	4
XP_016539319.1	fructose-1,6-bisphosphatase class 1	1.072	0		0	2.76	4
XP_016569326.1	2,3-bisphosphoglycerate-dependent phosphoglycerate mutase	0.805	27.34		13	5.53	4
XP_016540421.1	hexokinase-2 isoform X1	0.909	4.03		0	2.47	3
XP_016569741.1	dihydrolipoyllysine-residue acetyltransferase component 5 of pyruvate dehydrogenase complex, chloroplastic	1.21	4.51	0.066	25	7.46	2
XP_016577722.1	cytosolic enolase 3	0.735	0		20	2.04	2
XP_016546540.1	pyruvate dehydrogenase E1 component subunit beta-3, chloroplastic-like isoform X1	1.219	22.25	0.368	20	9.36	2

Ethylene is a plant hormone that is involved in a wide range of physiological and developmental processes, such as fruit ripening, leaf senescence, and responses to biotic and abiotic stress. Ethylene is known to indirectly influence the glycolysis pathway through its effects on gene expression and metabolism (Solomos & Laties, 1976, p. 1; C. H. Wang et al., 1962). Glycolysis is a central metabolic pathway that is involved in the breakdown of glucose to produce ATP, which is the main energy currency of cells. The pathway involves a series of enzymatic reactions that convert glucose to pyruvate, which can then be further metabolized in various ways, depending on the metabolic needs of the cell. Studies have shown that ethylene can influence the expression of genes involved in glycolysis and other metabolic pathways. For example, in tomato fruit, ethylene has been shown to alter the expression of genes encoding key glycolytic enzymes such as hexokinase (Karve et al., 2012) and phosphofructokinase (Mertens et al., 1987), leading to altered flux through the glycolysis pathway. ethylene has been shown to increase the levels of sugars such as glucose, fructose, and sucrose, which are key intermediates in the glycolysis pathway(Chidley et al., 2017). Ethylene can also affect the levels of other metabolites such as amino acids and organic acids, which can feed into the glycolysis pathway or be produced by it (Rodrigues et al., 2014). Though the role of ethylene on metabolites involved in the Crebs cycle, or the enzymes involved in the pathway, this study reports few dysregulated enzymes involved in the glycolysis.

4.3.7 Effect of 2,4D on chilli seedlings

Protein dysregulation suggest a strong influence of 2,4-D on the spliceosome pathway in chilli plants, potentially affecting their ability to properly process RNA and respond to stress. Alternative splicing is one of the key molecular mechanisms regulated by the spliceosome. Alternative splicing diversifies the mRNA and protein pool, allowing plants to adapt to stress conditions rapidly such as environmental changes and pest infestation (Mandadi et al., 2023). SR protein family and key spliceosomal components, are often upregulated during drought stress, leading to alternative splicing of specific drought-responsive genes (Syed et al., 2012). Similarly, temperature stress in Arabidopsis thaliana modifies the splicing patterns of thermotolerance-related genes (Yang et al., 2022). There is a cross-talk between spliceosome machinery and other stress-responsive pathways (J. Zhang et al., 2020).

Table *6:* List of dysregulated proteins in *Capsicum frutescens* seedlings upon the addition of 2,4D 3mg/L to the MS medium. These proteins are known to participate in the spliceosome (cann03040)

Accession	Description	Fold change	Variation (%)	Score (Mascot)	Score (Sequest HT)	P-Value	Coverage [%]
XP_016543065.1	heat shock cognate 70 kDa protein 2	1.153	0.3	3572	845.95	0.08	47
XP_016542521.1	heat shock cognate 70 kDa protein 2	1.061	21.84	3479	834.82	0.52	47
XP_016538990.1	stromal 70 kDa heat shock-related protein, chloroplastic	0.529	0.35	3517	780.71	0.01	43
XP_016572150.1	heat shock cognate 70 kDa protein 2-like	1.288	1.12	2712	735.73	0.01	47
XP_016577786.1	heat shock cognate 70 kDa protein 1	1.521	10.03	2922	665.94	0.04	37
XP_016547022.1	heat shock cognate 70 kDa protein	0.9	0	2295	634.11		39
XP_016579722.1	heat shock 70 kDa protein-like	2.002	0	774	277.52		14
XP_016561611.1	heterogeneous nuclear ribonucleoprotein 1	1.532	1.3	458	113.34	0.09	23
XP_016554478.1	heterogeneous nuclear ribonucleoprotein 1	1.436	5.15	663	107.42	0.07	30
XP_016548950.1	stromal 70 kDa heat shock-related protein, chloroplastic-like	0.872	2.52	880	240.87	0.03	10
XP_016558591.1	UBP1-associated protein 2C-like	1.277	7.03	315	100.47	0.07	23
XP_016572541.1	THO complex subunit 4D isoform X1	1.391	3.79	325	59.73	0.08	26
XP_016543064.1	THO complex subunit 4A-like	1.456	2.37	298	51.18	0.09	29
XP_016573050.1	LOW QUALITY PROTEIN	1.491	13.04	193	43.43	0.04	11
XP_016577661.1	transcription initiation factor TFIID subunit 15b	1.307	3.2	324	72.4	0.04	16
XP_016577972.1	UBP1-associated protein 2A-like	1.251	1.08	163	32.7	0.02	11
XP_016563017.1	U2 small nuclear ribonucleoprotein A'	1.189	10.01	245	53.96	0.11	18
XP_016545965.1	NHP2-like protein 1	2.376	14.7	84	36.69	0.02	30
XP_016579008.1	heterogeneous nuclear ribonucleoprotein A2 homolog 1-like	1.148	12.75	289	52.25		19
XP_016541641.1	UBP1-associated protein 2C-like	1.461	2.35	229	65.31	0.03	19

XP_016561308.1	glycine-rich RNA-binding protein 3, mitochondrial-like	1.112	3.03	187	38.95	0.30	11
XP_016560604.1	U1 small nuclear ribonucleoprotein 70 kDa	0.871	1.42	108	37.32	0.98	8
XP_016551530.1	sm-like protein LSM3A isoform X1	0.979	6.78	176	46.66	0.49	37
XP_016554349.1	eukaryotic initiation factor 4A-3	1.43	14.75	98	57.48	0.09	16
XP_016578007.1	sm-like protein LSM8	2.247	9.33	547	32.59	0.03	46
XP_016551398.1	probable small nuclear ribonucleoprotein G	1.739	5.44	109	35.53	0.08	30
XP_016575505.1	DEAD-box ATP-dependent RNA helicase 56-like isoform X1	1.14	1.49	139	42.03	0.13	9
XP_016540392.1	splicing factor U2af large subunit A-like isoform X1	1.732	22.63	25	10.23		11
XP_016542947.1	sm-like protein LSM7	1.845	9.76	146	31.31	0.05	34
XP_016553155.1	splicing factor 3B subunit 4	1.253	67.15	66	16.93	0.65	11
XP_016566047.1	pre-mRNA-processing factor 19	1.237	0.43	92	18.47	0.02	4
XP_016542821.1	splicing factor 3A subunit 2	0.958	40.85	36	14.64	0.93	12
XP_016565771.1	small nuclear ribonucleoprotein Sm D2 isoform X1	1.413	9.56	204	22.92	0.08	17
XP_016543603.1	glycine-rich RNA-binding protein 7	1.719	88.29	55	39.87	0.56	11
XP_016560437.1	LOW QUALITY PROTEIN	1.238	1.45	213	27.98	0.03	8
XP_016538051.1	small nuclear ribonucleoprotein-associated protein B'-like	1.001	2.48	184	31.4	0.50	6
XP_016554773.1	serine/arginine-rich splicing factor RSZ22-like	1.23	42.9	225	36.22	0.45	13
XP_016549205.1	serine/arginine-rich splicing factor RSZ22	1.161	7.04	231	49.35	0.11	12
XP_016571856.1	zinc finger CCCH domain-containing protein 49-like	1.193	8.68	47	5.71		5
XP_016555044.1	UBP1-associated protein 2A-like	1.818	25.4	80	6.47		3
XP_016558775.1	small nuclear ribonucleoprotein SmD3b-like	1.405	17.67	79	20.25	0.13	13
XP_016558682.1	nuclear cap-binding protein subunit 2	1.554	12.15	42	15	0.08	11
XP_016556239.1	THO complex subunit 4A	1.181	11.52	20	9.78	0.95	6
XP_016538285.1	LOW QUALITY PROTEIN	1.711	4.86	154	17.48	0.02	10
XP_016572056.1	THO complex subunit 4D	1.989	0	31	5.78		7

XP_016550372.1	DEAD-box ATP-dependent RNA helicase 20	1.235	20.48	29	5.93		4
XP_016562778.1	pre-mRNA-splicing factor SPF27 homolog	1.33	11.77	23	8.51	0.09	8
XP_016554774.1	uncharacterized protein At4g14342-like	1.043	50.86	57	13.3	0.80	13
XP_016560588.1	splicing factor U2af large subunit A isoform X1	1.659	3.8	69	6.19		2
XP_016540447.1	SNW/SKI-interacting protein	0.983	0	42	6.71		3
XP_016539223.1	serine/arginine-rich splicing factor SC35	1.572	7.68	106	18.27		6
XP_016577375.1	small nuclear ribonucleoprotein Sm D1-like	1.016	51.59	33	6.85	0.97	10
XP_016569289.1	serine/arginine-rich splicing factor SC35-like	1.394	0	24	5.2		6
XP_016569341.1	apoptotic chromatin condensation inducer in the nucleus-like isoform X1	1.853	14.18	0	4.75	0.05	2
XP_016543963.1	sm-like protein LSM36B	1.626	14.68	59	12.65	0.06	16
XP_016550072.1	serine/arginine-rich SC35-like splicing factor SCL30A isoform X1	1.223	23.67	21	12.03		4
XP_016572257.1	cell division cycle 5-like protein isoform X1	1.125	0	0	2.68		1
XP_016581010.1	DEAD-box ATP-dependent RNA helicase 46-like	0.987	0	14	2.98		1
XP_016577647.1	U2 small nuclear ribonucleoprotein B"-like	2.316	0	0	2.68		3
XP_016559015.1	glycine-rich RNA-binding protein 4, mitochondrial-like	2.604	21.98	27	13.1	0.03	3
XP_016553865.1	protein BUD31 homolog 2	1.103	0		2.58		8
XP_016569759.1	RNA-binding protein 8A-like	0.897	11.62	19	7.99		4
XP_016558805.1	protein mago nashi homolog	1.612	0	0	2.71		7

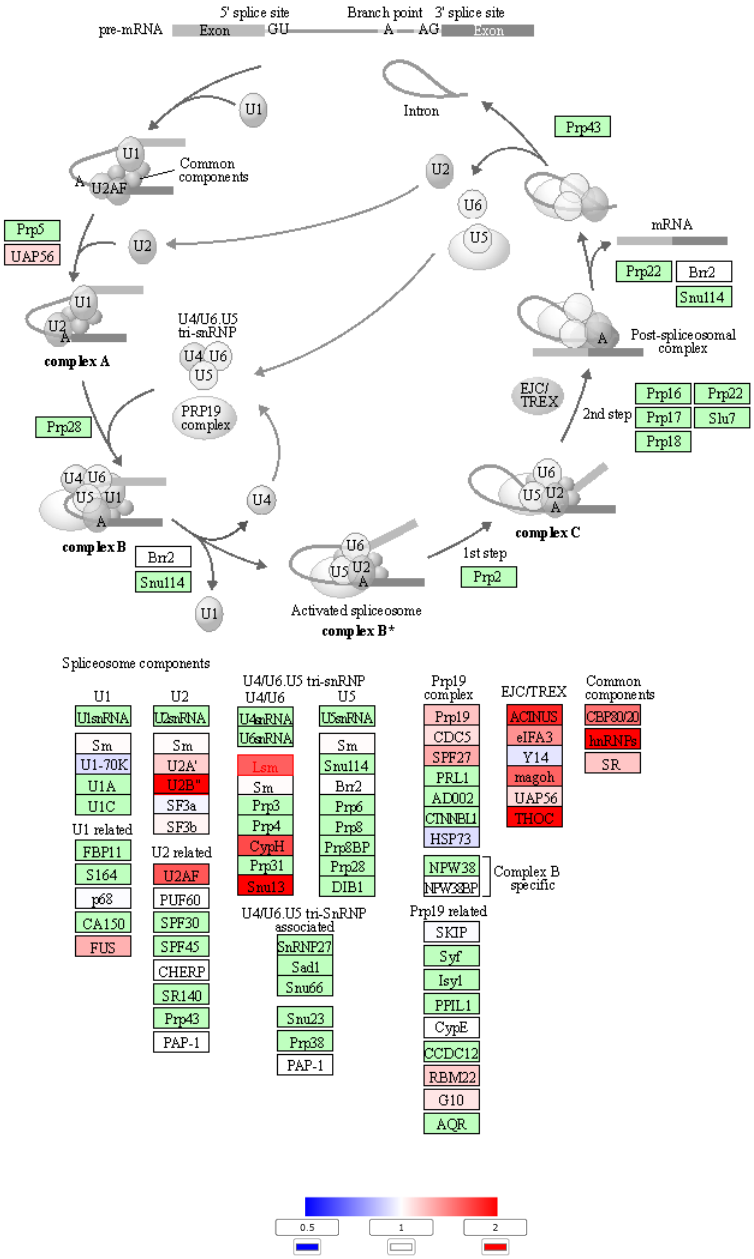

Figure 19: Effect of 2,4D on spliceosome pathway.The colour scale is used to illustrate the extent of dysregulation in relation to the fold change of the identified protein, where a deep red hue signifies the degree of overexpression, and a deep blue hue signifies the degree of downregulation.

4.3.8 Effect of DICAMBA on chilli seedlings

Protein translocation is a critical process in plants that involves the movement of proteins from one cellular compartment to another. This process is necessary for various functions in plants, including photosynthesis, respiration, and signalling (Neumann et al., 2003). DICAMBA is a broad-spectrum herbicide that is widely used to control weeds in various crops. While DICAMBA is primarily known for its herbicidal properties and is also used as a growth regulator in plant tissue culture (Akoyi et al., 2013) there are no reports of the role of DICAMBA on protein export mechanism. Herbicides in general, are known to disrupt multiple pathways such as tubulin

proteins (Gaines et al., 2020), photosynthesis (Gronwald, 1997), fatty acid synthesis (Bolton & Harwood, 1976), carotenoid synthesis (Burns et al., 1971, p. 1). DICAMBA is also reported to stimulate stress-responsive genes (Gleason et al., 2011) This study reports the role of DICAMBA on the protein export mechanism.

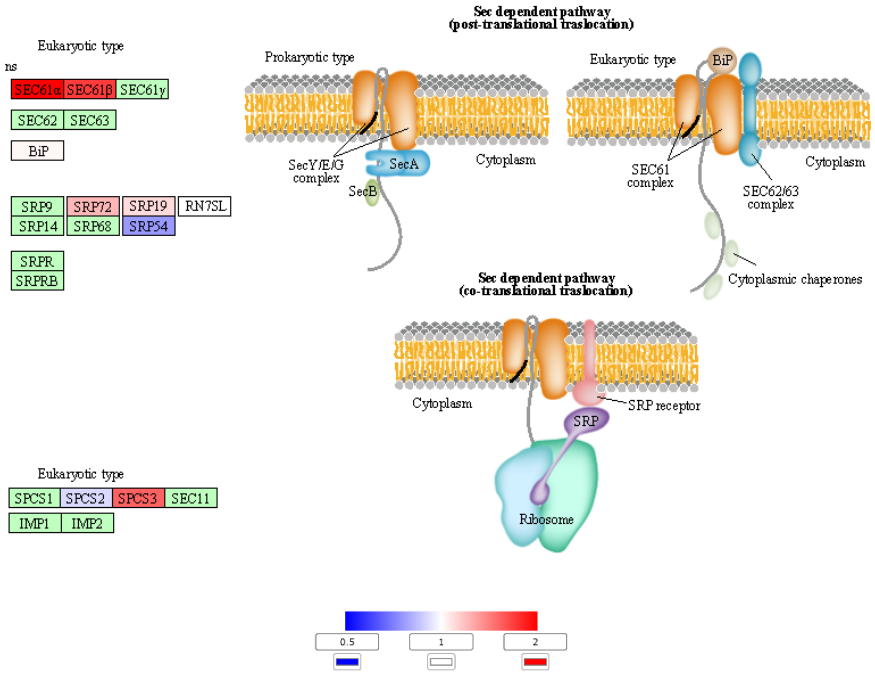

Figure 20: Effect of DICAMBA on protein export pathway. The colour scale is used to illustrate the extent of dysregulation in relation to the fold change of the identified protein, where a deep red hue signifies the degree of overexpression, and a deep blue hue signifies the degree of downregulation.

Table 7: List of dysregulated proteins in *Capsicum frutescens* seedlings upon the addition of DICAMBA 3mg/mL to the MS medium. These proteins are known to participate in the Protein export mechanism (cann03060).

Accession	Description	Fold change	Percentage variation	P-Value	Score (Mascot)	Score (Sequest HT)	Coverage [%]
XP_016564341.1	luminal-binding protein 5	1.035	1.5	0.119	2645	724.88	46
XP_016565558.1	luminal-binding protein	1.035	6.65	0.413	2299	653.09	37
XP_016545924.1	signal recognition particle subunit SRP72	1.277	15.44		103	15.88	6
XP_016542994.1	signal recognition particle 54 kDa protein, chloroplastic	0.639	5.5	0.079	120	26.76	7
XP_016559596.1	protein transport protein Sec61 subunit alpha-like	2.065	8.71	0.033	130	22.36	4
XP_016565746.1	signal recognition particle 19 kDa protein	1.142	23.58		16	15.97	10
XP_016575300.1	protein transport protein Sec61 subunit beta	1.752	8.66	0.180	26	19.63	18
XP_016573085.1	protein transport protein Sec61 subunit beta-like	1.763	12.09		89	6.63	13
XP_016556512.1	probable signal peptidase complex subunit 2	0.856	0		25	3.75	6
XP_016575635.1	cell division protein FtsY homolog, chloroplastic	0.714	1.4	0.046	51	14.71	3
XP_016538552.1	signal peptidase complex subunit 3B-like	1.616	3.04	0.033	70	16.07	5

XP_016538378.1	sec-independent protein translocase protein TATA, chloroplastic	1.102	3.92	0.492	19	8.46	5
XP_016562874.1	signal recognition particle 54 kDa protein 1	0.599	0		0	2.05	2

4.3.9 Effect of PICLORAM on chilli seedlings

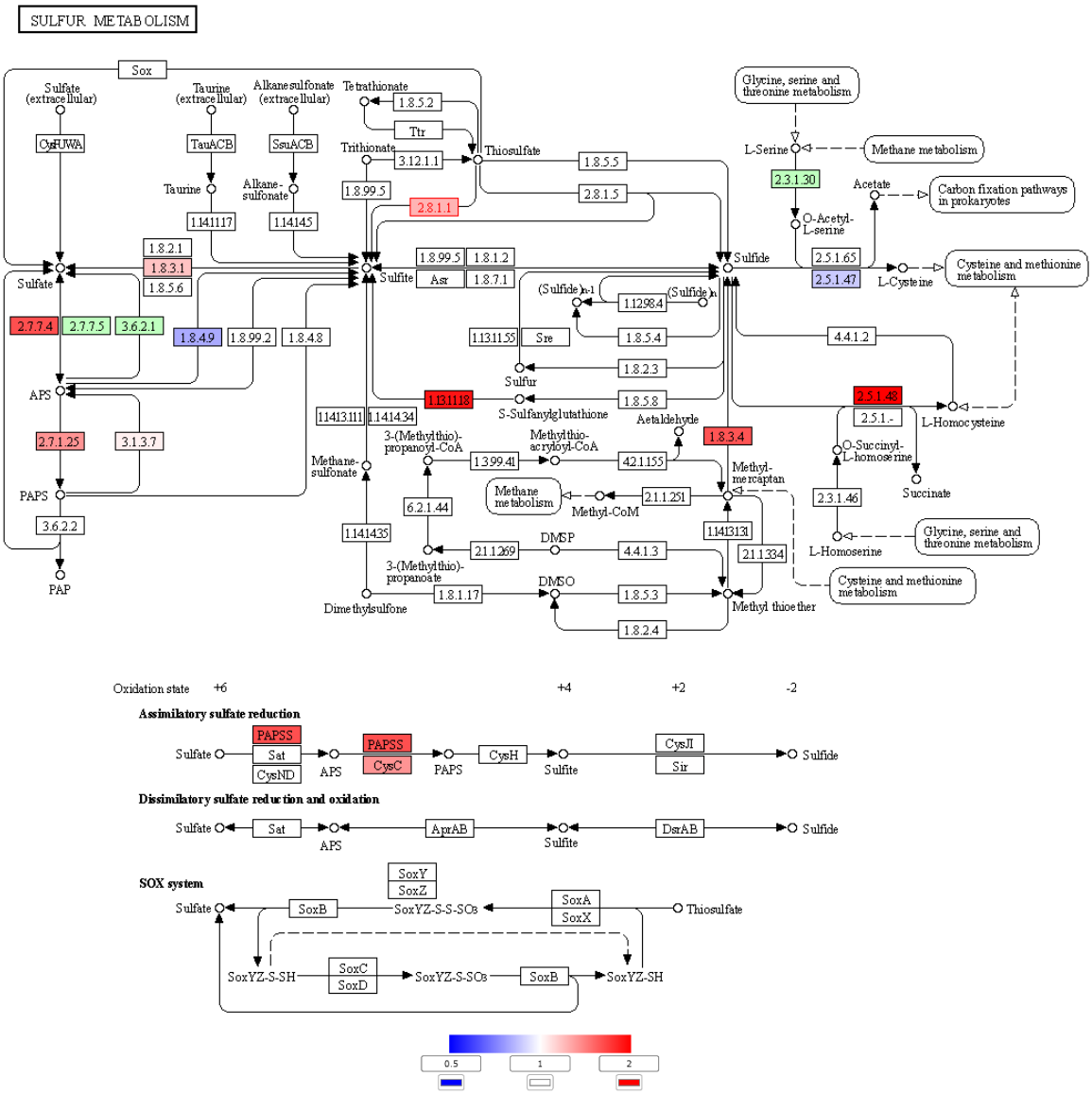

Figure 21: Effect of PICLORAM on sulphur metabolism pathway. The colour scale is used to illustrate the extent of dysregulation in relation to the fold change of the identified protein, where a deep red hue signifies the degree of overexpression, and a deep blue hue signifies the degree of downregulation.

PICLORAM is a broad-spectrum herbicide also a synthetic auxin, that is commonly used to control weeds in a variety of agricultural and plant tissue cultures (Ahmed et al., 2011). While its primary mode of action is to inhibit plant growth and development, there is limited research on the direct effects of PICLORAM on plant nutrient uptake and metabolism (Dumancas, 2014), and there is limited resource on uptake, transport and metabolism of PICLORAM itself (Kathare et al., 2020)

Table 8: List of dysregulated proteins in *Capsicum frutescens* seedlings upon the addition of PICLORAM 3mg/mL to the MS medium. These proteins are known to participate in the Sulfur metabolism pathway (cann00920).

Accession	Description	Fold change	Percentage variation	P-Value	Score (Mascot)	Score (Sequest HT)	Coverage [%]
XP_016565845.1	cysteine synthase	0.926	1.67	0.0722	1041	282.08	47
XP_016554536.1	sulfite reductase 1 [ferredoxin], chloroplastic isoform X1	1.002	10.22	0.9808	446	116.75	16
XP_016581537.1	thiosulfate/3-mercapto pyruvate sulfurtransferase 1, mitochondrial-like	1.294	3.97	0.0280	522	100.2	23
XP_016556137.1	cysteine synthase, chloroplastic/chromoplastic	0.463	7.03	0.1994	498	99.3	14
XP_016538470.1	cysteine synthase-like isoform X1	1.586	16.01	0.0669	137	59.27	29
XP_016566179.1	selenium-binding protein 1-like	1.67	1.44	0.0264	271	49.65	11
XP_016538083.1	bifunctional L-3-cyanoalanine synthase/cysteine synthase 2, mitochondrial isoform X1	0.793	0.11	0.0249	417	89.8	11
XP_016570661.1	ATP sulfurylase 1, chloroplastic-like	0.752	0.45	0.0267	129	66.65	14
XP_016552000.1	SAL1 phosphatase-like	1.058	13.66	0.4683	188	51.09	8
XP_016570659.1	ATP sulfurylase 1, chloroplastic-like	1.689	8.1	0.0294	104	31.05	10
XP_016581053.1	persulfide dioxygenase ETHE1 homolog, mitochondrial isoform X1	1.922	20.44	0.0512	14	14.19	12
XP_016558999.1	cystathionine gamma-synthase 1, chloroplastic-like	2.821	21.72		54	7.4	2
XP_016560132.1	5'-adenylylsulfate reductase 1, chloroplastic	0.665	0.91			4.96	3
XP_016561725.1	sulfite oxidase	1.237	19.84		0	3.97	2
XP_016548801.1	adenylyl-sulfate kinase 3-like	1.419	0		20	2.03	4

4.3.10 Effect of TIBA on chilli seedlings

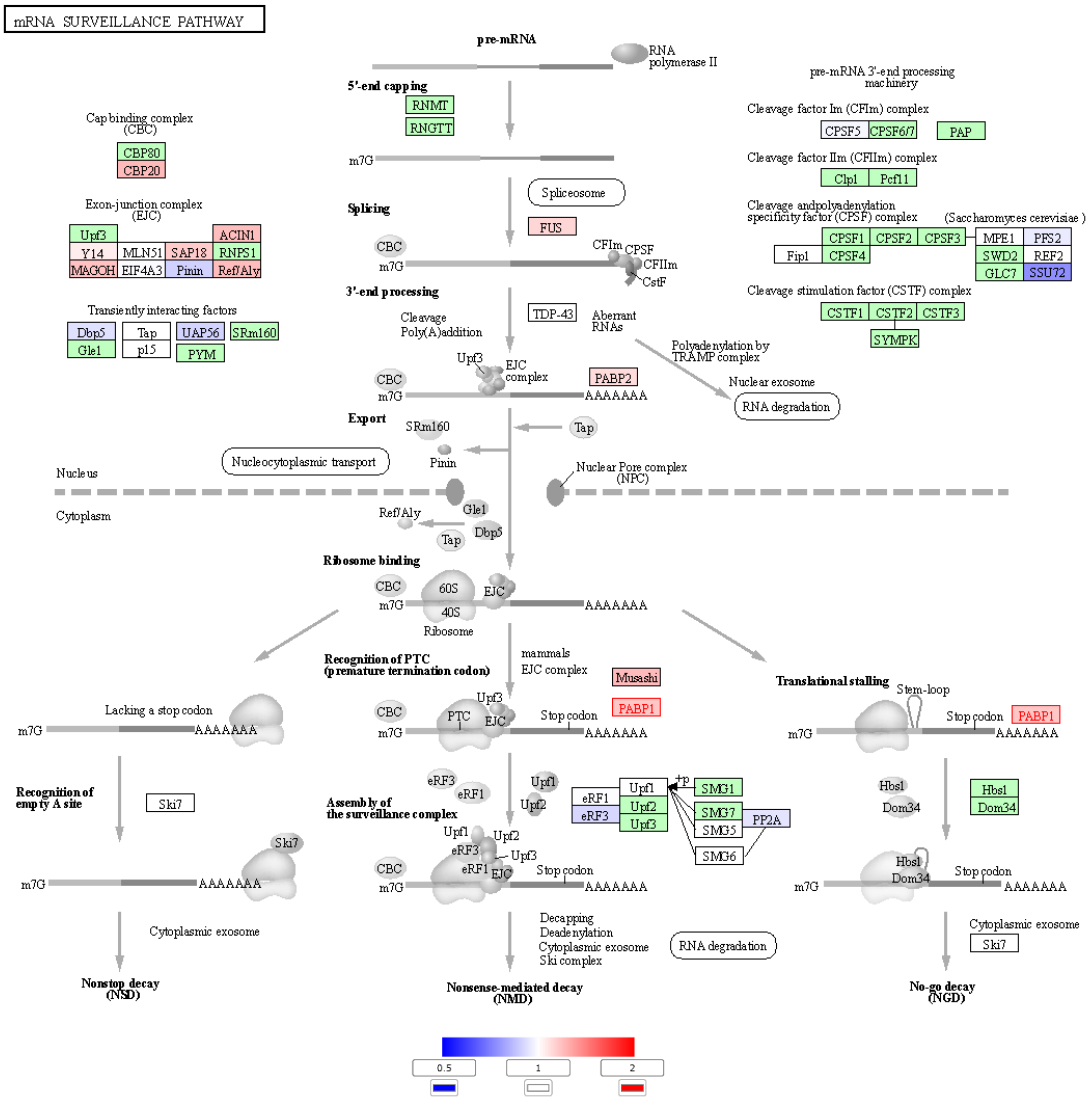

Figure 22: Effect of TIBA on mRNA surveillance pathway. The colour scale is used to illustrate the extent of dysregulation in relation to the fold change of the identified protein, where a deep red hue signifies the degree of overexpression, and a deep blue hue signifies the degree of downregulation.

The mRNA splicing machinery called the spliceosome, removes introns from pre-mRNA and connects exons to form mature mRNA that can be translated into proteins (Punzo et al., 2020). In plants, alternative splicing plays a critical role in response to abiotic and biotic stresses. Alternative splicing can produce different protein isoforms from a single gene, and this process can be regulated by stress signals. Several stress-responsive genes have been identified in plants that undergo alternative splicing in response to environmental stress, including genes involved in plant defence and stress tolerance (Gu et al., 2020).

Table 9: List of dysregulated proteins in *Capsicum frutescens* seedlings upon the addition of TIBA 3mg/mL to the MS medium. These proteins are known to participate in mRNA surveillance pathway (cann03015)

Accession	Description	Fold change	Fold change Variability [%]:	Abundance Ratio (P-Value)	Score (Mascot)	Score (Sequest HT)	Coverage [%]
XP_016539541.1	polyadenylate-binding protein 8-like isoform X1	1.166	3.19	0.107	1184	206.06	24
XP_016550576.1	polyadenylate-binding protein 2-like isoform X1	1.444	16.59	0.087	978	179.05	17
XP_016550760.1	eukaryotic peptide chain release factor subunit 1-3-like	0.992	9.39	0.877	298	70.13	16
XP_016572541.1	THO complex subunit 4D isoform X1	1.433	9.15	0.070	325	59.73	26
XP_016543064.1	THO complex subunit 4A-like	1.645	0.62	0.055	298	51.18	29
XP_016577661.1	transcription initiation factor TFIID subunit 15b	1.323	18.76	0.117	324	72.4	16
XP_016566062.1	heterogeneous nuclear ribonucleoprotein 1	1.166	3.25	0.047	136	57.07	13
XP_016570622.1	heterogeneous nuclear ribonucleoprotein 1-like	1.575	2.81	0.016	168	73.71	10
XP_016555910.1	eukaryotic peptide chain release factor GTP-binding subunit ERF3A-like isoform X1	0.84	0.26	0.055	96	42	17
XP_016554349.1	eukaryotic initiation factor 4A-3	0.986	12.72	0.667	98	57.48	16
XP_016575505.1	DEAD-box ATP-dependent RNA helicase 56-like isoform X1	0.826	4.7	0.258	139	42.03	9
XP_016553057.1	histone deacetylase complex subunit SAP18	1.418	5.23	0.027	69	43.4	27
XP_016555914.1	serine/threonine-protein phosphatase 2A 65 kDa regulatory subunit A beta isoform-like	0.766	5.87	0.096	77	13.25	7
XP_016545279.1	heterogeneous nuclear ribonucleoprotein 1 isoform X1	1.152	6.69		84	14.29	6
XP_016543143.1	DEAD-box ATP-dependent RNA helicase 38	0.879	0.91		55	17.81	13
XP_016564658.1	pre-mRNA cleavage factor Im 25 kDa subunit 2	0.965	32.9	0.583	21	5.23	15

XP_016558682.1	nuclear cap-binding protein subunit 2	1.542	2.35	0.023	42	15	11
XP_016556239.1	THO complex subunit 4A	1.217	3.25	0.166	20	9.78	6
XP_016572056.1	THO complex subunit 4D	1.529	0		31	5.78	7
XP_016551213.1	serine/threonine protein phosphatase 2A 55 kDa regulatory subunit B beta isoform-like	0.771	4.84	0.393	0	10.53	4
XP_016561089.1	RNA-binding protein Musashi homolog 2 isoform X1	1.257	12.9		32	11.15	5
XP_016580559.1	heterogeneous nuclear ribonucleoprotein 1-like				24	3.76	3
XP_016569341.1	apoptotic chromatin condensation inducer in the nucleus-like isoform X1	1.513	9.07	0.123	0	4.75	2
XP_016564033.1	RNA polymerase II subunit A C-terminal domain phosphatase SSU72 isoform X1	0.557	4.65		36	6.38	6
XP_016537887.1	flowering time control protein FY	0.92	0		30	2.71	1
XP_016543149.1	serine/threonine-protein phosphatase PP2A-5 catalytic subunit	0.892	15.76		0	6.41	4
XP_016565118.1	heterogeneous nuclear ribonucleoprotein 1-like	1.531	0		0	2.82	3
XP_016539149.1	pinin	0.818	11.19		33	3.76	2
XP_016569759.1	RNA-binding protein 8A-like	1.143	0.45		19	7.99	4
XP_016565010.1	polyadenylate-binding protein 1-like	1.285	1.07		0	2.29	3
XP_016573749.1	serine/threonine protein phosphatase 2A regulatory subunit B"beta-like	0.895	0			0	2
XP_016558805.1	protein mago nashi homolog	1.485	0		0	2.71	7

4.4 Conclusion:

The proteomic study on *Capsicum frutescens* (Bird's eye chilli) seedlings under abiotic stress conditions instigated by different plant growth regulators such as BAP, IAA, ABA, GA3, and Ethylene as well as weedicides like 2,4-D, DICAMBA, TIBA, and PICLORAM on protein expression. Notably, each of the plant growth regulators exhibited a unique footprint on protein expression. BAP significantly dysregulated the photosynthetic pathway, affecting various proteins associated with photosystem I and II, the cytochrome b6/f complex, and the electron transport system. IAA, influenced the light harvesting complex of the photosynthetic pathway, dysregulating multiple proteins of LHC. ABA, on the folate one-carbon pool pathway, is a critical pathway involved in various cellular processes including DNA repair and synthesis. GA3 was found to impact the valine leucine degradation pathway, which is crucial for amino acid metabolism. The finding not only enhances our understanding of GA3's role in plant physiology but also provides critical insights that could guide future research in improving plant resilience to stress conditions. Ethylene's influence was notable in the glycolysis pathway, similarly, 2,4-D has a strong influence on the spliceosome pathway, affecting the plant's ability to process RNA and respond to stress. DICAMBA affected the protein export pathway TIBA and PICLORAM affected the mRNA surveillance pathway and Sulfur metabolism pathway. These effects are the first to be documented.

CHAPTER 5

Morphological, Histological and Biochemical Studies of *Capsicum frutescens* (Birds Eye Chilli) Seedlings upon Biotic Stress Induced by *Polyphagotarsonemus latus* (Broad Mite)

5 Morphological, Histological and biochemical studies of *Capsicum frutescens* (Birds eye chilli) seedlings upon biotic stress induced by *Polyphagotarsonemus latus* (Broad mite)

5.1 Introduction

Morphological changes are often the first visible signs of plant stress and can serve as early indicators for the presence of broad mites. Previous studies have reported symptoms such as leaf curling, discolouration, and dieback in various crops due to mites (Gerson, 1992). This chapter extends these observations to chilli plants, providing a detailed account of the morphological

alterations, including the appearance of new shoots following the application of effective miticides. The use of microscopic techniques, both light and scanning electron microscopy, offers a more nuanced understanding of the mite's external anatomy and life stages. These observations can be crucial for the identification and development of targeted control measures. The chapter presents microscopic images of various life stages of broad mites, including eggs, nymphs, and adults. Molecular techniques like mitochondrial COI sequencing are increasingly being used for the accurate identification of mites. This chapter employs these techniques to confirm the identity of the broad mites infesting the chilli plants.

Understanding the efficacy of various pesticides is crucial for developing integrated pest management strategies. Previous research has shown varying levels of effectiveness among different pesticides in controlling mite populations (A. Kumar et al., 2018). This chapter evaluates the efficacy of several commercially available pesticides, providing valuable data for future pest management.

5.2 Materials and methods

5.2.1 Sample processing for microscopy

Light microscopy images were taken using an Olympus BX41 microscope fitted with a DP73 CCD camera connected to the Olympus CellSens standard software. Samples were dehydrated using absolute alcohol and dried in a desiccator under vacuum (-400 mmHg) before scanning electron microscopy. SEM images were taken using Hitachi TM3030 tabletop SEM under 15kV mode. Gold sputtering was done using the SPI-ModuleTM sputter coater. Other Photographs were taken using Fujifilm X-T100 24.2 MP Mirrorless Camera attached to XC 15-45 mm Lens.

5.2.2 Pathogenicity test:

To conform the Koch's postulates for the pathogenicity, healthy plants germinated from *in vitro* origin were grown in aseptic conditions and broad mites were inoculated on to healthy plants as described in 5.2.4. plants and pathogens were monitored for increment of number of mites, appearance of disease symptoms. This exercise is repeated to confirm the reappearance of disease symptoms and growth in number of pathogens when re-isolated and re-inoculated on to healthy plants.

5.2.3 Molecular identification : DNA Extraction and polymerase chain reaction

The sample was initially ground using liquid nitrogen and DNA was isolated using a Quiagen kit (cat no: 69104). Quality was evaluated using 0.1% agarose gel to conform single band high molecular weight DNA. The mitochondrial COX gene is amplified using BDT v3. 1 Cycle sequencing kit using the BioRad CFX96 PCR machine. Cytochrome c oxidase subunit I (COI) gene was targeted using universal forward primer LCO -1490 (5'-GGTCAACAAATCATAAAGATATTGG-3') and reverse primer HCO - 2198 (5'-TAAACTTCAGGGTGACCAAAAAATCA-3'). PCR conditions were set according to (Marullo et al., 2020). PCR amplicons were sequenced using Sanger sequencing technology at Barcode Biosciences, Bengaluru. Consensus sequences are generated using CodonCode Aligner software. Sequences are submitted to the DDBJ (DNA Data Bank of Japan) repository (Accession number: LC605048). Samples were maintained in the laboratory, at -80^{0}C (accession number: LAB013).

5.2.4 Effective miticides against broad mite

30 days old Seedlings germinated on agar medium were planted in a autoclaved potting mix containing 1:1:1 ratio of soil: sand: vermicompost, The plants were grown under controlled environmental conditions, which included a temperature of 27°C, a humidity range of 50-70% and a light-dark cycle of 16:8 hours. The light was provided by cool white fluorescent tubes, emitting approximately 270 μmol photons per square meter per second. After additional growth of 30 days on the potting mix, plants were segregated further, uninfected plants were inoculated with leaves containing live, motile mites. An infected leaf is attached to a healthy plant with the help of a cello tape. Healthy plants were grown separately in different room with a same light, temperature and humidity conditions to avoid cross contamination of mite infection. 25 days after mite inoculation, various pesticides were tested at doses prescribed by the manufacturers. The following pesticides were used in this study: EM-1® (Emamectin Benzoate 5% SG), Dhanuka Agritech Limited, dosage: 80g/acre; Omite® (Propargite 57% EC), Dhanuka Agritech Limited, dosage: 600ml/acre; Mit – 505® (Ethion 50 % EC) SWAL Corporation Limited, dosage : 500ml/acre; Actara® (Thiamethoxam 25% WG), Syngenta India Limited, dosage: 24g/acre; Harrier® (Acetamiprid 20% SP), ADAMA India Private Limited, dosage: 40g/acre. Deionized water was used as a control. Experiments are carried out in triplicates.

5.2.5 Preparation of Plant materials for biochemical analysis:

Plants for biochemical analysis were harvested. Leaf, stem and roots were separated and finely ground into powder using mortar and pestle and liquid nitrogen. The ground powder was stored at -80^0C until further analysis. Subsequent biochemical analysis was carried out using this sample.

5.2.6 Malondialdehyde assay (MDA)

To confirm the status of stress, and to determine the statistical point of a particular concentration and a particular day at which the sample is selected for further investigation, MDA analysis was carried out using Himedia EZAssayTM TBARS Estimation Kit for Lipid Peroxidation, Product Code: CCK023. Procedure was followed as per the manufacturer's instructions, 10mg of fresh samples were used to carry out the analysis. 60 days old plants (30 days old germinated seedlings from agar medium, transferred to potting mix and allowed to grow 30 more days in potting mix) are infected with broad mites as described in section 5.2.4, uninfected plants were considered as control. MDA content of roots, stem and leaves of infected and uninfected plants were monitored.

5.2.7 Selection of seedlings for biochemical, histological studies:

On the 80th day, after infection of broad mites, leaf and stem samples were chosen for experiments. This selection was based on, an analysis of MDA content as described in section 5.2.6 and 5.3.7 which aimed to assess the biotic stress levels of the seedlings. Which indicated the significant increment of MDS levels in leaves and stem.

5.2.8 Analysis of total carbohydrate content (TCC) by Anthrone method:

Methods are followed as described in section 3.2.6

5.2.9 Estimation of Total soluble sugars (TSS) by Anthrone method:

Methods are followed as described in section 3.2.7

5.2.10 Total lipid content (TL) by gravimetry Bligh and Dyer method:

Methods are followed as described in section 3.2.8

5.2.11 Total phenolic content (TPC) by Folin-Ciocalteu method (FC method):

Methods are followed as described in section 3.2.9

5.2.12 Analysis of Antioxidant activity using the DPPH method:

Methods are followed as described in section 3.2.10

5.2.13 Statistics for biochemical analysis:

Methods are followed as described in section 3.2.11

5.2.14 Histology

Methods are followed as described in section 3.2.12

5.3 Results and discussion

5.3.1 Morphological observations of broad mite infection in chilli plants

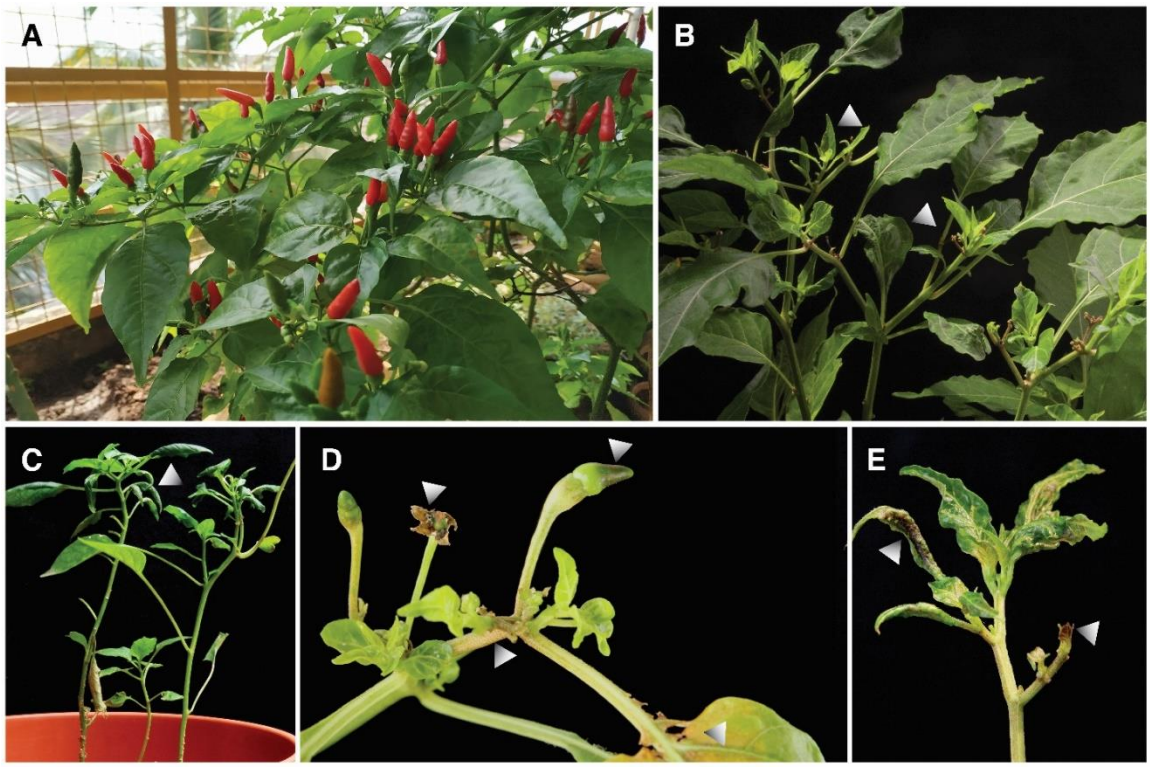

Figure 23 : (A-E): Morphological observations of broad mite infection in chilli plants.

A) Healthy *Capsicum frutescens* plant bearing highly pungent erect fruits. Green unripe fruits turn red when matured.
B) New shoots are emerging following the application of effective miticides.
C) Curled leaves, rigid apical meristem and young foliage of infested chilli plant.

D) Aborted bloom and downward curled leaf showing dieback symptoms in chilli pepper plant infested by the broad mite.
E) The leaves exhibit brownish blotches or bronze-like discolouration. The presence of broad mites can cause the leaf surface to develop a wrinkled or puckered appearance.

5.3.2 Light microscopic observations

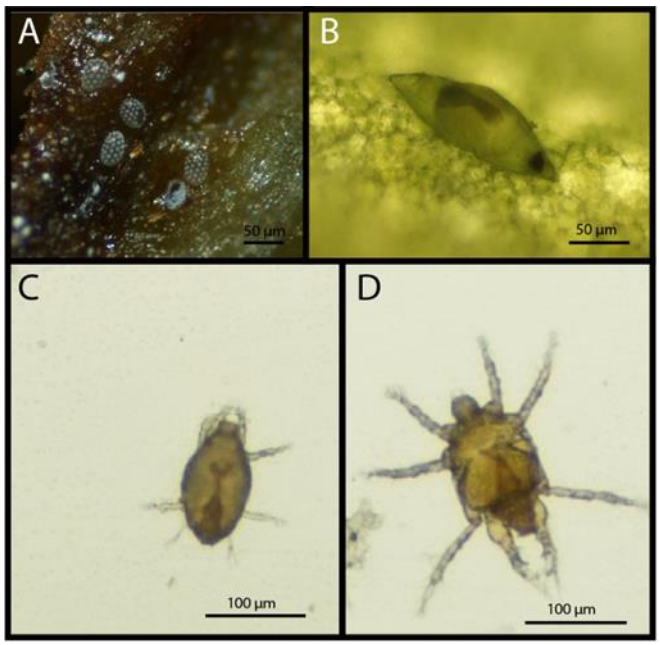

Figure 24: Broad mites under the light microscope A: eggs, B: Nymphal stage, C: Adult female D: Adult male.

5.3.3 Scanning electron microscopic observations

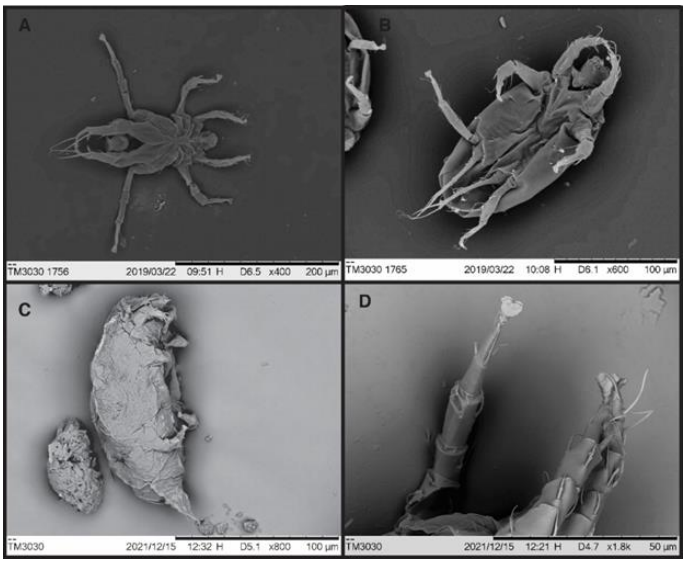

Figure 25: Broad mites observed under scanning electron microscope A: Adult male, B: Adult feale C: Nymphal stage, D: heart-shaped claw on the leg of the adult male

5.3.4 Molecular identification

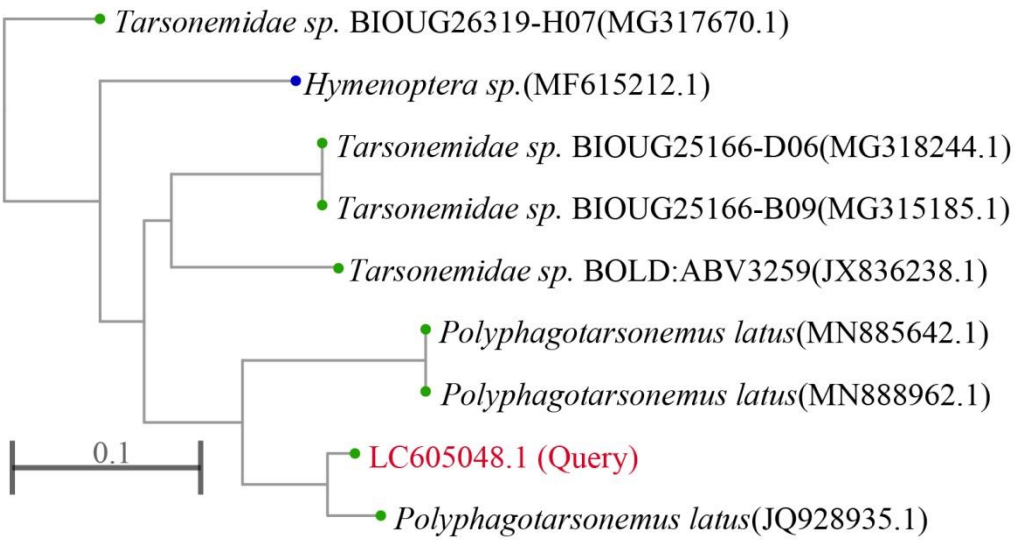

Figure 26: The Fast-Minimum Evolution model tree of mitochondrial COI sequences of mites, Query sequences showed close similarity to *Polyphagotarsonemus latus*.

5.3.5 Pathogenicity test

The presence of broad mites and the appearance of symptoms of infestation confirmed pathogenicity. After 5 +/- 2 days, initial symptoms appeared, i.e., stunted apical meristem. After 9 days subtending leaves started curling downwards, and meristem growth was halted and turned to the darker color. After 25 days subsequent healthy leaves showed curly leaf symptoms, and meristem appeared brownish-green in colour. Growth was halted.

5.3.6 Efficacy of miticides to control broad mite infestation on chilli plant

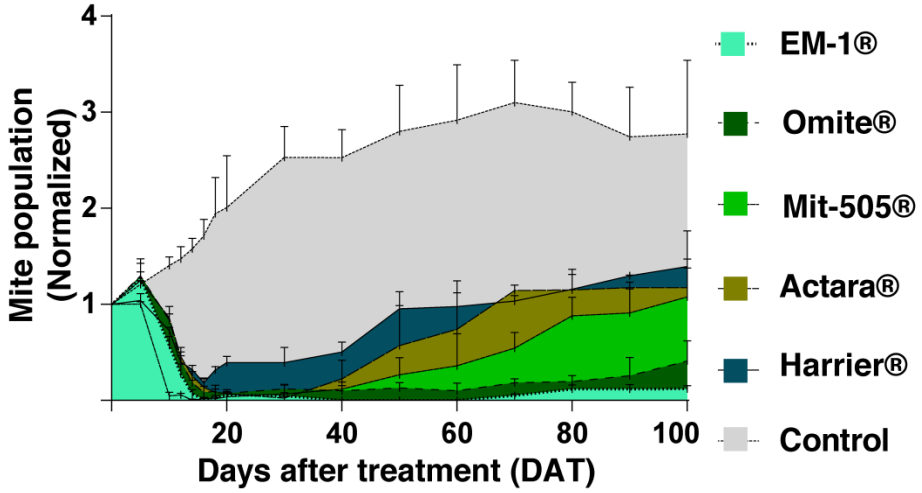

Figure 27: Efficacy of various pesticides to control broad mite infestation on chilli plant. EM-1® (Emamectin Benzoate 5% SG), Dhanuka Agritech Limited, dosage: 80g/acre; Omite® (Propargite 57% EC), Dhanuka Agritech Limited, dosage: 600ml/acre; Mit – 505® (Ethion 50 % EC) SWAL Corporation Limited, dosage : 500ml/acre; Actara® (Thiamethoxam 25% WG), Syngenta India Limited, dosage: 24g/acre; Harrier®

(Acetamiprid 20% SP), ADAMA India Private Limited, dosage: 40g/acre. (N=3), DAT: Days After Treatment

5.3.7 Variation of the Malondialdehyde content of biotic stress caused by broad mite infestation in chilli plant

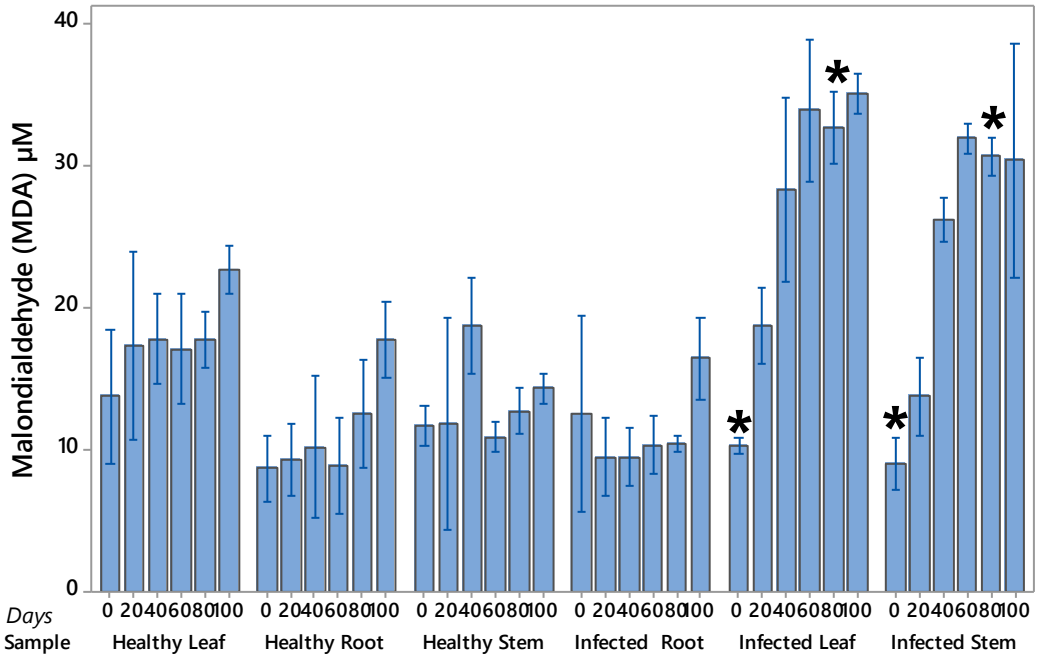

Figure 28: Variation of the Malondialdehyde content of biotic stress caused by broad mite infestation in chilli plant. Data shown are means ± standard deviations of the means (SD). Groups were compared using the one-way ANOVA. * denotes $p < 0.001$.

MDA levels in infected roots and healthy stems and healthy roots did not show significant alterations. This suggests that roots are less susceptible to oxidative stress or that the mite infestation primarily targets aerial parts of the plant. The increase in MDA levels may be indicative of the activation of various stress-responsive pathways. Such as antioxidant defence mechanisms like catalase and superoxide dismutase (SOD) activities, aimed at neutralizing oxidative damage (Sajedi et al., 2011).

5.3.8 Histological observations

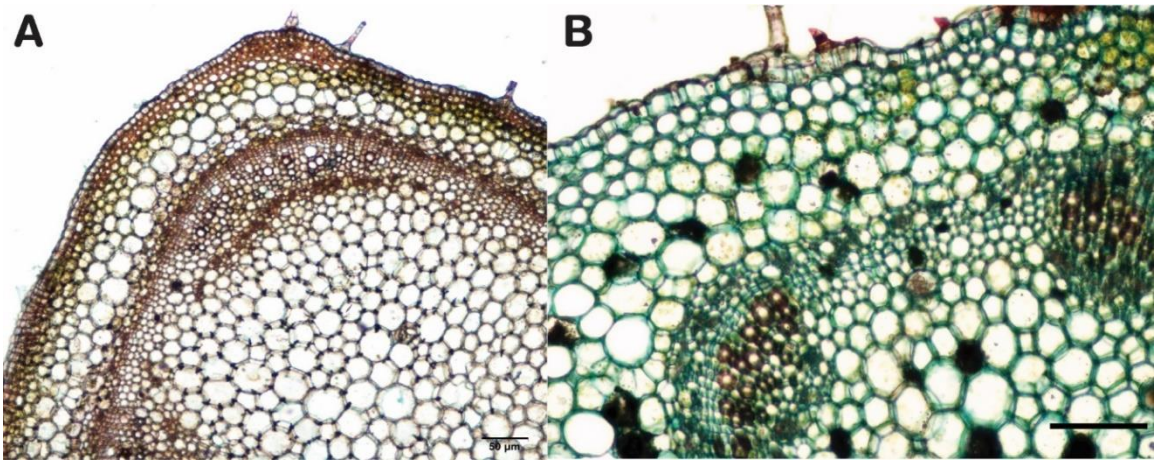

Figure 29: Biotic stress caused by broad mite infestation in chilli plant: Histological observations (stem) (scale: 50µm) A: Healthy stem: Epidermis, hypodermis, xylem, phloem and pith are observed. B: Infected stem: Epidermis, hypodermis, xylem, and phloem are small in size compared to healthy stem. Secretory canals were observed, and pith to epidermis distance was less.

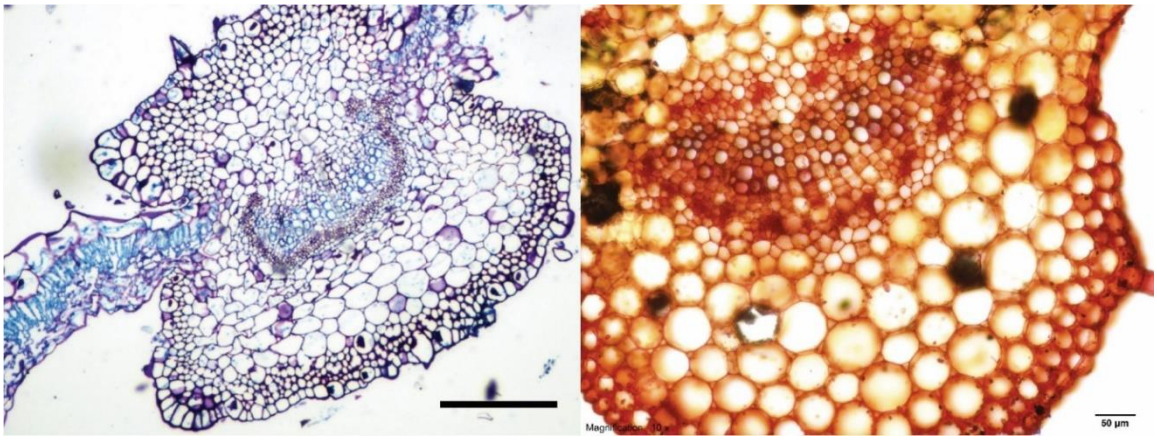

Figure 30: Biotic stress caused by broad mite infestation in chilli plant: Histological observations (leaf) (scale: 50µm) A: Healthy leaves: Vascular bundle was clear, large, xylem and phloem tissues were visible, cells of upper epidermis were large. Mesophyll consisted tightly packed palisade parenchyma and loosely arranged spongy parenchyma, leaves were large and many compared to control. B: Infected leaves: The vascular bundle was large, distribution of the xylem was reduced compared to healthy leaves. xylem and phloem tissues were visible, and cells of the upper epidermis were large and consisted waxy layer. Secretory canals were more observed in parenchymatous cells but were not observed in healthy leaves.

5.3.9 Biochemical investigation of biotic stress caused by broad mite infestation in chilli plant

5.3.9.1 Soluble sugar content

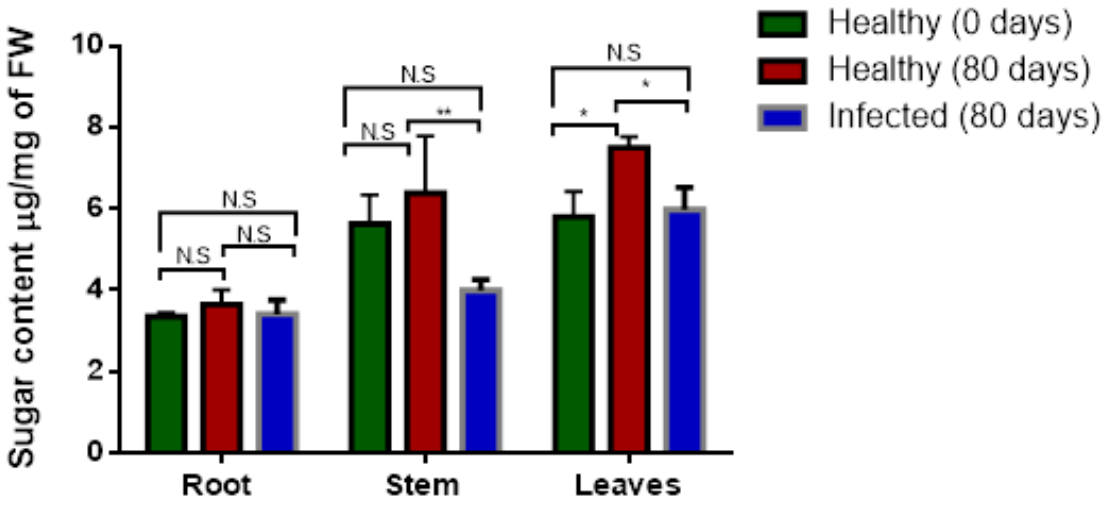

Figure 31: Variation of soluble sugar content upon biotic stress caused by broad mite infestation on chilli plant. Data shown are means ± standard deviations of the means (SD). $P \leq 0.01$ (overall ANOVA). Individual groups were compared using the one-way ANOVA. N.S: not significant, * $p < 0.05$, ** $p < 0.01$, *** $p < 0.001$, N=3.

Plants encounter a wide range of pathogens and pests, leading to various changes in their metabolism. Free sugars, including glucose, fructose, and sucrose, play a critical role in plant growth and development and plant-pathogen interaction (Y.-H. Liu et al., 2022). Biotrophic pathogens rely on the host plant's resources to survive and reproduce. They often induce an increase in free sugar content in infected tissues, which can be beneficial for their growth and development. Necrotrophic pathogens, cause cell death and tissue degradation, leading to a decrease in free sugar content (Morkunas & Ratajczak, 2014). The availability of carbon and energy sources can also affect free sugar content upon pathogen infection. As a result of dysregulation of enzymes that participate in photosynthesis and energy metabolism (P. Li et al., 2019). The observed alteration can indicate the metabolic shifts initiated by the pathogenic invasion. Infestation can cause reallocation of metabolic resources towards defensive pathways, thereby hampering regular physiological functions such as growth and cellular maintenance (Rojas et al., 2014). This could account for the reduced sugar availability in infected tissues, considering that sugars not only serve as energy substrates but also as signalling molecules in plant stress responses (M. Wang et al., 2020).

5.3.9.2 Total carbohydrate content

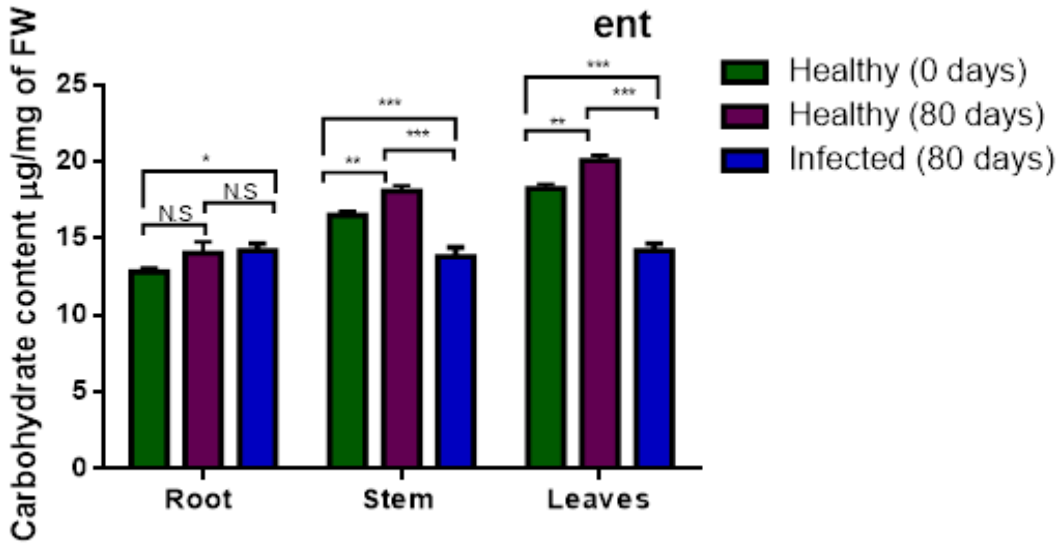

Figure 32: Variation of total carbohydrate content upon biotic stress caused by broad mite infestation on chilli plant. Data shown are means ± standard deviations of the means (SD). N.S: not significant,* $p < 0.05$, ** $p < 0.01$, *** $p < 0.001$, N=3.

Carbohydrate distribution and accumulation are tightly regulated processes in plants, influenced by both developmental cues and environmental stressors (M. Wang et al., 2020). Pathogen attacks involve the activation of various defence-related genes, including those involved in the synthesis and modification of polysaccharides in the cell wall. During the infection of wheat spikes by *F. graminearum*, the fungus secretes pectin lyases, cellulases, and xylanases that degrade the components of the plant cell wall to facilitate infection (S. Wu et al., 2014). Plant carbon energy metabolism can also redirect carbon resources to support defence responses to produce defence-related proteins and phytohormones via the activation of calcium-dependent protein kinases (CDPKs) (Alves et al., 2021). These responses require significant amounts of carbon resources, often resulting in a decrease in the plant's growth and development (Yip Delormel & Boudsocq, 2019). The increase in carbohydrate content in healthy plants is likely reflective of standard physiological processes that support growth and development. The root carbohydrate content was unaffected in infested plants, which could signify a compensatory mechanism to maintain root function and nutrient absorption, or it may indicate that the root system is less sensitive to the broad mite infestation.

5.3.9.3 DPPH free radicle assay

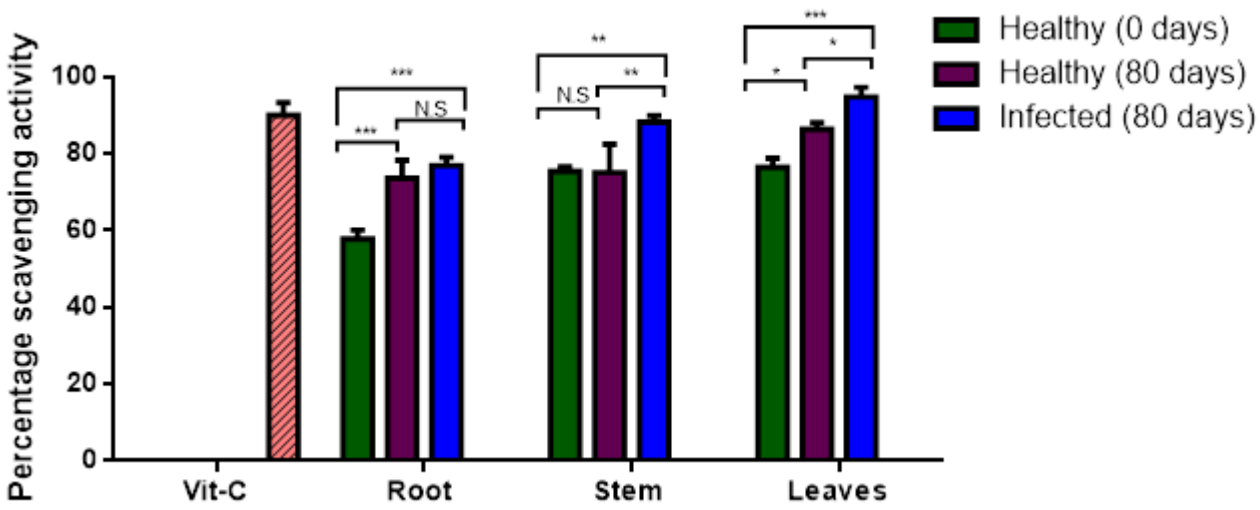

Figure 33: Variation of free radicle scavenging capacity (DPPH method) of chilli plant upon biotic stress caused by broad mite infestation on chilli plant. Data shown are means ± standard deviations of the means (SD). N.S: not significant, * $p < 0.05$, ** $p < 0.01$, *** $p < 0.001$, N=3.

Plants under stress conditions exhibit increased production of secondary metabolites, including phenolic compounds, as a form of defence (Ainsworth & Gillespie, 2007). Likewise, the increment in scavenging capacity in healthy plants as they age could be linked to the natural physiological maturation process, which often involves the accumulation of secondary metabolites (Jan et al., 2021). The roots did not display a drastic change in scavenging ability, which suggests that root cells have different antioxidant mechanisms or are less responsive to broad mite infestation (Pandey et al., 2017a). Examples such as the infection of tomato plants with the bacterial pathogen *Pseudomonas syringae* leads alteration of hydroxyl-free radicles (D.-D. Cheng et al., 2016). Similarly, in Arabidopsis, the pathogenic fungus *Botrytis cinerea* leads to altered levels of superoxide dismutase, an important antioxidant enzyme (Zhu et al., 2021). Pathogen attack can also affect the expression of genes involved in the biosynthesis and regulation of free radical scavenging molecules. The infection of cabbage plants with the bacterial pathogen *Xanthomonas campestris* leads to an upregulation of genes involved in the biosynthesis of flavonoids, a class of antioxidants (Sun et al., 2022). Similarly, in the flax plant, biosynthesis of carotenoids, another class of free radicle scavengers, influences the plant's ability to resist *Fusarium culmorum* and *Fusarium oxysporum* infection (Boba et al., 2011).

5.3.9.4 Total phenolic content

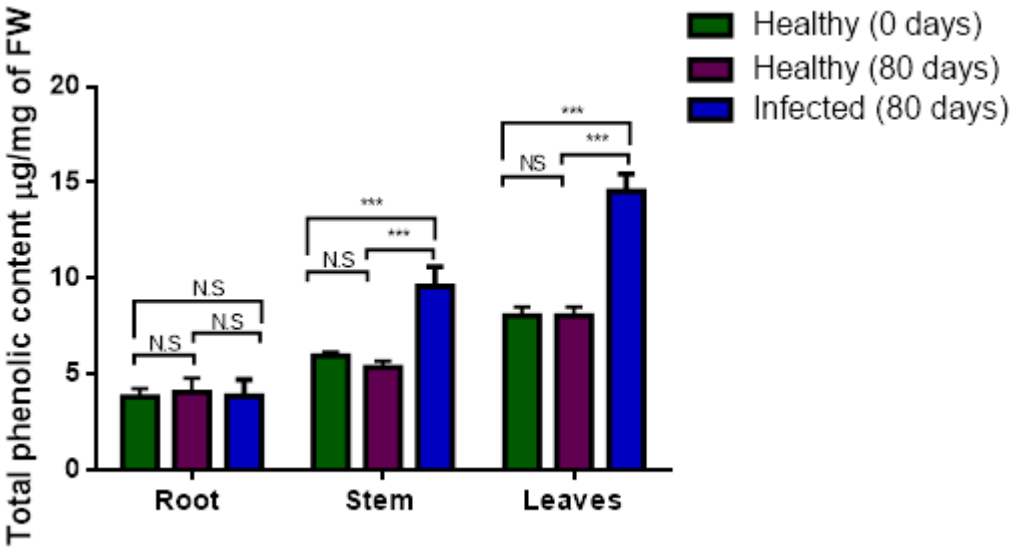

Figure 34: Variation of the total phenolic content of chilli plant upon biotic stress caused by broad mite infestation on chilli plant. Data shown are means ± standard deviations of the means (SD). N.S: not significant, * $p < 0.05$, ** $p < 0.01$, *** $p < 0.001$, N=3.

Phenolic compounds play various roles in plant growth, development, and defence against environmental stresses including pathogen attacks. Phenolic compounds have antimicrobial properties and can help to limit the spread of the pathogen within the plant tissues. The level of phenolic compounds produced by the plant may also be influenced by the type of pathogen, the severity of the infection, and the stage of the infection (Chowdhary et al., 2021). In healthy plants, a rise in TPC was not observed over an 80-day observation period, further suggesting that the increase in TPC may be stressor-specific. The preferential accumulation of these phenolic compounds in leaves compared to stems could be attributed to the leaves being the primary site of photosynthesis, also a site for the synthesis of several phenolic compounds and thus more exposed to environmental stressors such as broad mite infestation. When plants are under stress, photosynthesis can be impacted, leading to reactive oxygen species (ROS) production, Phenolic compounds, such as flavonoids, serve as natural antioxidants that can scavenge ROS, thereby protecting the cellular machinery involved in photosynthesis (Dadáková et al., 2020).

5.3.9.5 Total lipid content

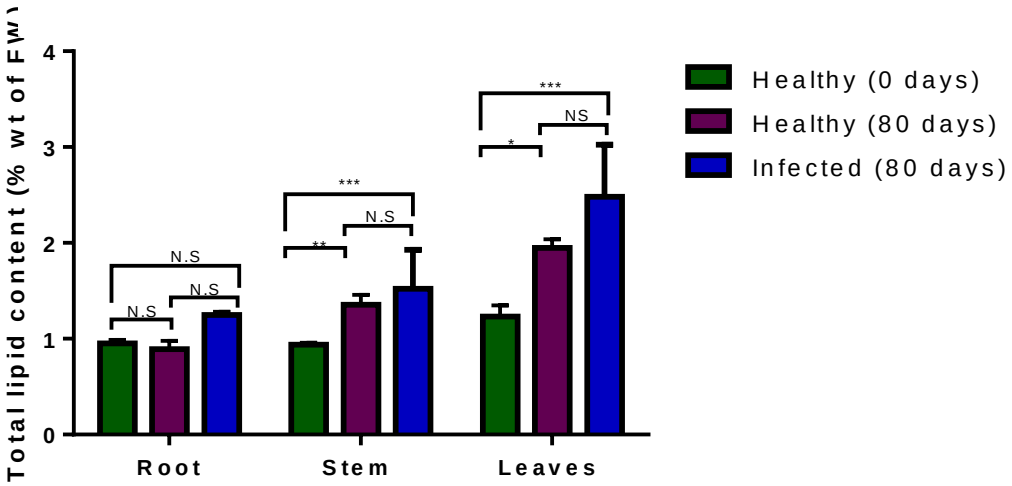

Figure 35: Variation of the total lipid content of chilli plant upon biotic stress caused by broad mite infestation on chilli plant. Data shown are means ± standard deviations of the means (SD). N.S: not significant, * $p < 0.05$, ** $p < 0.01$, *** $p < 0.001$, N=3.

Pathogen attacks are known to induce various biochemical and physiological changes in plants, one of which is the alteration in lipid composition. Changes in lipid profiles are thought to serve as a part of the plant's defence mechanism against invading pathogens. Various membrane lipids have been shown to undergo remodelling in response to bacterial or fungal attacks, often resulting in increased levels of certain phospholipids and galactolipids, which may contribute to membrane integrity and function (S. Wu et al., 2014). Lipid-derived signalling molecules like jasmonic acid and oxylipins play critical roles in initiating defence responses. These lipid alterations not only act as immediate response mechanisms but also mediate signal transduction pathways that lead to systemic acquired resistance, thereby providing long-term defence capabilities (Blée, 2002; Q. Zhang & Xiao, 2015). These changes can be correlated with an alteration in the expression of genes involved in lipid metabolism and defence against pathogens. These changes can contribute to variations in total lipid content in the plant.

5.4 Conclusion

The present study offers an in-depth exploration of the impact of broad mite infestation on chilli plants, covering morphological, biochemical, and molecular dimensions. Morphologically, the study identifies a range of symptoms that are indicative of broad mite infestation. These include leaf curling, dieback, and a range of discolourations, which are critical for early detection and timely intervention. The use of light and scanning electron microscopy offers a detailed view of the mites' life stages and anatomical features. This microscopic and histological analysis not only aids in the accurate identification of the mites but also provides information about interaction mechanisms with the host plant at the cellular level. It identifies significant alterations in

Malondialdehyde (MDA) levels, soluble sugar content, total carbohydrate content, free radical scavenging capacity, total phenolic content, and total lipid content in infected plants when compared to healthy controls. The elevation in MDA levels is particularly noteworthy as it suggests heightened oxidative stress within the infected leaves and stems. The changes in soluble sugars and carbohydrates point to disrupted metabolic pathways, likely a result of the plant's stress response to the infestation.

The study also investigates the efficacy of various pesticides in controlling broad mite infestations. Emamectin Benzoate 5% SG was found to be the most effective miticide, showing long-term control of broad mite infestation. This finding is crucial for the development of integrated pest management strategies for chilli cultivation. Along with the development of pesticide resistance in the mite population Ethion 50% EC.

CHAPTER 6

Proteomic Investigation of Biotic Stress Caused by Broad Mite (*Polyphagotarsonemus latus*) Infestation on Chilli

6 Proteomic investigation of biotic stress caused by broad mite (*Polyphagotarsonemus latus*) infestation on chilli plant

6.1 Introduction

Capsicum frutescens is a culturally and economically significant chilli pepper plant widely cultivated across the globe. Plant-pathogen interactions are ecologically delicate events that significantly impact agriculture, food production and the economy. Broad mite, *Polyphagotarsonemus latus*, is a multi-host pathogen that infests crops including chilli pepper limiting its yield thereby leading to economic loss.

In general, the plant responds to its pathogen via a unique pathogen recognition system. Pathogen infestation results in cellular, biochemical and physiological changes. Necrosis, withering of leaves, altered metabolic and physiological rates, production of aromatic molecules, resins and

other secondary metabolites are some of the responses against the pathogen (Klepzig et al., 1995; Pandey et al., 2017b). Such plant defense mechanisms are governed by various cellular pathways (Ku et al., 2018; Lecourieux et al., 2006); (Jalmi & Sinha, 2015a).

The molecular mechanisms (de)activated in chilli following broad mite infestation remain poorly understood from the standpoint of systems biology. Global quantitative analysis of proteomics changes in chilli infested with broad mite is an important research frontier in mapping plant-pathogen interactions and offers the potential for innovation in pest management methods whose ecological footprints are better understood.

This study report here a gel-free, TMT labeled mass spectrometry-based quantitative proteomic analysis of the leaves and apical meristems of healthy versus chilli pepper plants infested with broad mite.

6.2 Materials and Methods

6.2.1 Sample collection

The sample collection was carried out from a broad mite-infested field. Plants grew at an ambient temperature of 27^0C with a relative humidity of 65-85%. Samples were collected from 80 days old infested and healthy plants. Apical meristem and leaf samples from healthy and infected plants were collected, snap-frozen in liquid nitrogen and were stored at -80^0C until further analysis. Figure *36* depicts the schematic representation of the workflow followed in the experiment. Ethics committee approval was not required for this study

6.2.2 Protein extraction

Samples were ground in liquid nitrogen using a mortar and pestle. Two grams of the ground sample was transferred into a 50 ml pre-chilled centrifuge tube containing 10ml of homogenization buffer [50 mM HEPES-KOH (pH 7.5), 1 mM EDTA (pH 7.5) beta-mercaptoethanol (1%), sucrose (40%)] and vortexed immediately. To the homogenate, 15 ml of Tris equilibrated phenol was added and vortexed again. This mixture was placed on a rocker at 4^0C for 30min followed by centrifugation at 5000g for 15 min to collect the phenol phase. The collected phenol phase was subjected to overnight precipitation using 5 volumes of methanol containing 0.1 mM ammonium acetate at -20^0C. Samples were centrifuged to collect the protein pellet and washed with 80% acetone. The pellet was air-dried and resuspended in resuspension buffer [2 M thiourea, 8 M urea, and CHAPS (2%)].

6.2.3 Trypsin digestion

From each sample, 100 µg of protein was used for trypsin digestion. Proteins were reduced first using 5mM dithiothreitol (DTT) at 60^0C for 45 min, alkylated using iodoacetamide (IAA) in dark at room temperature for 30 min. Reduced and alkylated proteins were subjected to enzymatic digestion using sequencing grade modified trypsin (Promega, Madison, WI. Cat #: V5111) overnight at 37^0C (trypsin: protein ratio of 1:20). Enzymatic digestion was confirmed by running SDS-PAGE of pre-digest and post-digest samples. Peptides obtained after trypsin digestion were vacuum dried before storage at -80^0C until further use. For TMT labeling, vacuum dried peptides were suspended in 50mM TEABC and the TMT labels were reconstituted in anhydrous acetonitrile. TMT labeling was carried out as per manufacturers' instructions. Peptides obtained

from samples, i.e., infected leaf, infected meristem, healthy meristem and healthy leaf were labeled with TMTsixplex kit labels 126, 128, 129 and 130 respectively. Labeling efficiency for each sample was confirmed by running 2 µg equivalent peptides in the mass spectrometer. TMT-labeled peptides were then pooled from all conditions and fractionated using the basic reverse-phase liquid chromatography (bRPLC) into 96 fractions and then concatenated into 12 fractions. The separation was carried out using XBridge C18, 4.6 mm column (Waters, Milford, MA). The separation was done using a gradient of 0-100% of solvent A (10 mM TEABC in the water at, pH 8.5) to solvent-B (10mM TEABC, 90% ACN), for 120 minutes.

6.2.4 Mass spectrometry analysis

The fractionated peptides were desalted using SCX Stage Tip based method. Samples were solubilized in Trifluoracetic acid [TFA (0.1%)]. SCX columns were equilibrated using 0.1% TFA and the samples were loaded to the column. Columns were then washed using 0.2% TFA. Sample elution was carried out with 500mM of ammonium acetate in 50% on acetonitrile. Technical triplicates were used to acquire the data using Thermo Scientific Orbitrap Fusion Tribrid mass spectrometer (Thermo Fischer Scientific, Bremen, Germany) connected to an Easy-nLC-1200 nanoflow liquid chromatography system (Thermo Scientific). Desalted peptides were reconstituted in 0.1% formic acid and loaded onto a 2 cm trap column (NanoViper, 3 µm C18 Aq) (Thermo Fisher Scientific). Peptides were separated using a 15 cm analytical column (NanoViper, 75 µm silica capillary, 2 µm C18 Aq) at a flow rate of 300 nl/min.

The solvent gradients were set from 5-35% from Solvent A (0.1% formic acid) to solvent B (80% acetonitrile in 0.1% formic acid). The total run time for each fraction was 120 min. Global MS survey scan was carried out at a scan range of 400-1600 m/z (120,000 mass resolution at 200 m/z) in a data-dependent mode using Orbitrap mass analyzer. The maximum injection time was 5 ms. Only peptides with a charge state of 2-6 were considered for the analysis. The dynamic exclusion rate was set to 30 ms. For MS/MS analysis, data acquisition was carried out at top speed mode with 3s cycles and subjected to higher collision energy dissociation with 34% normalized collision energy. MS/MS scans were carried out at a range of 100-1600 m/z using the Orbitrap mass analyzer at a resolution of 60,000 at 200 m/z. The maximum injection time was 120ms. Internal calibration was carried out using a lock mass option (m/z 445.1200025) from ambient air.

6.2.5 Data analysis

Proteome Discoverer V2.1 platform (Thermo Scientific) with SequestHT and Mascot V.2.4 algorithms were used to carry out the data analysis. Mass spectrometric data were searched against the NCBI *Capsicum annuum* (Pepper Zunla 1 Ref_v1.0) which contained 40,627 proteins. The search parameters were set as following: precursor mass tolerance was set to 20ppm, fragment mass tolerance was set to 0.05Da. TMT label at the peptide N terminus and Lys residues, acetylation at the protein N terminus and oxidation of Met were set as variable modifications. Carbamidomethylation of Cys was set as a fixed modification. Other search parameters included two missed cleavages by trypsin and a 1% false discovery rate (FDR). Since *Capsicum sp.* Protein IDs are not supported by Gene Ontology and STRING analysis tools, the protein list obtained from Proteome Discoverer was subjected to reciprocal BLAST (Blastp)

against the *Arabidopsis thaliana* with the settings 60% identity and 80% query coverage to fetch the respective counterparts in *Arabidopsis thaliana* proteome. Gene Ontology analysis was carried out using PANTHER (Mi et al., 2017), protein-protein interaction analysis was carried out using STRING V.11.0 tool., with the help of *Arabidopsis thaliana* protein IDs. Pathway analysis was done using the KEGG pathways tool (*Capsicum annuum*).

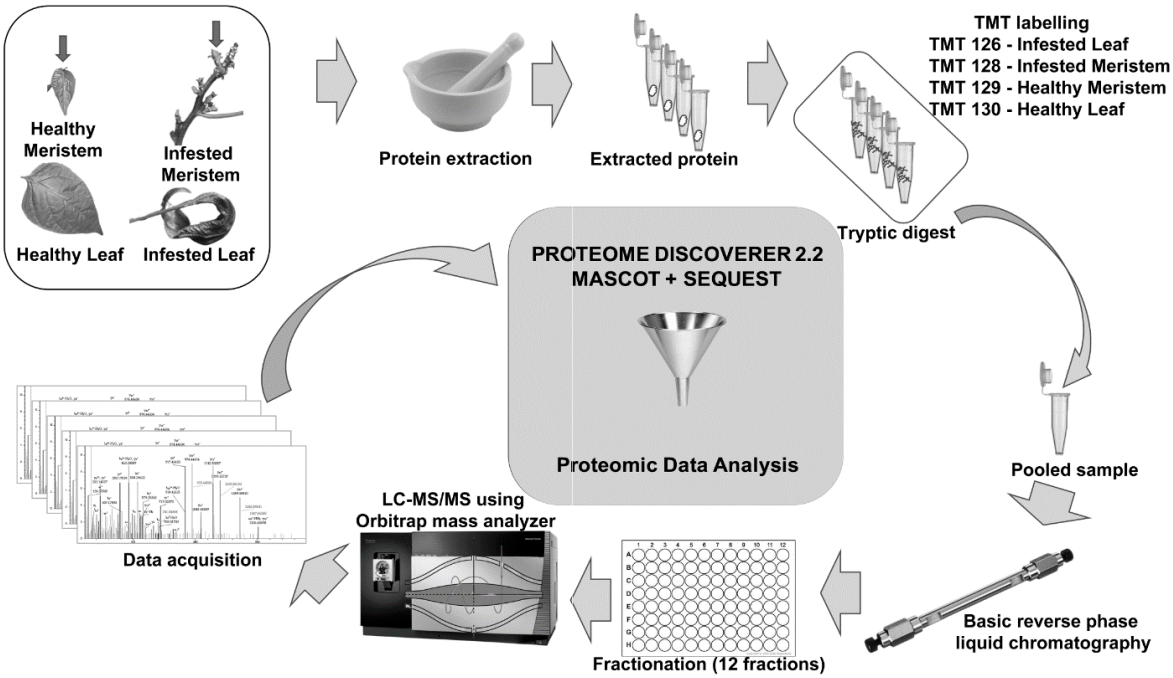

Figure 36: Schematic representation of the experimental plan for the proteomic analysis of broad mite infestation in Chilli: a workflow showing the steps involved in the proteomic analysis of meristem and leaf of the plant infected by broad mite. Proteins were extracted for from the tissues, and estimated using BCA. The proteins were then digested with trypsin and labelled with Tandem Mass Tags (TMT). Labelled peptides were analyzed on the Orbitrap Fusion Tribrid mass spectrometer. The acquired data from the mass spectrometer were searched against the *Capsicum annuum* (Pepper Zunla 1 Ref_v1.0) database using both Sequest HT and Mascot.

6.2.6 Data availability

The mass spectrometry raw data and the Proteome Discoverer output MSF files obtained from this study have been uploaded to the ProteomeXchange Consortium (http://proteomecentral.proteomexchange.org) through the PRIDE partner repository (Project accession: PXD018653).

6.3 Results and Discussion

6.3.1 Proteins and peptides identified

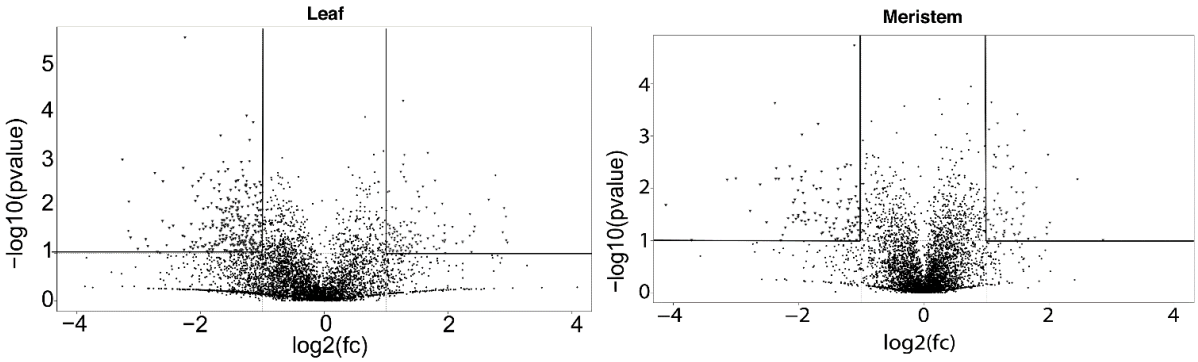

Figure 37: Volcano plot representing differentially regulated (FDR adjusted p-value<0.05) proteins in leaf, A p value of 0.1 and a fold change of 2 are indicated by non axial line. Right region reflects proteins increased by a ratio of >2.0 while left region reflects protein decreased by a ratio <0.5.

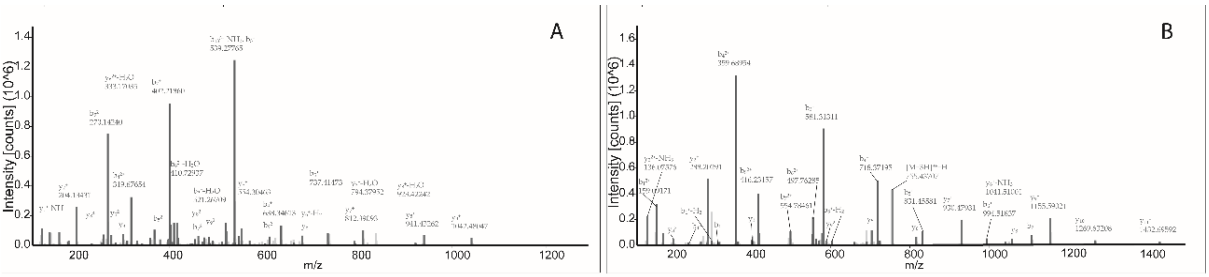

Figure 38: Representative MS/MS spectra of some peptides. (A) The peptide GDHVVTEEEHNVGK is derived from pathogenesis-related protein STH-2-like protein and (B) the peptide STYHLYNPQNINWDLR is derived from pathogenesis-related protein 4.

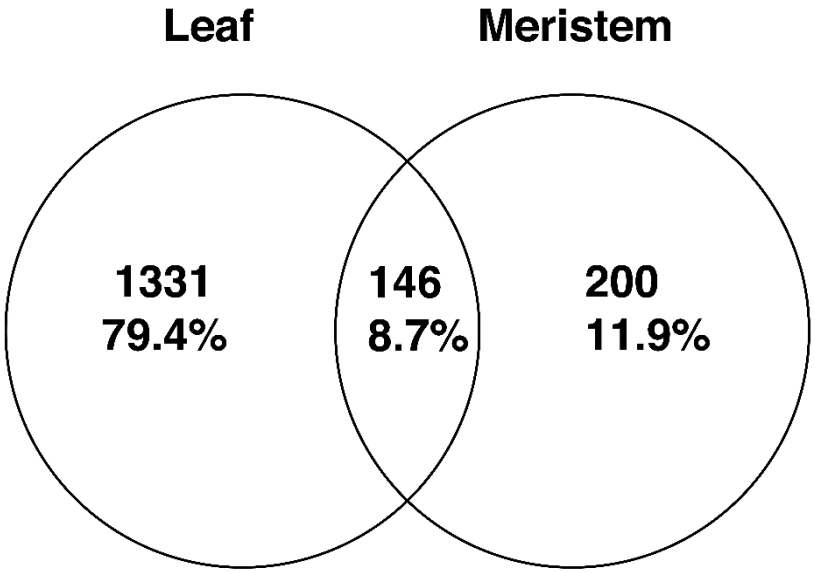

Figure 39: Venn diagram of differentially regulated proteins across sample sets (2 folds overexpressed + 2 fold downregulated). In leaf, a total of 1331 and in the meristem, 200 proteins were differentially expressed.

Proteomic data analysis resulted in the identification of 5,807 protein groups supported by 48,555 unique peptides and 1,279,655 peptide-spectrum matches. Individually, 5,186 proteins were detected in healthy leaf samples, 5,193 in infested leaf sample, 5194 proteins in healthy meristem sample and 5196 proteins in infested meristem sample. A threshold of 2-fold was set to fetch the differentially regulated (up- or down-regulated). Of the total number of proteins identified, 1677 were found to be differentially regulated in the infected samples. The distribution of several up-regulated and down-regulated proteins is represented by a Venn diagram (Figure *39*). Representative MS/MS spectra of two candidate proteins (pathogenesis-related protein STH-2-like and pathogenesis-related protein 4) that were found to be differentially regulated is shown in Figure *38*. Differentially regulated proteins across the leaf and meristem samples were visualized using a volcano plot Figure *37*. The non-axial vertical lines denote ±2.0-fold change while the non-axial horizontal line denotes P = 0.1. Proteins that are highly overexpressed (fold change ≥ 4) both infected leaf and meristem are presented in *Table 11*. Highly Downregulated (fold change ≤ 0.5) proteins both in infected leaf and infected meristem are presented in

Table 10.

Table 10: Partial list of significantly overexpressed proteins identified in *Capsicum frutescens* leaf and meristem upon broad mite infestation with fold change ≥ 4.

Gene ID	**RefSeq Access No.**	**Name of the Protein**	**Fold change in leaf (infected/healthy)**	**Fold change meristem (infected/healthy)**
A0A1U8F298	XP_016552766.1	defensin-like protein	8.91	5.19
A0A1U8HGT2, B0FYW8	XP_016579689.1	flower-specific defensin-like	5.84	4.01
A0A1U8H8L1	XP_016579665.1	ribonuclease S-7-like	4.04	4.16
A0A1U8G957	XP_016564563.1	peroxidase P7-like isoform X1	6.29	4.4
A0A1U8G7L7, A0A2G3ADZ2	XP_016567337.1	P21-like	9.58	5.14
A0A2G3ADX5	XP_016567370.1	osmotin-like protein OSML13	5.74	4.73
A0A1U8DWJ0, O65157	XP_016539393.1	basic form of pathogenesis-related protein 1-like	4.43	4.01
A0A1U8F686	XP_016551719.1	ATP-dependent RNA helicase DEAH11, chloroplastic-isoform X1	14.36	17.37
A0A1U8FZ64, A0A2G3ACP3	XP_016561693.1	lysine histidine transporter 1-like	6.67	4.24
A0A1U8E8Z1, A0A2G2YNL0	XP_016543667.1	protein trichome birefringence-like	4.65	4.56
A0A1U8FN99, A0A2G3AAS0	XP_016560687.1	abscisic acid and environmental stress-inducible pro TAS14-like	7.14	6

Table 11: Partial list of significantly downregulated proteins identified in *Capsicum frutescens* leaf and meristem upon broad mite infestation with fold change ≤ 0.5

Gene ID	RefSeq Accession No.	Name of the protein	Fold change in leaf (Infected/healthy)	Fold change in meristem (Infected/healthy)
A0A1U8F1W7	XP_016552636.1	putative UDP-rhamnose:rhamnosyltransferase 1	0.41	0.35
A0A1U8GY46	XP_016576025.1	putative UDP-rhamnose:rhamnosyltransferase 1	0.47	0.48
A0A1U8GLZ2	XP_016569778.1	anthocyanidin 3-O-glucoside 2'''-O-xylosyltransferase-like	0.48	0.35
A0A1U8E6L8	XP_016542879.1	heterodimeric geranylgeranyl pyrophosphate synthase small subunit, chloroplastic	0.44	0.42
A0A1U8G059	XP_016561354.1	UDP-glycosyltransferase 708D1-like	0.49	0.25
A0A1U8GTP3	XP_016574622.1	probable carboxylesterase 8	0.41	0.47
A0A1U8QDA4, J7H3W2	YP_006666078.1	ribosomal protein L32 (chloroplast)	0.42	0.49
A0A1U8ERZ9	XP_016546664.1	phosphomannomutase	0.26	0.45
A0A1U8QCI5, J7H9N4	YP_006666064.1	ribosomal protein L36 (chloroplast)	0.13	0.37
A0A1U8QC72, J7H9E5	YP_006666009.1	ribosomal protein S12 (chloroplast)	0.13	0.38
A0A1U8DXE4	XP_016539698.1	long chain acyl-CoA synthetase 2-like	0.18	0.47

6.3.2 Gene Ontology and protein interactions

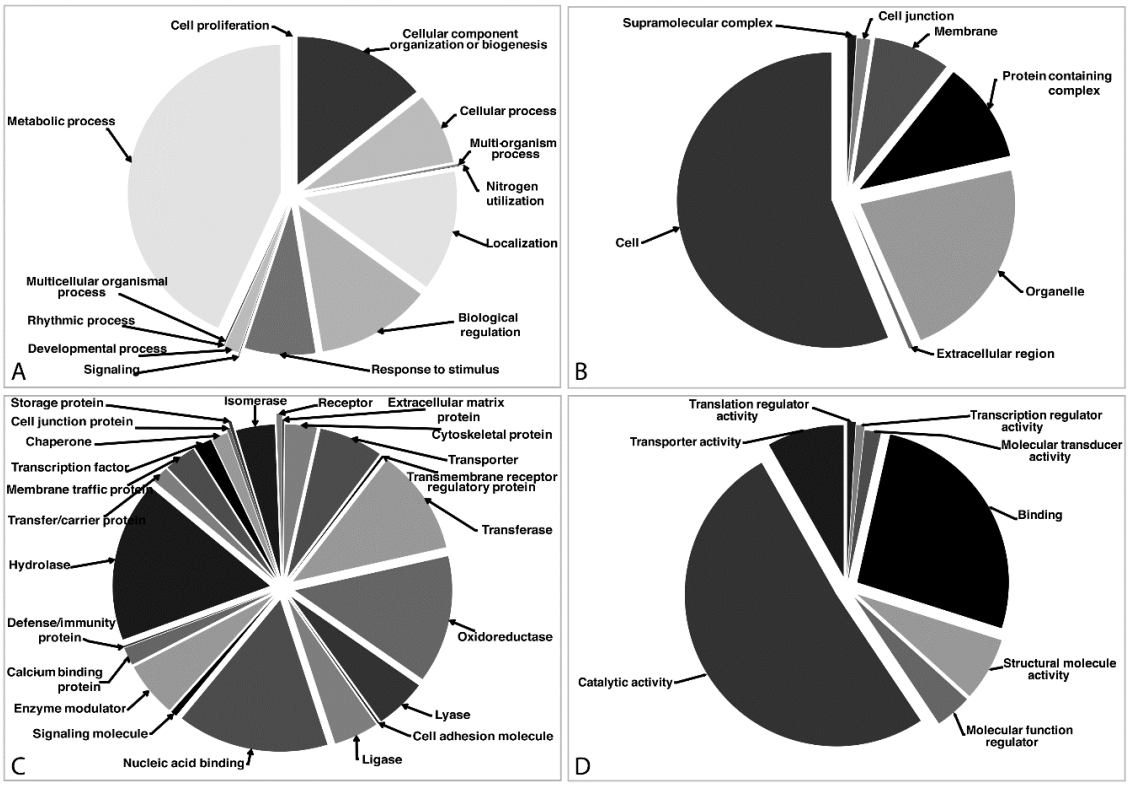

Figure 40: Subcellular localization and functional annotation of proteins identified in leaf and apical meristem tissues. (A) Biological process, (B) Cellular components, (C) Protein classes, (D) Molecular functions.

Various metabolic processes associated with plant immunity and metabolites related to defense mechanisms were found to be activated upon broad mite infestation. These are coordinated by the activation of different biological processes, cellular components, protein classes and molecular functions that are represented in Figure *40*. Gene ontology (GO) analysis for biological processes suggested a large number of proteins that mapped to metabolic processes (GO:00081521) and response to a stimulus (GO:0050896) which suggests some biological processes as being overexpressed by a stimulus received due to pest infestation. GO analysis with respect to cellular components, represents the mapping of the highest number of proteins to the term cell (GO: 0005623). GO analysis of protein classes revealed that the small portion of the proteins mapped to the term (PC:000901) corresponds to defense and immunity-related proteins.

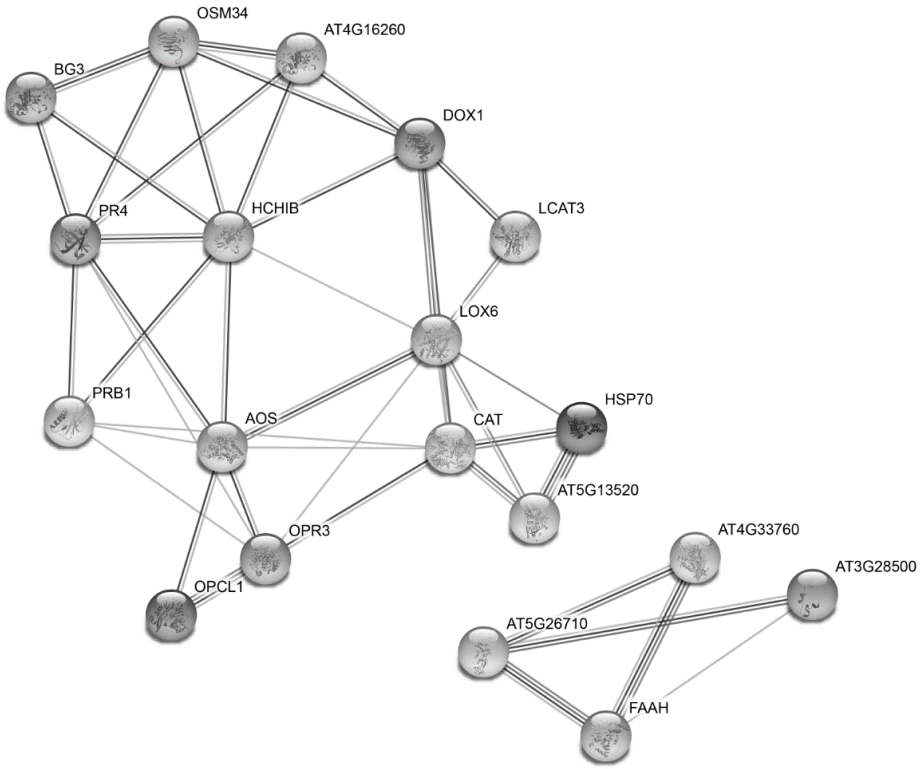

Figure 41:Putative protein-protein interaction predicted through STRING analysis of proteins identified and which participate in plant defence mechanism. Due to unavailability of *Capsicum frutescence* dataset in STRING, protein IDs were converted to respective Arabidopsis thaliana (AT) IDs using reciprocal BLAST analysis

Protein-protein interaction analysis using the STRING software tool showed the clustering of several proteins related to RNA regulation, protein synthesis, wound responsive proteins etc. (Figure *41*). An interaction network of defense and oxidative stress-responsive proteins was generated to visualize the interactions. Oxidative stress-responsive proteins not only play an important role in reducing oxidative damage caused by reactive oxygen species but also influence pathways such as jasmonate biosynthesis and propanoid pathways (Ahmad et al., 2016; Grace & Logan, 2000; Nakabayashi et al., 2014). Oxidative imbalance in the intracellular environment triggers various cell-mediated responses governed by interacting protein network of oxidoreductase and peroxidase superfamily proteins (Almagro et al., 2009; Caverzan et al., 2012; Cvetkovska & Vanlerberghe, 2013). These proteins are mainly present in peroxisomes, cytosol, chloroplasts and mitochondria to synthesize secondary metabolites via a series of various enzyme-mediated redox reactions as a result of various types of biotic stress-related pathways (e.g., jasmonate biosynthesis (J. Wang et al., 2019), biosynthesis of lignin via phenylpropanoid pathway (Moura et al., 2010).

6.3.3 Proteins associated with the plant-pathogen response

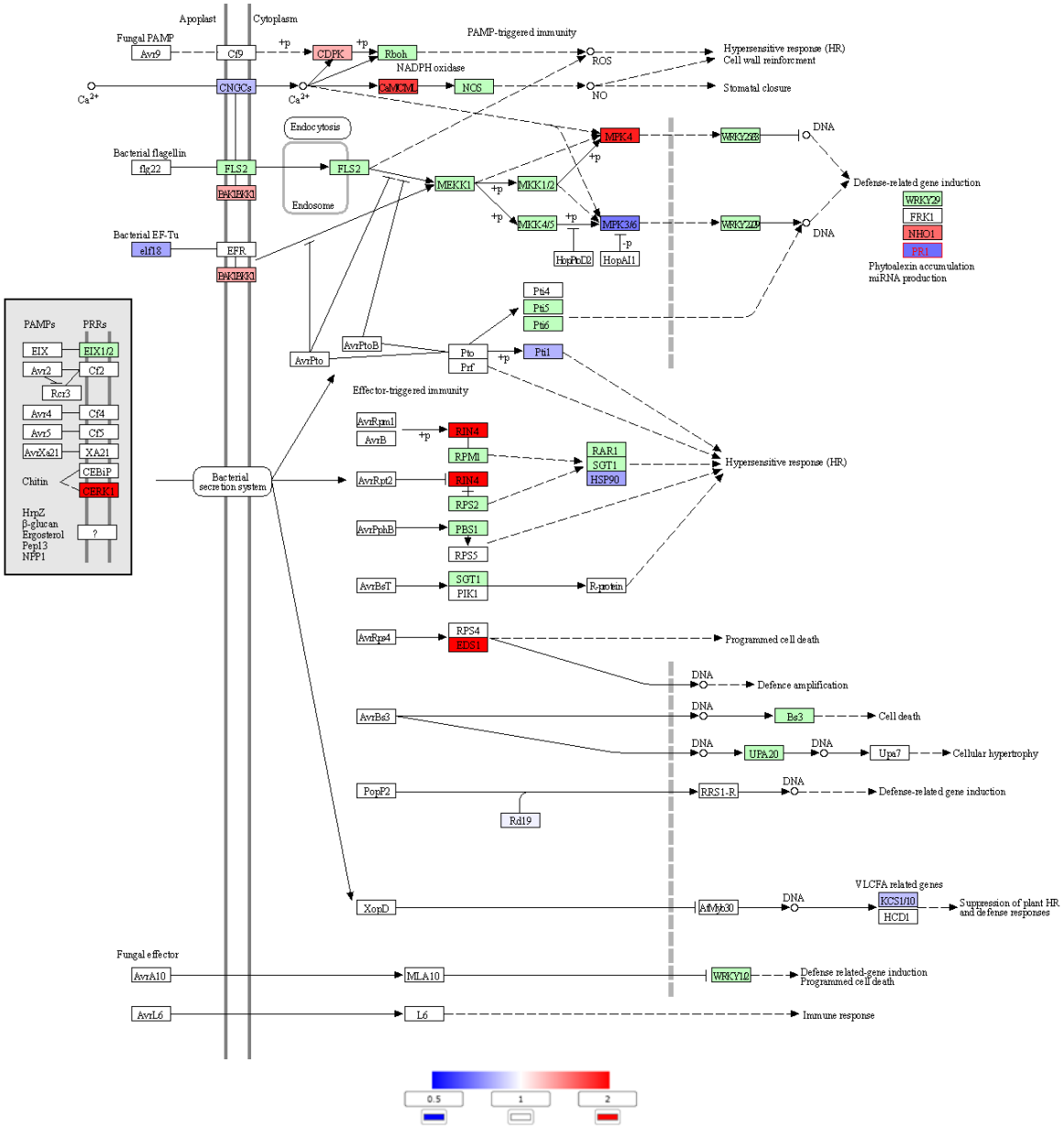

Figure 42:KEGG pathway representing disregulated Proteins associated with the plant-pathogen response. The colour scale is used to illustrate the extent of dysregulation in relation to the fold change of the identified protein, where a deep red hue signifies the degree of overexpression, and a deep blue hue signifies the degree of downregulation.

Calcium/ calmodulin-dependent, ROS and stimulus dependent responses are the triggering factors to produce various cellular and physiological responses against pathogen attack (Afzal et al., 2008; Cheval et al., 2013; Kunze et al., 2004; N. Suzuki et al., 2011). Apart from these, pathogen responsive genes, programmed cell death and miRNA production also acts as first line of defense against pathogens (Jha et al., 2016; S.-R. Liu et al., 2017; Santos & Aragão, 2009; Yuan et al., 2018; Zipfel et al., 2006). This study observed overexpression of calcium-dependent

protein kinase 11-like (*CDPK9*) in the chilli leaf. *CDPK9* protein participates in calcium-dependent nitric oxide synthase, which is responsible for stomatal closure (Gayatri et al., 2013). This study also noted the overexpression of probable calcium-binding protein *CML49* in the leaf, which has been reported to take part in nitric oxide regulation (Aoyagi et al., 2003). Overexpression of serine/threonine-protein kinase CDL1-like (*PBS1*) was found in infected leaf samples. Overexpression of Cyclic nucleotide-gated ion channel (*CNGC*) was also differentially regulated in the infected meristem sample. Differential regulation of proteins belonging to CaM/CAL signaling cascade, such as calmodulin, calmodulin-binding transcription activator 4 suggested the activity of calmodulin-dependent membrane signaling pathways. Apart from these, overexpression of chitin elicitor receptor kinase 1-like, RPM1-interacting protein 4, disease resistance protein RPM, probable disease resistance protein At4g14610, heat shock cognate protein 80-like are strong proteomic evidence to prove chitin elicited plant hyper response against broad mite infestation (Nicaise et al., 2009; Ramonell et al., 2005) overexpression of protein EDS1-like protein in leaf suggested activation of programmed cell death-related pathways (Bernacki et al., 2018), which could be the evidence for the leaf senescence observed upon broad mite infestation

6.3.4 Proteins associated with the MAPK pathway

Mitogen-activated protein kinase (MAPK) pathways play an important role in the signal transduction of extracellular factors to the nucleus to bring about necessary cellular responses (Meng & Zhang, 2013; Sinha et al., 2011). MAPK pathway is activated upon external stimuli such as flagellin fragment of the pathogen such as flg22 (Asai et al., 2002; Frei dit Frey et al., 2014), oxidative stress caused by pathogen attack (Son et al., 2011), plant hormones such as jasmonic acid, ethylene, and abscisic acid. Cold stress, heat shock, osmotic, salt and drought stress have also been found to activate this pathway (Taj et al., 2010) (Ichimura et al., 2002). This study identified 32 proteins both in infested leaf and infested meristem; participating in the mitogen-activated protein kinase pathway. The basic form of pathogenesis-related protein 1-like (*PR-1*) is found to be highly overexpressed in the infected leaf, whereas catalase isozyme 1(*CAT-1*) was downregulated. In the meristem, endochitinase 4 (*chi4*) was found to be overexpressed and nucleoside diphosphate kinase 2 (*NDK-1*) is down-regulated protein. Up-regulation of the basic form of pathogenesis-related protein 1-like (*LOC107768379*) and endochitinase 4 indicates activation of the MAPK pathway due to mite infestation.

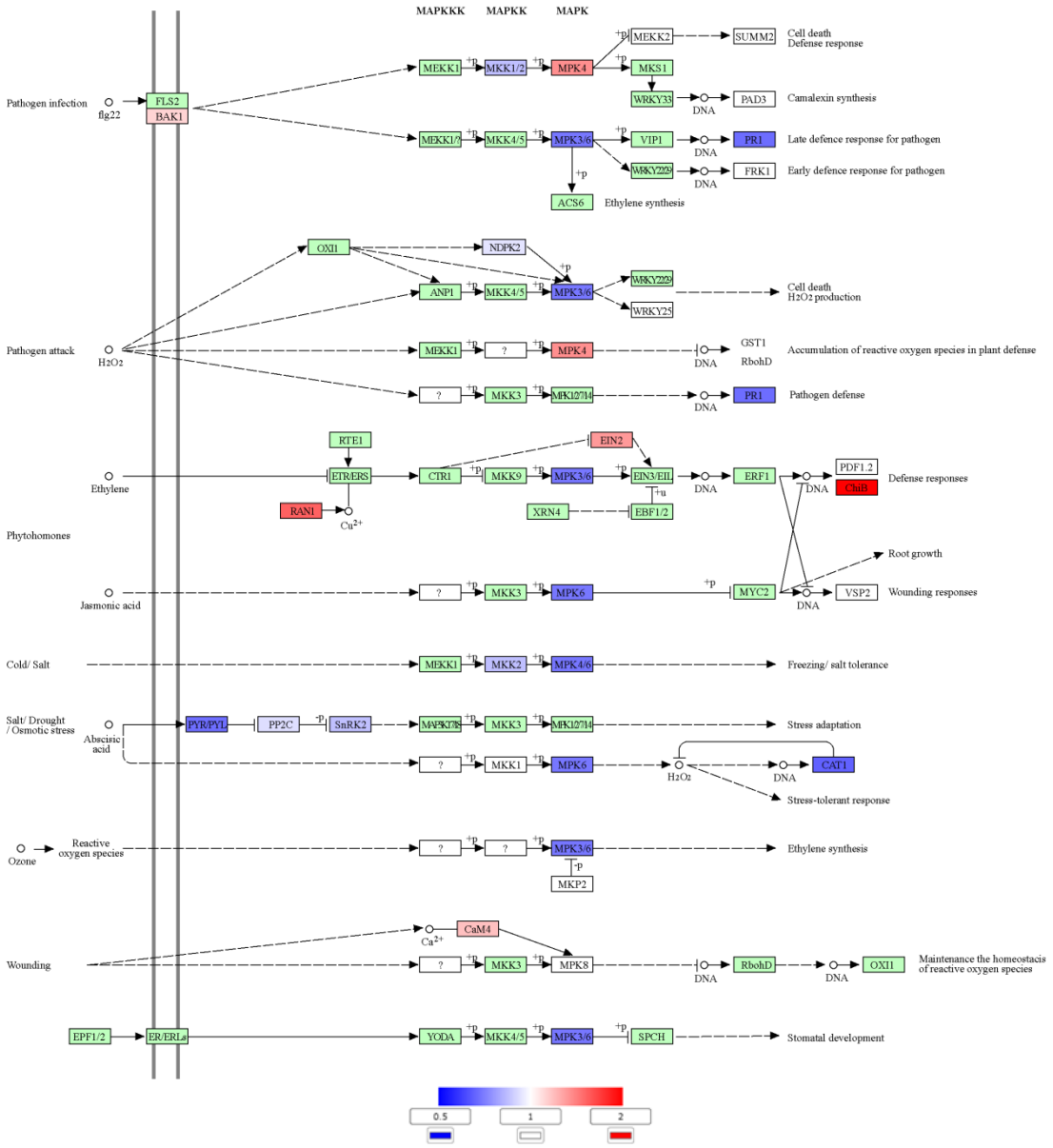

Figure 43: Disregulated Proteins associated with the MAPK signalling pathway upon broad mite infestation. The colour scale is used to illustrate the extent of dysregulation in relation to the fold change of the identified protein, where a deep red hue signifies the degree of overexpression, and a deep blue hue signifies the degree of downregulation.

6.3.5 Proteins associated with plant hormone regulation

It has been previously noted that auxin-responsive genes are differentially expressed in response to biotic stress. *GH3, Aux/IAA, SAUR* and *ARF* gene families are known to be overexpressed upon biotic stress (Ghanashyam & Jain, 2009; Ma & Ma, 2016). Modulation in plant hormones either stimulates growth-related responses such as lateral bud induction, changes in leaf, flower sizes, changes in root develop patterns and plant senescence (Spoel & Dong, 2008). In our data, auxin influx carrier (*LAX1*) an AUX family-related protein were overexpressed. Also, noted the

up-regulation of histidine-containing phosphotransfer protein 1 (*AHP3*). This protein is known to participate in cytokinin modulation. AHP belongs to His-containing phosphotransfer (HPt) factor family of proteins (Mizuno, 1998), which has been known to bring about histidine to aspartate (His-to-Asp) phosphorelay signal transduction (Tanaka et al., 2004). Overexpression of AHP proteins results in an increased sensitivity towards cytokinin uptake (T. Suzuki et al., 2002). AHP also participates in Zeatin biosynthesis. This study noted overexpression of probable serine/threonine-protein kinase (*BSK2*), a BR-signaling kinase protein that participates in brassinosteroid signaling. Brassinosteroid is antagonistically interacting with ethylene, gibberellic acid and jasmonic acid, thereby influencing the plant defense mechanism (Saini et al., 2015). Overexpression of proteins such as transcription factor TGA (*TGA9*) and pathogenesis-related protein, a CAP superfamily protein indicated the influence of salicylic acid and its corresponding defense-related pathways in response to the mite infestation. All the above-discussed proteins are preferentially overexpressed in leaf compared to meristem.

6.3.6 Proteins associated with alpha-linolenic acid metabolism and jasmonate synthesis

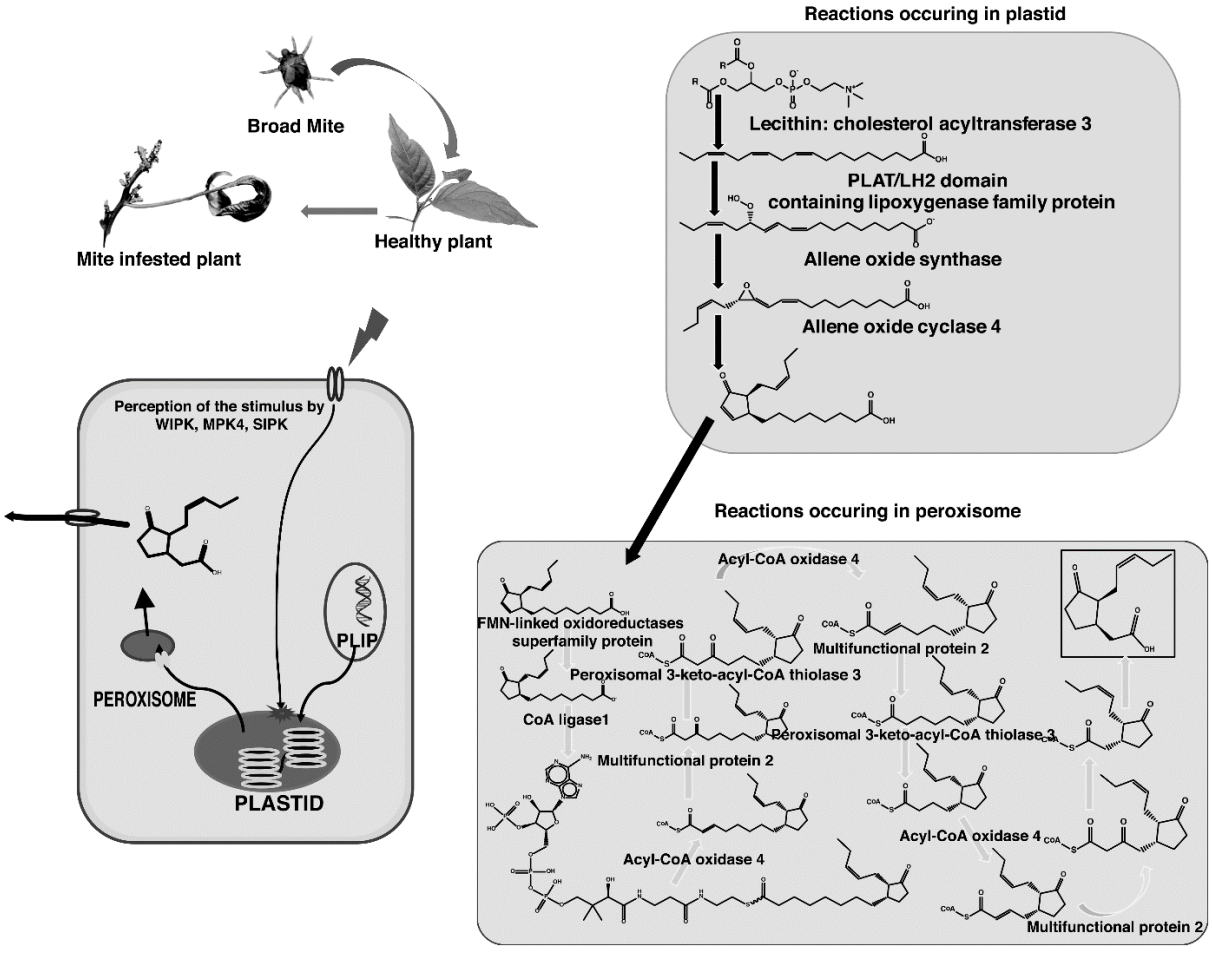

Figure 44: Alpha-linolenic acid metabolism and jasmonate synthesis. The infestation of broad mite triggers cellular responses via the MAPK pathway. Subcellular events trigger

the synthesis of jasmonic acid - a key messenger molecule for defence-related responses;via sequential actions of oxidases, multi-function and thiolases enzymes.

Alpha-linolenic acid metabolism and jasmonate synthesis is a well-known pathway in plant defense mechanism activated against biotic and abiotic stress (Figure *44*) (Ahmad et al., 2016; Wasternack & Hause, 2013). Alpha-linolenic acid pathway has been known to produce jasmonates (Liechti & Farmer, 2006), which actively participate in spreading the wound signals throughout the plant via JAZ proteins (Larrieu & Vernoux, 2016). Jasmonates were also known to affect plant growth and sterility of the flowers. Volatile methyl jasmonates also act as a signaling molecule to the neighboring plants and thereby influencing the defense response of the close by plants (Okada et al., 2015). Few opportunistic herbivorous pathogens are attracted to jasmonates producing weak, wounded or infested plants and manipulate the jasmonate induced signaling pathway (L. Zhang et al., 2017). Evidence suggests that beneficial microbes detour jasmonate mediated defense mechanisms by secreting certain molecules, which either stop or bypass jasmonate mediated plant defense (Yan & Xie, 2015). KEGG pathway analysis of our data revealed enrichment of the alpha-linolenic acid pathway. Acyl-CoA oxidase 4 (*ACX4*) was the highly overexpressed protein in the leaf whereas 12-oxophytodienoate reductase 1 (*OPR3*) is overexpressed in the mite-infested meristem. Various intermediates and enzymes involved in jasmonate synthesis which are recorded in our data are presented in *Table 12*. Jasmonate synthesis occurs at peroxisomes in the plant cell. Peroxisomes are rich in oxidase enzymes such as ACX1 (Schilmiller et al., 2007). Acyl-coenzyme A oxidase (*ACX1*) often found to be elevated under salicylic acid stress, injury and dehydration. Proteins such as peroxisomal 3-ketoacyl-CoA thiolase 2 (*KAT5*) and peroxisomal 3-keto-acyl-CoA thiolase 4 (*PKT4*) have also been reported to take part in the wound response (Cruz Castillo et al., 2004; J. Wu & Baldwin, 2009)

Gene symbol	Refseq Protein ID	Name of the protein	Fold Change Leaf	Fold Change Meristem
ACX5	XP_016569524.1	acyl-CoA oxidase 5	0.76	0.90
AMP-dependent synthetase ligase family protein	XP_016550360.1	AMP-dependent synthetase and ligase family protein	0.77	1.21
AMP-dependent synthetase ligase family protein	XP_016550360.2	AMP-dependent synthetase and ligase family protein	0.77	1.21
OPCL1	XP_016550360.3	CoA ligase1	0.77	1.21
MFP2	XP_016550653.1	multifunctional protein 2	0.78	1.29
FMN-linked oxidoreducta superfamily protein	XP_016554786.1	FMN-linked oxidoreductases superfamily protein	0.79	1.55
PKT4	XP_016566389.1	peroxisomal 3-ketoacyl-CoA thiolase 4	0.81	1.61
A0A1U8FBV9	XP_016556161.1	Oxidoreductase, zinc-binding dehydrogenase fan protein	1.06	1.54
LOX6	XP_016547545.1	PLAT/LH2 domain-containing lipoxygenase family prot	1.07	1.04
PKT3	XP_016541790.1	peroxisomal 3-ketoacyl-CoA thiolase 3	1.25	1.02
AOC4	XP_016555194.1	allene oxide cyclase 4	1.43	1.65
AOS	XP_016548437.1	allene oxide synthase	1.62	1.63
LCAT3	XP_016550818.1	lecithin:cholesterol acyltransferase 3	1.70	1.25
AIM1	XP_016540509.1	Enoyl-CoA hydratase/isomerase family	1.80	1.42
DOX1	XP_016561515.1	Peroxidase superfamily protein	2.04	1.42
OPR3	XP_016579932.1	12-oxophytodienoate reductase 1	2.06	1.71
ACX4	XP_016543215.1	acyl-CoA oxidase 4	2.26	1.54
ACX2	XP_016550464.1	acyl-CoA oxidase 2	Under LOQ	Under LOQ

Table 12: List of identified proteins which take part in alpha linolenic acid metabolism (jasmonate synthesis)

6.3.7 Proteins associated with the phenylpropanoid pathway:

Mite infestation resulted in the overexpression of several enzymes involved in the phenylpropanoid pathway. Lignin, a complex structural polymer is one of the results of this pathway, plays a plant defense-related role upon biotic stress (Moura et al., 2010). This study have observed overexpression of enzymes such as 4-coumarate-CoA ligase 1 (*4CL2*), which ligates coenzyme A to phenolic acids such as cinnamic acid, p-coumaric acid, caffeic acid, ferulic acid, 5-hydroxyferrulic acid, sinapic acid into respective phenolic CoA products, enzymes such as trans-cinnamate 4-monooxygenase (*C4H*) converts cinnamic acid, cinnamic CoA, p-coumaric acid, p-coumaric acid CoA into caffeic acid or caffeic acid caffeic acid CoA via shikimate conjugation. CoA undergoes reduction to produce respective phenolic aldehydes. In the presence of enzyme cinnamyl alcohol dehydrogenase 1 (*CAD5*) phenolic aldehydes are converted into respective phenolic alcohols. In the presence of peroxidase superfamily proteins, it undergoes polymerization to produce lignin. The enzymes mentioned before were found to be overexpressed both in leaf and meristem samples.

6.4 Conclusions

This study provides the first in-depth comparative proteomic analysis of broad mite (*Polyphagotarsonemus latus*) infestation in chilli *Capsicum frutescens*. Proteomic analysis revealed the dysregulation of various pathways that take part in plant defense mechanisms. Altered signaling pathways and plant hormone regulations can inform future efforts to understand the pest induced structural and physiological damage. Dysregulation of proteins involved in the synthesis and utilization of precursors of various secondary metabolites may also contribute to further research to understand physiological alterations and yield loss due to pest infestation. Designing novel molecules that could target these proteins may pave way for better strategies to manage pests and post-infestation damage. These findings can broadly enable further ecological and agri-proteomic research in prevention and management of plant-pathogen induced damages.

CHAPTER 7

Common Pathways Dysregulated Upon Abiotic and Biotic Stress caused by Plant Hormones and Broad Mite Infestation in Chilli

7 Common pathways dysregulated upon abiotic and biotic stress caused by plant hormones and broad mite infestation in chilli plant

7.1 Introduction

The study of plant proteins and their expression concerning various external factors has become increasingly relevant to understanding how plants interact and respond to their surroundings. This is particularly true when considering the impact of plant growth regulators and external stressors like pests on the overall health and productivity of the plant. Plant growth regulators such as Benzyl aminopurine (BAP), Indole-3-acetic acid (IAA), Abscisic acid (ABA), and Gibberellic acid 3 (GA3) and ethylene play pivotal roles in plant development and stress response. These chemicals are involved in a plethora of physiological processes including cell division, root initiation, flowering, and responses to environmental stresses. Similarly, though used as weedicides, 2,4-D (2,4-Dichlorophenoxyacetic acid), DICAMBA, TIBA (2,3,5-Triiodobenzoic acid), and PICLORAM are also important in modulating plant growth and development in *in vitro* conditions. Among abiotic factors, the role of plant hormones in modulating stress responses is increasingly gaining attention. Their influence extends from cellular processes to whole-plant physiology, affecting gene expression, metabolic pathways, and ultimately, plant health. However, the molecular mechanisms through which these hormones mediate stress responses are not yet fully understood.

On the other side of the spectrum, plants are also susceptible to various biotic stresses, including pest infestations. Among the numerous pests, broad mites pose a significant threat to chilli, and other commercial crops. Broad mites inject toxins into the plant tissues, triggering a cascade of physiological changes that can alter protein expression and metabolic pathways. Understanding the protein expression in plants in response to these mite infestations can provide valuable insights into plant defense mechanisms.

This study aims to explore the common proteins expressed in plants when treated with the aforementioned plant growth regulators and upon broad mite infestation by using advanced techniques to profile these proteins and their fold changes.

7.2 Materials and methods

The RAW data was subjected to *de novo* peptide sequencing in Proteome Discoverer ver. 2.1, as mentioned in the sections 4.2.5 and 6.2.5. Subsequently, the list of proteins was analyzed using KEGG pathway analysis, utilizing Gene IDs and fold change values for the analysis of common proteins participating in the specific pathways. For discussion in the thesis, three pathways were selected.

7.3 Results and discussion

7.3.1 Role of ubiquitin-mediated proteolysis in biotic and abiotic stress in chilli caused by hormonal stress and broad mite infestation

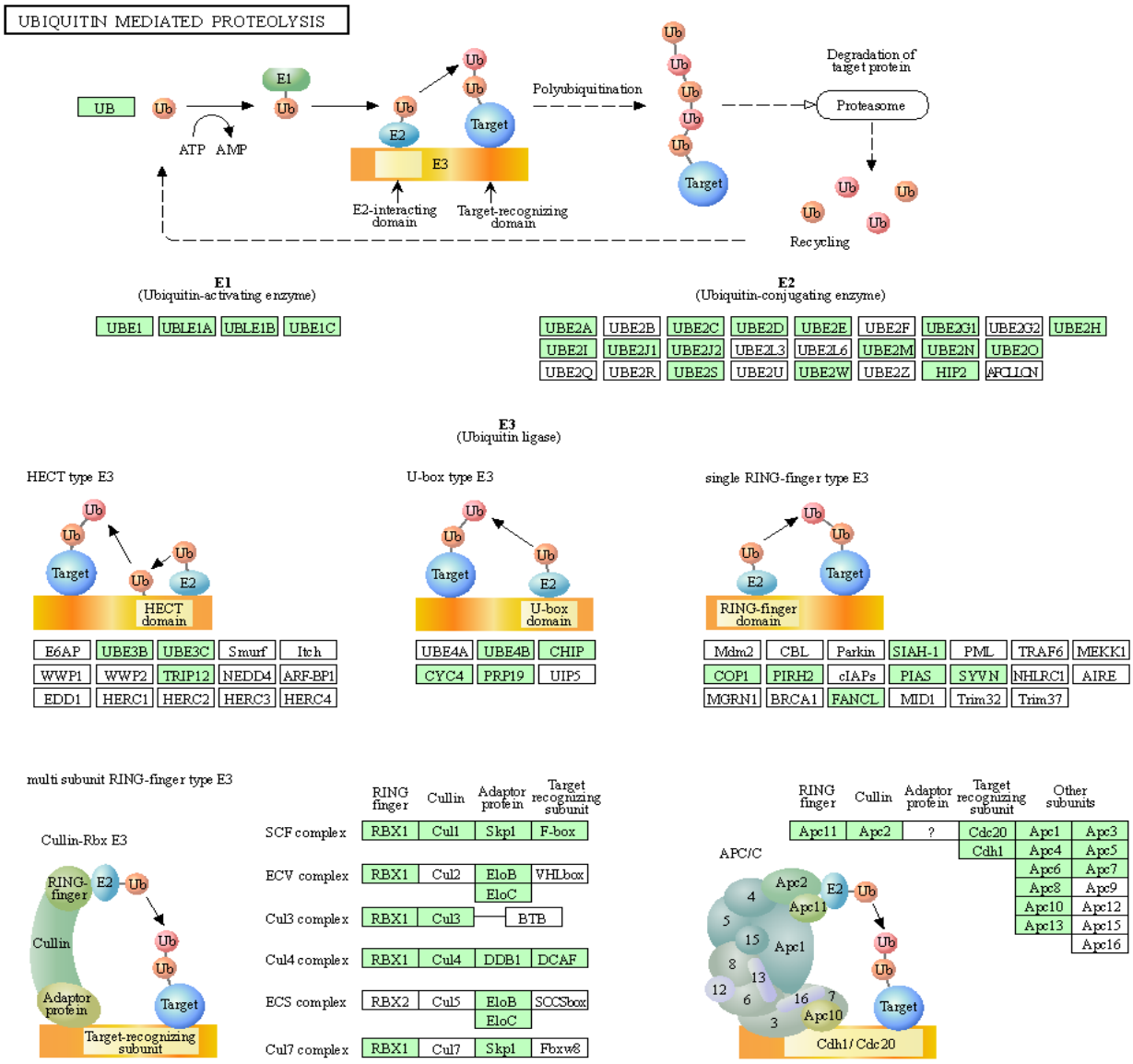

Figure 45: KEGG pathway depicting ubiquitin-mediated proteolysis (cann 04120)

Table 13: List of common dysregulated proteins of ubiquitin mediated proteolysis (cann04120) in *Capsicum frutescens* seedlings upon stress caused by plant hormones and broad mite infestation.

Protein ID	Description of the protein	BAP	IAA	ABA	GA3	ETH	24D	DICAMBA	TIBA	PICLORAM	Leaf	meristem
XP_016537856.1	anaphase-promoting complex subunit 5 isoform X1										1.72	1.05
XP_016538173.1	ubiquitin-conjugating enzyme E2 28-like	0.82	1.06	1.00	1.19	1.13	1.55	1.36	1.25	1.57		
XP_016538254.1	ubiquitin-60S ribosomal protein L40										1.22	0.47
XP_016539785.1	SUMO-activating enzyme subunit 2	0.67	0.73	0.48	0.55	0.54	0.51	0.69	0.45	0.56	1.22	0.82
XP_016539955.1	E3 ubiquitin-protein ligase UPL3	1.01	1.02	0.96	0.99	1.07	1.09	1.03	1.28	1.12	0.85	2.46
XP_016539969.1	SKP1-like protein 1B	0.98	0.88	0.69	0.82	1.04	1.34	1.06	0.72	0.96	1.03	1.02
XP_016540684.1	NEDD8-activating enzyme E1 catalytic subunit isoform X1										0.68	0.83
XP_016542098.1	ubiquitin-activating enzyme E1 1-like										1.00	0.74
XP_016542112.1	anaphase-promoting complex subunit 7 isoform X1										1.73	1.30
XP_016542284.1	cullin-1-like										2.17	1.19
XP_016543308.1	ubiquitin-conjugating enzyme E2 10-like										0.77	0.68
XP_016545285.1	ubiquitin-conjugating enzyme E2 36	1.38	1.17	1.15	1.07	1.16	1.41	1.32	1.59	1.54	0.96	1.00
XP_016548218.1	ubiquitin-conjugating enzyme E2-23 kDa-like										0.35	0.77
XP_016548220.1	ubiquitin-conjugating enzyme E2-23 kDa-like	0.91	0.96	1.21	0.96	1.16	1.31	1.32	1.26	1.20		
XP_016551576.1	ubiquitin-40S ribosomal protein S27a										1.46	0.86

XP_016554632.1	ubiquitin-40S ribosomal protein S27a-like	1.97	1.12	1.29	1.23	1.16	1.48	1.23	1.53	1.57	0.51	0.58
XP_016557036.1	DNA damage-binding protein 1 isoform X1										1.04	1.23
XP_016558560.1	cullin-4-like										0.68	1.33
XP_016560698.1	probable ubiquitin-conjugating enzyme E2 18										1.67	1.08
XP_016561349.1	probable ubiquitin conjugation factor E4										0.66	0.95
XP_016561411.1	cullin-3A-like										3.31	1.35
XP_016561429.1	ubiquitin-conjugating enzyme E2 2-like	1.14	1.11	0.76	0.99	1.00	1.40	1.23	1.25	1.28		
XP_016566047.1	pre-mRNA-processing factor 19	1.03	1.00	1.07	0.83	0.89	1.24	1.28	1.05	1.02	0.79	0.87
XP_016566696.1	ubiquitin-conjugating enzyme E2 5-like	0.86	1.21	1.06	0.90	1.04	1.16	1.25	1.73	1.63	1.99	0.85
XP_016568621.1	NEDD8-conjugating enzyme Ubc12-like isoform X1	0.74	1.26	1.02	0.99	0.87	1.90	1.69	1.69	1.90		
XP_016572152.1	ubiquitin-conjugating enzyme E2 7-like										1.10	0.79
XP_016573909.1	ubiquitin isoform X1	1.05	0.98	0.81	0.79	1.79	1.16	1.02	1.12	0.99	2.12	1.00
XP_016576007.1	ubiquitin-activating enzyme E1 1-like isoform X1	0.86	1.41	1.01	1.21	1.59	1.51	1.23	1.08	1.47	1.14	0.98
XP_016578150.1	ubiquitin-conjugating enzyme E2 27	1.06	1.13	1.01	0.98	0.74	1.57	1.32	1.55	1.65	0.60	1.03
XP_016578212.1	SUMO-activating enzyme subunit 1B-1-like										2.86	1.28
XP_016578531.1	RING-box protein 1a-like isoform X1										0.82	1.18
XP_016581140.1	ubiquitin-conjugating enzyme E2 35										1.40	1.06
XP_016581501.1	ubiquitin-conjugating enzyme E2 28	0.93	1.17	1.04	1.05	0.94	1.42	1.30	1.50	1.50		
XP_016581502.1	ubiquitin-conjugating enzyme E2 28										1.14	1.00

Ubiquitin-mediated proteolysis plays a critical role in plant stress signalling, as it regulates the abundance of key proteins involved in stress responses. Ubiquitin is a small, highly conserved protein that is covalently attached to lysine residues on target proteins, marking them for degradation by the proteasome (Zuin et al., 2014). The process of ubiquitination is carried out by a cascade of enzymes that includes E1 (ubiquitin-activating enzyme), E2 (ubiquitin-conjugating enzyme), and E3 (ubiquitin ligase) enzymes. The specificity of the ubiquitination reaction is largely determined by the E3 enzyme, which recognizes and binds to specific target proteins (Damgaard, 2021). In plant stress signalling, ubiquitin-mediated proteolysis plays a key role in regulating the abundance of key proteins involved in stress responses (Doroodian & Hua, 2021), such as transcription factors and signalling molecules (Adams & Spoel, 2018). For example, in response to drought stress, the transcription factor DREB2A is ubiquitinated and degraded by the proteasome, leading to the activation of downstream stress-responsive genes (Qin et al., 2008). Recent studies have also shed light on the regulation of ubiquitin-mediated proteolysis in plant hormone-mediated stress signalling. For example, the E3 ligase UBR1 has been shown to regulate the degradation of the transcription factor ABI5 in response to abscisic acid (ABA) signalling (F. Yu et al., 2016). Another E3 ligase, RGLG1, has been shown to regulate the degradation of the transcription factor WRKY33 in response to pathogen infection (B. Liu et al., 2021). E3 ligase COP1 has been shown to regulate the abundance of multiple stress-responsive proteins, including the transcription factor HY5 and the ABA receptor PYL8 (Hardtke et al., 2000). Similarly, the E3 ligase PUB22 has been shown to regulate the abundance of multiple proteins involved in oxidative stress responses (Furlan et al., 2017).

7.3.2 Role of mitogen-activated protein kinases (MAPKs) in biotic and abiotic stress in chilli caused by hormonal stress and broad mite infestation

Mitogen-activated protein kinases (MAPKs) play a critical role in plant stress signalling by transmitting extracellular signals into the cell, leading to the activation of various cellular responses. The activation of MAPKs is initiated by different abiotic and biotic stress factors, including salt, drought, cold, heat, pathogen attack, and oxidative stress. Once activated, MAPKs activate downstream transcription factors, leading to the expression of genes involved in stress tolerance (Sinha et al., 2011). Studies have shown that MAPKs are involved in various stress responses, including the regulation of stomatal closure (Lee et al., 2016), and the production of reactive oxygen species (ROS) (Jalmi & Sinha, 2015b). MAPKs also play a crucial role in the regulation of plant growth and development, as well as in the response to hormone signalling. In plants, the MAPK cascade consists of three different kinases, namely the MAPK kinase kinase (MAPKKK), MAPK kinase (MAPKK), and MAPK. The activation of MAPKs is initiated by the phosphorylation of MAPKKK, which in turn activates MAPKK, leading to the phosphorylation and activation of MAPK (Jagodzik et al., 2018). Genes such as AtMPK3, AtMPK4, and AtMPK6 are activated by different stress signals and are involved in the regulation of different stress responses in Arabidopsis thaliana (Yuasa et al., 2001). Similarly, OsMAPK3 and OsMAPK6 are involved in the regulation of the stress and yield response in rice (S. Liu et al., 2015). Upstream regulators of MAPK signalling, such as receptor-like kinases (RLKs), calcium-dependent protein kinases (CDPKs) (Wurzinger et al., 2011), and reactive oxygen species (ROS). Can also influence the activation of the MAPK signalling cascade (R. R. Kumar et al., 2020).

7.3.3 Role of Plant hormone signal transduction in biotic and abiotic stress in chilli caused by hormonal stress and broad mite infestation

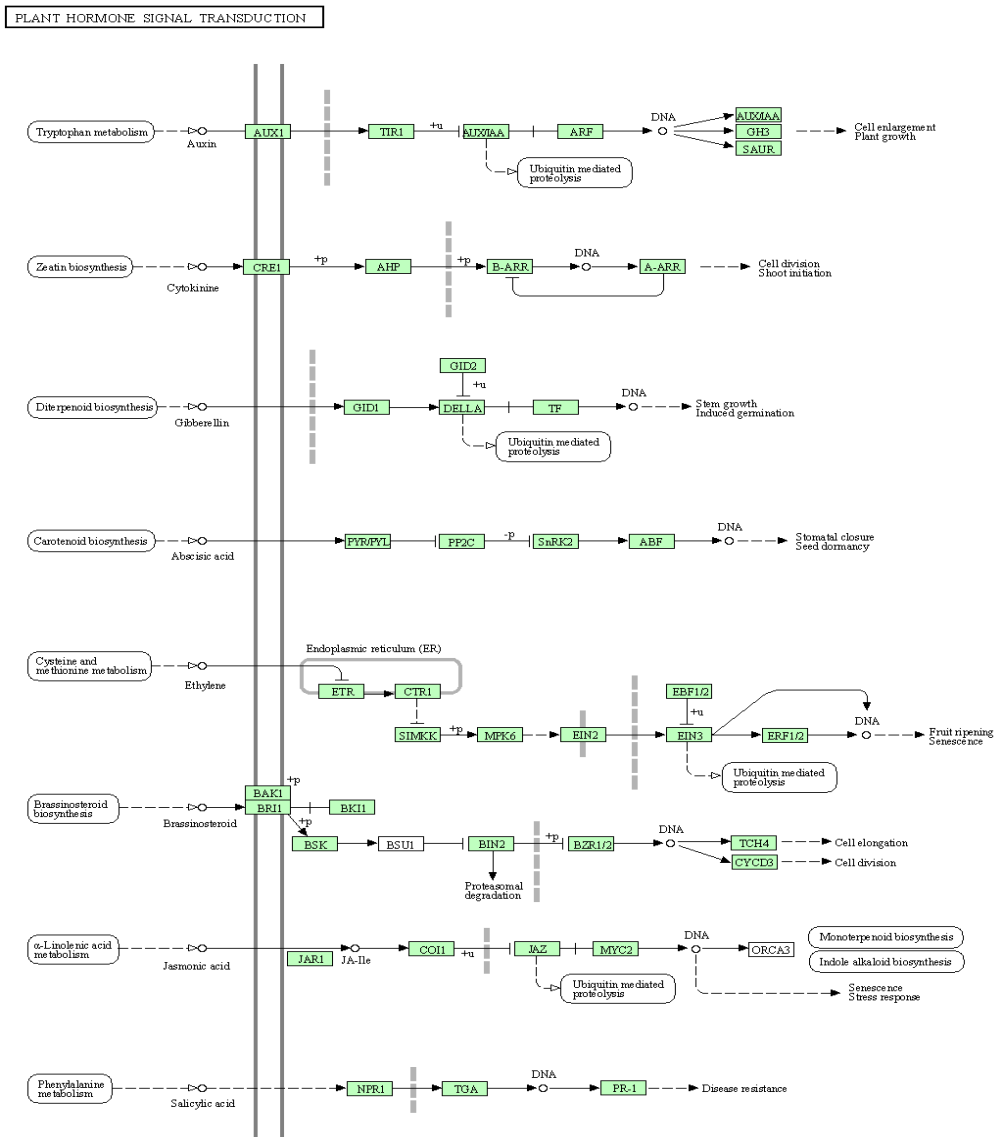

Figure 46: KEGG pathway depicting Plant hormone signal transduction (KEGG pathway: cann04016)

Plant hormones play a pivotal role in regulating responses to various biotic and abiotic stressors. In the context of pathogen defense, Salicylic Acid is crucial for combating biotrophic pathogens by activating defense-related genes and inducing systemic acquired resistance (SAR) (Klessig et al., 2018). On the other hand, Jasmonic Acid and Ethylene are vital for defense against necrotrophic pathogens, promoting the activation of defense genes and the production of antimicrobial compounds. JA also serves as a central player in herbivore defense, triggering the release of volatile organic compounds and toxic substances upon herbivore damage (N. Li et al., 2019). SA and JA pathways can antagonize each other to prioritize the type of pathogen defense. In terms of abiotic stress, Abscisic Acid (ABA) is the primary hormone for drought stress response, inducing stomatal closure and regulating stress-related gene expression (Muhammad Aslam et al., 2022).

Table 14: List of common dysregulated proteins of Environmental Information Processing: signal transduction (cann04075) in *Capsicum frutescens* seedlings upon stress caused by plant hormones and broad mite infestation.

Protein ID	Description of the protein	BAP	IAA	ABA	GA3	Ethylene	24D	DICAMBA	TIBA	PICLORAM	Leaf	Meristem
XP_016549771.1	abscisic acid receptor PYL2			0.77	0.69	0.68	0.67	0.68	0.84	0.72	0.73	0.68
XP_016555804.1	abscisic acid receptor PYL9-like	0.43	1.53									
XP_016554091.1	abscisic acid receptor PYR1-like											
XP_016575021.1	abscisic acid receptor PYR1-like			0.80	1.04	0.78	0.85	1.01	0.86	0.97	0.85	0.92
XP_016554091.1	abscisic acid receptor PYR1-like	0.87	1.29	0.88	1.08	0.79	0.99	1.14	1.13	1.02	1.08	1.18
XP_016575021.1	abscisic acid receptor PYR1-like	0.47	0.77	0.80	1.04	0.78	0.85	1.01	0.86	0.97	0.85	0.92
XP_016539579.1	ABSCISIC ACID-INSENSITIVE 5-like protein 7	3.33	1.09									
XP_016542238.1	auxin transporter-like protein 4	1.61	1.44									
XP_016576817.1	auxin-induced protein 22D-like			1.08	0.80	0.76	0.70	0.94	0.90	0.74	0.81	0.72
XP_016582337.1	basic form of pathogenesis-related protein 1-like			0.88	1.15	0.93	0.97	1.12	1.62	1.31	1.33	2.15
XP_016539393.1	basic form of pathogenesis-related protein 1-like	4.44	4.01									
XP_016582337.1	basic form of pathogenesis-related protein 1-like	6.36	2.10	0.88	1.15	0.93	0.97	1.12	1.62	1.31	1.33	2.15
XP_016539195.1	BRASSINOSTEROID INSENSITIVE 1-associated receptor kinase 1 isoform X1	1.34	1.12	3.73	1.23	1.04	0.97	1.12	2.15	1.33	1.22	2.17
XP_016542746.1	ethylene-insensitive protein 2	1.80	1.04									
XP_016577355.1	histidine-containing phosphotransfer protein 1-like			0.85	1.04	0.63	0.88	0.81	1.64	1.23	0.99	1.59

XP_016538521.1	histidine-containing phosphotransfer protein 1-like	1.58	1.74	0.72	1.06	0.99	1.11	0.97	0.92	0.95	1.02	1.22
XP_016577355.1	histidine-containing phosphotransfer protein 1-like	4.00	1.15	0.85	1.04	0.63	0.88	0.81	1.64	1.23	0.99	1.59
XP_016581313.1	indole-3-acetic acid-amido synthetase GH3.6			1.46	0.60	0.81	0.77	0.62	2.18	1.43	1.09	2.33
XP_016580705.1	indole-3-acetic acid-amido synthetase GH3.6-like			0.96	0.60	0.68	0.69	0.60	1.71	1.37	0.99	1.98
XP_016547427.1	mitogen-activated protein kinase homolog NTF4	0.47	1.16									
XP_016541443.1	pathogenesis-related leaf protein 4-like	0.43	0.65									
XP_016542442.1	pathogenesis-related leaf protein 6											
XP_016542442.1	pathogenesis-related leaf protein 6	1.29	1.23	5.35	0.47	1.90	0.67	0.59	1.13	1.00	2.10	2.41
XP_016582333.1	pathogenesis-related protein 1A-like			2.63	1.36	0.96	0.96	0.82	4.13	3.41	3.91	10.02
XP_016582339.1	pathogenesis-related protein 1B-like			1.54	1.57	1.26	1.44	1.31	6.92	5.89	10.27	13.86
XP_016539472.1	probable indole-3-acetic acid-amido synthetase GH3.1			1.51	1.72	1.08	1.00	1.53	1.56	1.37	1.34	2.07
XP_016560988.1	probable indole-3-acetic acid-amido synthetase GH3.1			0.71	0.90	0.72	0.75	0.83	2.29	1.34	0.97	2.68
XP_016537783.1	probable protein phosphatase 2C 6	0.87	1.64									
XP_016568302.1	probable serine/threonine-protein kinase At4g35230	1.44	1.08									
XP_016544093.1	probable serine/threonine-protein kinase At4g35230 isoform X1	2.97	1.10									
XP_016577309.1	protein TRANSPORT INHIBITOR RESPONSE 1	0.36	0.98									

XP_016570753.1	serine/threonine-protein kinase SAPK3-like			0.87	1.09	0.78	0.88	0.89	1.37	1.15	1.00	1.31
XP_016539059.1	serine/threonine-protein kinase SRK2B	0.80	0.93	0.94	1.21	0.89	1.02	1.04	1.52	1.38	0.92	1.37
XP_016539642.1	serine/threonine-protein kinase SRK2E	0.75	1.25									

7.4 Conclusions:

This study employs advanced proteomic techniques to explore the molecular underpinnings of stress responses in *Capsicum frutescens* seedlings. The focus is on both abiotic stresses induced by plant hormones and biotic stress from broad mite infestations. Notably, the study identifies the critical roles of MAPK and Plant Hormone Signal Transduction pathways, along with ubiquitin-mediated proteolysis, in modulating these responses. These findings are first to be reported thereby contributing to the broader applications in sustainable agriculture vis targeted interventions. The research serves as a valuable resource for understanding the complex mechanisms that govern stress responses in *Capsicum frutescens*.

8 References

1. Abbasi, B. H., Stiles, A. R., Saxena, P. K., & Liu, C.-Z. (2012). Gibberellic Acid Increases Secondary Metabolite Production in *Echinacea purpurea* Hairy Roots. *Applied Biochemistry and Biotechnology*, *168*(7), 2057–2066. https://doi.org/10.1007/s12010-012-9917-z
2. Adams, E. H. G., & Spoel, S. H. (2018). The ubiquitin–proteasome system as a transcriptional regulator of plant immunity. *Journal of Experimental Botany*, *69*(19), 4529–4537. https://doi.org/10.1093/jxb/ery216
3. Afzal, A. J., Wood, A. J., & Lightfoot, D. A. (2008). Plant receptor-like serine threonine kinases: Roles in signaling and plant defense. *Molecular Plant-Microbe Interactions: MPMI*, *21*(5), Article 5. https://doi.org/10.1094/MPMI-21-5-0507
4. Ahmad, P., Rasool, S., Gul, A., Sheikh, S. A., Akram, N. A., Ashraf, M., Kazi, A. M., & Gucel, S. (2016). Jasmonates: Multifunctional Roles in Stress Tolerance. *Frontiers in Plant Science*, *7*. https://doi.org/10.3389/fpls.2016.00813
5. Ahmed, A. B. A., Rao, A. S., Rao, M. V., & Taha, R. M. (2011). Effect of picloram, additives and plant growth regulators on somatic embryogenesis of *Phyla nodiflora* (L.) Greene. *Brazilian Archives of Biology and Technology*, *54*, 7–13. https://doi.org/10.1590/S1516-89132011000100002
6. Ainsworth, E. A., & Gillespie, K. M. (2007). Estimation of total phenolic content and other oxidation substrates in plant tissues using Folin–Ciocalteu reagent. *Nature Protocols*, *2*(4), Article 4. https://doi.org/10.1038/nprot.2007.102
7. Akoyi, J., Mgutu, A. J., Machuka, J., Van Lijsebettens, M., Taracha, C., & Anami, S. E. (2013). Dicamba growth regulator promotes genotype independent somatic embryogenesis from immature zygotic embryos of tropical maize inbred lines. *JOURNAL OF LIFE SCIENCES (LIBERTYVILLE, ILL.)*, *7*(7), Article 7.
8. Alabdallah, O., Ahou, A., Mancuso, N., Pompili, V., Macone, A., Pashkoulov, D., Stano, P., Cona, A., Angelini, R., & Tavladoraki, P. (2017). The Arabidopsis polyamine oxidase/dehydrogenase 5 interferes with cytokinin and auxin signaling pathways to control xylem differentiation. *Journal of Experimental Botany*, *68*(5), 997–1012. https://doi.org/10.1093/jxb/erw510
9. Almagro, L., Gómez Ros, L. V., Belchi-Navarro, S., Bru, R., Ros Barceló, A., & Pedreño, M. A. (2009). Class III peroxidases in plant defence reactions. *Journal of Experimental Botany*, *60*(2), 377–390. https://doi.org/10.1093/jxb/ern277

10. Alves, H. L. S., Matiolli, C. C., Soares, R. C., Almadanim, M. C., Oliveira, M. M., & Abreu, I. A. (2021). Carbon/nitrogen metabolism and stress response networks – calcium-dependent protein kinases as the missing link? *Journal of Experimental Botany*, *72*(12), 4190–4201. https://doi.org/10.1093/jxb/erab136
11. Aoyagi, M., Arvai, A. S., Tainer, J. A., & Getzoff, E. D. (2003). Structural basis for endothelial nitric oxide synthase binding to calmodulin. *The EMBO Journal*, *22*(4), 766–775. https://doi.org/10.1093/emboj/cdg078
12. Asai, T., Tena, G., Plotnikova, J., Willmann, M. R., Chiu, W.-L., Gomez-Gomez, L., Boller, T., Ausubel, F. M., & Sheen, J. (2002). MAP kinase signalling cascade in *Arabidopsis* innate immunity. *Nature*, *415*(6875), 977–983. https://doi.org/10.1038/415977a
13. Ashrafuzzaman, M., M Hossain, M., Razi Ismail, M., Haque, M., & M Shahidullah, S. (2009). Regeneration potential of seedling explants of chilli (*Capsicum annuum*). *African Journal of Biotechnology*, *8*, 591–596.
14. Baluška, F., Parker, J. S., & Barlow, P. W. (1993). A role for gibberellic acid in orienting microtubules and regulating cell growth polarity in the maize root cortex. *Planta*, *191*(2), 149–157. https://doi.org/10.1007/BF00199744
15. Bernacki, M. J., Czarnocka, W., Witoń, D., Rusaczonek, A., Szechyńska-Hebda, M., Ślesak, I., Dąbrowska-Bronk, J., & Karpiński, S. (2018). ENHANCED DISEASE SUSCEPTIBILITY 1 (EDS1) affects development, photosynthesis, and hormonal homeostasis in hybrid aspen (Populus tremula L. × P. tremuloides). *Journal of Plant Physiology*, *226*, 91–102. https://doi.org/10.1016/j.jplph.2018.04.014
16. Binenbaum, J., Weinstain, R., & Shani, E. (2018). Gibberellin Localization and Transport in Plants. *Trends in Plant Science*, *23*(5), 410–421. https://doi.org/10.1016/j.tplants.2018.02.005
17. Bjornson, R. D., Carriero, N. J., Colangelo, C., Shifman, M., Cheung, K.-H., Miller, P. L., & Williams, K. (2008). X!!Tandem, an Improved Method for Running X!Tandem in Parallel on Collections of Commodity Computers. *Journal of Proteome Research*, *7*(1). https://doi.org/10.1021/pr0701198
18. Blakeley, P., Overton, I. M., & Hubbard, S. J. (2012). Addressing Statistical Biases in Nucleotide-Derived Protein Databases for Proteogenomic Search Strategies. *Journal of Proteome Research*, *11*(11), 5221–5234. https://doi.org/10.1021/pr300411q
19. Blée, E. (2002). Impact of phyto-oxylipins in plant defense. *Trends in Plant Science*, *7*(7), 315–322. https://doi.org/10.1016/s1360-1385(02)02290-2
20. Bligh, E. G., & Dyer, W. J. (1959). A rapid method of total lipid extraction and purification. *Canadian Journal of Biochemistry and Physiology*, *37*(8), 911–917. https://doi.org/10.1139/o59-099
21. Boba, A., Kulma, A., Kostyn, K., Starzycki, M., Starzycka, E., & Szopa, J. (2011). The influence of carotenoid biosynthesis modification on the *Fusarium culmorum* and *Fusarium oxysporum* resistance in flax. *Physiological and Molecular Plant Pathology*, *76*(1), 39–47. https://doi.org/10.1016/j.pmpp.2011.06.002
22. Boja, E. S., & Fales, H. M. (2001). Overalkylation of a protein digest with iodoacetamide. *Analytical Chemistry*, *73*(15), 3576–3582. https://doi.org/10.1021/ac0103423

23. Bolton, P., & Harwood, J. L. (1976). Effect of thiocarbamate herbicides on fatty acid synthesis by potato. *Phytochemistry*, *15*(10), 1507–1509. https://doi.org/10.1016/S0031-9422(00)88925-6
24. Brust, G. E., & Gotoh, T. (2018). Chapter 5 - Mites: Biology, Ecology, and Management. In W. Wakil, G. E. Brust, & T. M. Perring (Eds.), *Sustainable Management of Arthropod Pests of Tomato* (pp. 111–130). Academic Press. https://doi.org/10.1016/B978-0-12-802441-6.00005-X
25. Burns, E. R., Buchanan, G. A., & Carter, M. C. (1971). Inhibition of Carotenoid Synthesis as a Mechanism of Action of Amitrole, Dichlormate, and Pyriclor 1. *Plant Physiology*, *47*(1), 144–148.
26. Camejo, D., Jiménez, A., Palma, J. M., & Sevilla, F. (2015). Proteomic identification of mitochondrial carbonylated proteins in two maturation stages of pepper fruits. *Proteomics*, *15*(15), 2634–2642. https://doi.org/10.1002/pmic.201400370
27. Caverzan, A., Passaia, G., Rosa, S. B., Ribeiro, C. W., Lazzarotto, F., & Margis-Pinheiro, M. (2012). Plant responses to stresses: Role of ascorbate peroxidase in the antioxidant protection. *Genetics and Molecular Biology*, *35*(4 Suppl), 1011–1019.
28. Chaki, M., Álvarez de Morales, P., Ruiz, C., Begara-Morales, J. C., Barroso, J. B., Corpas, F. J., & Palma, J. M. (2015). Ripening of pepper (*Capsicum annuum)* fruit is characterized by an enhancement of protein tyrosine nitration. *Annals of Botany*, *116*(4), 637–647. https://doi.org/10.1093/aob/mcv016
29. Chen, E. I., Cociorva, D., Norris, J. L., & Yates, J. R. (2007). Optimization of Mass Spectrometry Compatible Surfactants for Shotgun Proteomics. *Journal of Proteome Research*, *6*(7), 2529–2538. https://doi.org/10.1021/pr060682a
30. Chen, T.-K., Yang, H.-T., Fang, S.-C., Lien, Y.-C., Yang, T.-T., & Ko, S.-S. (2016). Hybrid-Cut: An Improved Sectioning Method for Recalcitrant Plant Tissue Samples. *Journal of Visualized Experiments : JoVE*, *117*, 54754. https://doi.org/10.3791/54754
31. Chen, Z., Li, W., Gaines, C., Buck, A., Galli, M., & Gallavotti, A. (2021). Structural variation at the maize WUSCHEL1 locus alters stem cell organization in inflorescences. *Nature Communications*, *12*(1), Article 1. https://doi.org/10.1038/s41467-021-22699-8
32. Chen, Z., Qin, C., Wang, M., Liao, F., Liao, Q., Liu, X., Li, Y., Lakshmanan, P., Long, M., & Huang, D. (2019). Ethylene-mediated improvement in sucrose accumulation in ripening sugarcane involves increased sink strength. *BMC Plant Biology*, *19*, 285. https://doi.org/10.1186/s12870-019-1882-z
33. Cheng, D.-D., Liu, M.-J., Sun, X.-B., Zhao, M., Chow, W. S., Sun, G.-Y., Zhang, Z.-S., & Hu, Y.-B. (2016). Light Suppresses Bacterial Population through the Accumulation of Hydrogen Peroxide in Tobacco Leaves Infected with *Pseudomonas syringae* pv. Tabaci. *Frontiers in Plant Science*, *7*. https://www.frontiersin.org/articles/10.3389/fpls.2016.00512
34. Cheng, Q., Li, T., Ai, Y., Lu, Q., Wang, Y., Sun, L., & Shen, H. (2019). Complementary Transcriptomic and Proteomic Analysis Reveals a Complex Network Regulating Pollen Abortion in GMS (msc-1) Pepper (*Capsicum annuum* L.). *International Journal of Molecular Sciences*, *20*(7), 1789. https://doi.org/10.3390/ijms20071789

35. Cheval, C., Aldon, D., Galaud, J.-P., & Ranty, B. (2013). Calcium/calmodulin-mediated regulation of plant immunity. *Biochimica et Biophysica Acta (BBA) - Molecular Cell Research*, *1833*(7), Article 7. https://doi.org/10.1016/j.bbamcr.2013.01.031
36. Chidley, H. G., Deshpande, A. B., Oak, P. S., Pujari, K. H., Giri, A. P., & Gupta, V. S. (2017). Effect of postharvest ethylene treatment on sugar content, glycosidase activity and its gene expression in mango fruit. *Journal of the Science of Food and Agriculture*, *97*(5), 1624–1633. https://doi.org/10.1002/jsfa.7912
37. Choi, D. S., & Hwang, B. K. (2011). Proteomics and functional analyses of pepper abscisic acid-responsive 1 (ABR1), which is involved in cell death and defense signaling. *The Plant Cell*, *23*(2), 823–842. https://doi.org/10.1105/tpc.110.082081
38. Chowdhary, V., Alooparampil, S., Pandya, R. V., Tank, J. G., Chowdhary, V., Alooparampil, S., Pandya, R. V., & Tank, J. G. (2021). Physiological Function of Phenolic Compounds in Plant Defense System. In *Phenolic Compounds—Chemistry, Synthesis, Diversity, Non-Conventional Industrial, Pharmaceutical and Therapeutic Applications*. IntechOpen. https://doi.org/10.5772/intechopen.101131
39. Chung, T.-Y., Kuo, C.-Y., Lin, W.-J., Wang, W.-L., & Chou, J.-Y. (2018). Indole-3-acetic-acid-induced phenotypic plasticity in Desmodesmus algae. *Scientific Reports*, *8*(1), Article 1. https://doi.org/10.1038/s41598-018-28627-z
40. Colangelo, C. M., Shifman, M., Cheung, K.-H., Stone, K. L., Carriero, N. J., Gulcicek, E. E., Lam, T. T., Wu, T., Bjornson, R. D., Bruce, C., Nairn, A. C., Rinehart, J., Miller, P. L., & Williams, K. R. (2015). YPED: An Integrated Bioinformatics Suite and Database for Mass Spectrometry-based Proteomics Research. *Genomics, Proteomics & Bioinformatics*, *13*(1), 25–35. https://doi.org/10.1016/j.gpb.2014.11.002
41. Conrath, U., Pieterse, C. M. J., & Mauch-Mani, B. (2002). Priming in plant–pathogen interactions. *Trends in Plant Science*, *7*(5), 210–216. https://doi.org/10.1016/S1360-1385(02)02244-6
42. Cruz Castillo, M., Martínez, C., Buchala, A., Métraux, J.-P., & León, J. (2004). Gene-specific involvement of beta-oxidation in wound-activated responses in Arabidopsis. *Plant Physiology*, *135*(1), 85–94. https://doi.org/10.1104/pp.104.039925
43. Cvetkovska, M., & Vanlerberghe, G. C. (2013). Alternative oxidase impacts the plant response to biotic stress by influencing the mitochondrial generation of reactive oxygen species. *Plant, Cell & Environment*, *36*(3), 721–732. https://doi.org/10.1111/pce.12009
44. Dadáková, K., Heinrichová, T., Lochman, J., & Kašparovský, T. (2020). Production of Defense Phenolics in Tomato Leaves of Different Age. *Molecules*, *25*(21), Article 21. https://doi.org/10.3390/molecules25214952
45. Damgaard, R. B. (2021). The ubiquitin system: From cell signalling to disease biology and new therapeutic opportunities. *Cell Death & Differentiation*, *28*(2), Article 2. https://doi.org/10.1038/s41418-020-00703-w
46. Dancy, B. C. R., Chen, S.-W., Drechsler, R., Gafken, P. R., & Olsen, C. P. (2015). 13C- and 15N-Labeling Strategies Combined with Mass Spectrometry Comprehensively Quantify Phospholipid Dynamics in C. elegans. *PLOS ONE*, *10*(11), e0141850. https://doi.org/10.1371/journal.pone.0141850

47. De Vries, D. P., & Dubois, L. A. M. (1988). The effect of BAP and IBA on sprouting and adventitious root formation of 'Amanda' rose single-node softwood cuttings. *Scientia Horticulturae*, *34*(1), 115–121. https://doi.org/10.1016/0304-4238(88)90081-7
48. Doroodian, P., & Hua, Z. (2021). The Ubiquitin Switch in Plant Stress Response. *Plants (Basel, Switzerland)*, *10*(2), 246. https://doi.org/10.3390/plants10020246
49. Dreger, M., & Szalata, M. (2022). The Effect of TIBA and NPA on Shoot Regeneration of Cannabis sativa L. Epicotyl Explants. *Agronomy*, *12*(1), Article 1. https://doi.org/10.3390/agronomy12010104
50. Dumancas, G. G. (2014). Picloram. In P. Wexler (Ed.), *Encyclopedia of Toxicology (Third Edition)* (pp. 948–951). Academic Press. https://doi.org/10.1016/B978-0-12-386454-3.00185-8
51. El-Shourbagy, M. N., A, B., Ghaffar, A., & El-Naggar, R. A. (1995). Effect of IAA and GA3 on the Anatomical Characteristics, Straw and Fiber Yield and Quality of Flax. *Journal of Agronomy and Crop Science*, *174*(1), 21–26. https://doi.org/10.1111/j.1439-037X.1995.tb00190.x
52. Eng, J. K., McCormack, A. L., & Yates, J. R. (1994). An approach to correlate tandem mass spectral data of peptides with amino acid sequences in a protein database. *Journal of the American Society for Mass Spectrometry*, *5*(11), 976–989. https://doi.org/10.1016/1044-0305(94)80016-2
53. Esteban, R., Royo, B., Urarte, E., Zamarreño, Á. M., Garcia-Mina, J. M., & Moran, J. F. (2016). Both Free Indole-3-Acetic Acid and Photosynthetic Performance are Important Players in the Response of *Medicago truncatula* to Urea and Ammonium Nutrition Under Axenic Conditions. *Frontiers in Plant Science*, *7*, 140. https://doi.org/10.3389/fpls.2016.00140
54. Fan, Y. Q., & Petitt, F. L. (1994). Biological Control of Broad Mite, *Polyphagotarsonemus latus* (Banks), by *Neoseiulus barkeri* Hughes on Pepper. *Biological Control*, *4*(4), Article 4. https://doi.org/10.1006/bcon.1994.1049
55. Fang Zhu, X., Sheng Zhao, X., Wu, Q., & Fang Shen, R. (2018). Abscisic acid is involved in root cell wall phosphorus remobilization independent of nitric oxide and ethylene in rice (*Oryza sativa*). *Annals of Botany*, *121*(7), 1361–1368. https://doi.org/10.1093/aob/mcy034
56. Fernández-Escalada, M., Zulet-González, A., Gil-Monreal, M., Royuela, M., & Zabalza, A. (2019). Physiological performance of glyphosate and imazamox mixtures on *Amaranthus palmeri* sensitive and resistant to glyphosate. *Scientific Reports*, *9*, 18225. https://doi.org/10.1038/s41598-019-54642-9
57. Finkelstein, R. R., & Gibson, S. I. (2002). ABA and sugar interactions regulating development: Cross-talk or voices in a crowd? *Current Opinion in Plant Biology*, *5*(1), 26–32. https://doi.org/10.1016/s1369-5266(01)00225-4
58. Fisher, D. A., Bayer, D. E., & Weier, T. E. (1968). Morphological and Anatomical Effects of Picloram on *Phaseolus vulgaris*. *Botanical Gazette*, *129*(1), 67–70.
59. Florencio-Ortiz, V., Sellés-Marchart, S., & Casas, J. L. (2021). Proteome changes in pepper (*Capsicum annuum* L.) leaves induced by the green peach aphid (*Myzus persicae* Sulzer). *BMC Plant Biology*, *21*(1), 12. https://doi.org/10.1186/s12870-020-02749-x

60. Frei dit Frey, N., Garcia, A. V., Bigeard, J., Zaag, R., Bueso, E., Garmier, M., Pateyron, S., de Tauzia-Moreau, M.-L., Brunaud, V., Balzergue, S., Colcombet, J., Aubourg, S., Martin-Magniette, M.-L., & Hirt, H. (2014). Functional analysis of Arabidopsisimmune-related MAPKs uncovers a role for MPK3 as negative regulator of inducible defences. *Genome Biology*, *15*(6), R87. https://doi.org/10.1186/gb-2014-15-6-r87
61. Furlan, G., Nakagami, H., Eschen-Lippold, L., Jiang, X., Majovsky, P., Kowarschik, K., Hoehenwarter, W., Lee, J., & Trujillo, M. (2017). Changes in PUB22 Ubiquitination Modes Triggered by MITOGEN-ACTIVATED PROTEIN KINASE3 Dampen the Immune Response[CC-BY]. *The Plant Cell*, *29*(4), 726–745. https://doi.org/10.1105/tpc.16.00654
62. Gaines, T. A., Duke, S. O., Morran, S., Rigon, C. A. G., Tranel, P. J., Küpper, A., & Dayan, F. E. (2020). Mechanisms of evolved herbicide resistance. *The Journal of Biological Chemistry*, *295*(30), 10307–10330. https://doi.org/10.1074/jbc.REV120.013572
63. Gantait, S., & Mahanta, M. (2021). Picloram-induced enhanced callus-mediated regeneration, acclimatization, and genetic clonality assessment of gerbera. *Journal of Genetic Engineering & Biotechnology*, *19*, 175. https://doi.org/10.1186/s43141-021-00269-1
64. Gant-Branum, R. L., Kerr, T. J., & McLean, J. A. (2009). Labeling strategies in mass spectrometry-based protein quantitation. *Analyst*, *134*(8), 1525–1530. https://doi.org/10.1039/B904643G
65. Gayatri, G., Agurla, S., & Raghavendra, A. S. (2013). Nitric oxide in guard cells as an important secondary messenger during stomatal closure. *Frontiers in Plant Science*, *4*. https://doi.org/10.3389/fpls.2013.00425
66. Gerson, U. (1992). Biology and control of the broad mite,*Polyphagotarsonemus latus* (Banks) (Acari: Tarsonemidae). *Experimental & Applied Acarology*, *13*(3), 163–178. https://doi.org/10.1007/BF01194934
67. Ghanashyam, C., & Jain, M. (2009). Role of auxin-responsive genes in biotic stress responses. *Plant Signaling & Behavior*, *4*(9), 846–848.
68. Ghorashy, S. R., Colville, W. L., & Ashworth, D. L. (1969). Effects of 2,3,5-Triiodobenzoic Acid on the Morphology and Anatomy of *Glycine max* (L.) Merrill1. *Crop Science*, *9*(4), cropsci1969.0011183X000900040001x. https://doi.org/10.2135/cropsci1969.0011183X000900040001x
69. Gleason, C., Foley, R. C., & Singh, K. B. (2011). Mutant Analysis in Arabidopsis Provides Insight into the Molecular Mode of Action of the Auxinic Herbicide Dicamba. *PLoS ONE*, *6*(3), e17245. https://doi.org/10.1371/journal.pone.0017245
70. González-Gordo, S., Palma, J. M., & Corpas, F. J. (2022). Peroxisomal Proteome Mining of Sweet Pepper (C*apsicum annuum* L.) Fruit Ripening Through Whole Isobaric Tags for Relative and Absolute Quantitation Analysis. *Frontiers in Plant Science*, *13*, 893376. https://doi.org/10.3389/fpls.2022.893376
71. Gorelova, V., De Lepeleire, J., Van Daele, J., Pluim, D., Meï, C., Cuypers, A., Leroux, O., Rébeillé, F., Schellens, J. H. M., Blancquaert, D., Stove, C. P., & Van Der Straeten, D. (2017). Dihydrofolate Reductase/Thymidylate Synthase Fine-Tunes the Folate Status

and Controls Redox Homeostasis in Plants. *The Plant Cell*, *29*(11), 2831–2853. https://doi.org/10.1105/tpc.17.00433

72. Grace, S. C., & Logan, B. A. (2000). Energy dissipation and radical scavenging by the plant phenylpropanoid pathway. *Philosophical Transactions of the Royal Society B: Biological Sciences*, *355*(1402), 1499–1510.
73. Gray, R. A. (1957). Alteration of Leaf Size and Shape and Other Changes Caused by Gibberellins in Plants. *American Journal of Botany*, *44*(8), 674–682. https://doi.org/10.2307/2438632
74. Grinberg, M., Perl-Treves, R., Palevsky, E., Shomer, I., & Soroker, V. (2005). Interaction between cucumber plants and the broad mite, *Polyphagotarsonemus latus*: From damage to defense gene expression. *Entomologia Experimentalis et Applicata*, *115*(1), Article 1. https://doi.org/10.1111/j.1570-7458.2005.00275.x
75. Gronwald, J. W. (1997). Resistance to PS II Inhibitor Herbicides. In R. De Prado, J. Jorrín, & L. García-Torres (Eds.), *Weed and Crop Resistance to Herbicides* (pp. 53–59). Springer Netherlands. https://doi.org/10.1007/978-94-011-5538-0_5
76. Gu, J., Ma, S., Zhang, Y., Wang, D., Cao, S., & Wang, Z.-Y. (2020). Genome-Wide Identification of Cassava Serine/Arginine-Rich Proteins: Insights into Alternative Splicing of Pre-mRNAs and Response to Abiotic Stress. *Plant & Cell Physiology*, *61*(1), 178–191. https://doi.org/10.1093/pcp/pcz190
77. Gururani, M. A., Mohanta, T. K., & Bae, H. (2015). Current Understanding of the Interplay between Phytohormones and Photosynthesis under Environmental Stress. *International Journal of Molecular Sciences*, *16*(8), 19055–19085. https://doi.org/10.3390/ijms160819055
78. Guschina, I. A., Everard, J. D., Kinney, A. J., Quant, P. A., & Harwood, J. L. (2014). Studies on the regulation of lipid biosynthesis in plants: Application of control analysis to soybean. *Biochimica et Biophysica Acta (BBA) - Biomembranes*, *1838*(6), 1488–1500. https://doi.org/10.1016/j.bbamem.2014.02.008
79. Hanus-Fajerska, E. (2006). Improvement of growth parameters of prune callus cultures destined to initiate cell suspensions. *Acta Societatis Botanicorum Poloniae*, *75*(1), Article 1. https://doi.org/10.5586/asbp.2006.001
80. Hardtke, C. S., Gohda, K., Osterlund, M. T., Oyama, T., Okada, K., & Deng, X. W. (2000). HY5 stability and activity in Arabidopsis is regulated by phosphorylation in its COP1 binding domain. *The EMBO Journal*, *19*(18), 4997–5006. https://doi.org/10.1093/emboj/19.18.4997
81. Hartung, W., Sauter, A., & Hose, E. (2002). Abscisic acid in the xylem: Where does it come from, where does it go to? *Journal of Experimental Botany*, *53*(366), 27–32. https://doi.org/10.1093/jexbot/53.366.27
82. Hildebrandt, T. M., Nunes Nesi, A., Araújo, W. L., & Braun, H.-P. (2015). Amino Acid Catabolism in Plants. *Molecular Plant*, *8*(11), 1563–1579. https://doi.org/10.1016/j.molp.2015.09.005
83. Hönig, M., Plíhalová, L., Husičková, A., Nisler, J., & Doležal, K. (2018). Role of Cytokinins in Senescence, Antioxidant Defence and Photosynthesis. *International Journal of Molecular Sciences*, *19*(12), Article 12. https://doi.org/10.3390/ijms19124045

84. Hou, B.-Z., Li, C.-L., Han, Y.-Y., & Shen, Y.-Y. (2018). Characterization of the hot pepper (*Capsicum frutescens*) fruit ripening regulated by ethylene and ABA. *BMC Plant Biology*, *18*(1), 162. https://doi.org/10.1186/s12870-018-1377-3
85. Hutson, S. (2001). Structure and function of branched chain aminotransferases. In *Progress in Nucleic Acid Research and Molecular Biology* (Vol. 70, pp. 175–206). Academic Press. https://doi.org/10.1016/S0079-6603(01)70017-7
86. Hynes, D. P. (2012). Effects of low dose applications of 2,4-D and dicamba on Cucurbitaceae and Solanaceae vegetables. *Theses and Dissertations Available from ProQuest*, 1–129.
87. Ichimura, K., Shinozaki, K., Tena, G., Sheen, J., Henry, Y., Champion, A., Kreis, M., Zhang, S., Hirt, H., Wilson, C., Walker, J. C. (2002). Mitogen-activated protein kinase cascades in plants: A new nomenclature. *Trends in Plant Science*, *7*(7), 301–308. https://doi.org/10.1016/S1360-1385(02)02302-6
88. Inada, S., Tominaga, M., & Shimmen, T. (2000). Regulation of root growth by gibberellin in Lemna minor. *Plant & Cell Physiology*, *41*(6), 657–665. https://doi.org/10.1093/pcp/41.6.657
89. Iqbal, N., Khan, N. A., Ferrante, A., Trivellini, A., Francini, A., & Khan, M. I. R. (2017). Ethylene Role in Plant Growth, Development and Senescence: Interaction with Other Phytohormones. *Frontiers in Plant Science*, *8*. https://www.frontiersin.org/articles/10.3389/fpls.2017.00475
90. Irigoyen, J. J., Einerich, D. W., & Sánchez-Díaz, M. (1992). Water stress induced changes in concentrations of proline and total soluble sugars in nodulated alfalfa (*Medicago sativa*) plants. *Physiologia Plantarum*, *84*(1), 55–60. https://doi.org/10.1111/j.1399-3054.1992.tb08764.x
91. Isensee, A. R., Jones, G. E., & Turner, B. C. (1971). Root Absorption and Translocation of Picloram by Oats and Soybeans. *Weed Science*, *19*(6), 727–731.
92. Iwaniuk, P., & Lozowicka, B. (2022). Biochemical compounds and stress markers in lettuce upon exposure to pathogenic Botrytis cinerea and fungicides inhibiting oxidative phosphorylation. *Planta*, *255*(3), 61. https://doi.org/10.1007/s00425-022-03838-x
93. Jagodzik, P., Tajdel-Zielinska, M., Ciesla, A., Marczak, M., & Ludwikow, A. (2018). Mitogen-Activated Protein Kinase Cascades in Plant Hormone Signaling. *Frontiers in Plant Science*, *9*. https://www.frontiersin.org/articles/10.3389/fpls.2018.01387
94. Jalmi, S. K., & Sinha, A. K. (2015a). ROS mediated MAPK signaling in abiotic and biotic stress- striking similarities and differences. *Frontiers in Plant Science*, *6*. https://doi.org/10.3389/fpls.2015.00769
95. Jalmi, S. K., & Sinha, A. K. (2015b). ROS mediated MAPK signaling in abiotic and biotic stress- striking similarities and differences. *Frontiers in Plant Science*, *6*, 769. https://doi.org/10.3389/fpls.2015.00769
96. Jan, R., Asaf, S., Numan, M., Lubna, & Kim, K.-M. (2021). Plant Secondary Metabolite Biosynthesis and Transcriptional Regulation in Response to Biotic and Abiotic Stress Conditions. *Agronomy*, *11*(5), Article 5. https://doi.org/10.3390/agronomy11050968
97. Jaswanthi, N., Krishna, M. S. R., Sahitya, U. L., & Suneetha, P. (2019). Apoplast proteomic analysis reveals drought stress-responsive protein datasets in chilli (*Capsicum annuum* L.). *Data in Brief*, *25*, 104041. https://doi.org/10.1016/j.dib.2019.104041

98. Jenks, M. A., Eigenbrode, S. D., & Lemieux, B. (2002). Cuticular Waxes of Arabidopsis. *The Arabidopsis Book / American Society of Plant Biologists*, *1*. https://doi.org/10.1199/tab.0016
99. Jeong, K., Kim, S., & Bandeira, N. (2012). False discovery rates in spectral identification. *BMC Bioinformatics*, *13*(Suppl 16), S2. https://doi.org/10.1186/1471-2105-13-S16-S2
100. Jha, S. K., Sharma, M., & Pandey, G. K. (2016). Role of Cyclic Nucleotide Gated Channels in Stress Management in Plants. *Current Genomics*, *17*(4), Article 4. https://doi.org/10.2174/1389202917666160331202125
101. Jing, H.-C., Schippers, J. H. M., Hille, J., & Dijkwel, P. P. (2005). Ethylene-induced leaf senescence depends on age-related changes and OLD genes in Arabidopsis. *Journal of Experimental Botany*, *56*(421), 2915–2923. https://doi.org/10.1093/jxb/eri287
102. Jones, K. A., Kim, P. D., Patel, B. B., Kelsen, S. G., Braverman, A., Swinton, D. J., Gafken, P. R., Jones, L. A., Lane, W. S., Yeung, A. T. (2013). Immunodepletion plasma proteomics by tripleTOF 5600 and Orbitrap elite/LTQ-Orbitrap Velos/Q exactive mass spectrometers. *Journal of Proteome Research*, *12*(10), 4351–4365. https://doi.org/10.1021/pr400307u
103. Jones, R. L., & Kaufman, P. B. (1983). The role of gibberellins in plant cell elongation. *Critical Reviews in Plant Sciences*, *1*(1), 23–47. https://doi.org/10.1080/07352688309382170
104. Kamble, S. I. (2013). Effect of Agrochemical (2,4-D) on Anatomical Aspects of *Cassia tora* Linn. *Biosciences Biotechnology Research Asia*, *10*(2). https://www.biotech-asia.org/vol10no2/effect-of-agrochemical-24-d-on-anatomical-aspects-of-cassia-tora-linn/
105. Karabaghli-Degron, C., Sotta, B., Bonnet, M., Gay, G., & LE Tacon, F. (1998). The auxin transport inhibitor 2,3,5-triiodobenzoic acid (TIBA) inhibits the stimulation of in vitro lateral root formation and the colonization of the tap-root cortex of Norway spruce (*Picea abies*) seedlings by the ectomycorrhizal fungus *Laccaria bicolor*. *The New Phytologist*, *140*(4), 723–733. https://doi.org/10.1046/j.1469-8137.1998.00307.x
106. Karve, A., Xia, X., & Moore, B. d. (2012). Arabidopsis Hexokinase-Like1 and Hexokinase1 Form a Critical Node in Mediating Plant Glucose and Ethylene Responses1[C][W][OA]. *Plant Physiology*, *158*(4), 1965–1975. https://doi.org/10.1104/pp.112.195636
107. Kathare, P. K., Dharmasiri, S., Vincill, E. D., Routray, P., Ahmad, I., Roberts, D. M., & Dharmasiri, N. (2020). Arabidopsis PIC30 encodes a major facilitator superfamily transporter responsible for the uptake of picolinate herbicides. *The Plant Journal: For Cell and Molecular Biology*, *102*(1), 18–33. https://doi.org/10.1111/tpj.14608
108. Kedare, S. B., & Singh, R. P. (2011). Genesis and development of DPPH method of antioxidant assay. *Journal of Food Science and Technology*, *48*(4), 412–422. https://doi.org/10.1007/s13197-011-0251-1
109. Kempa, S., Krasensky, J., Dal Santo, S., Kopka, J., & Jonak, C. (2008). A Central Role of Abscisic Acid in Stress-Regulated Carbohydrate Metabolism. *PLoS ONE*, *3*(12), e3935. https://doi.org/10.1371/journal.pone.0003935
110. Khadr, A., Wang, G.-L., Wang, Y.-H., Zhang, R.-R., Wang, X.-R., Xu, Z.-S., Tian, Y.-S., & Xiong, A.-S. (2020). Effects of auxin (indole-3-butyric acid) on growth characteristics,

lignification, and expression profiles of genes involved in lignin biosynthesis in carrot taproot. *PeerJ*, *8*, e10492. https://doi.org/10.7717/peerj.10492

111. Kim, H., & Lim, J. (2019). Leaf-induced callus formation in two cultivars: Hot pepper "CM334" and bell pepper "Dempsey." *Plant Signaling & Behavior*, *14*(7), 1604016. https://doi.org/10.1080/15592324.2019.1604016
112. Kisa, D., İmamoğlu, R., Genç, N., Şahin, S., Qayyum, M. A., & Elmastaş, M. (2021). The interactive effect of aromatic amino acid composition on the accumulation of phenolic compounds and the expression of biosynthesis-related genes in *Ocimum basilicum*. *Physiology and Molecular Biology of Plants: An International Journal of Functional Plant Biology*, *27*(9), 2057–2069. https://doi.org/10.1007/s12298-021-01068-1
113. Klepzig, K. D., Kruger, E. L., Smalley, E. B., & Raffa, K. F. (1995). Effects of biotic and abiotic stress on induced accumulation of terpenes and phenolics in red pines inoculated with bark beetle-vectored fungus. *Journal of Chemical Ecology*, *21*(5), 601–626. https://doi.org/10.1007/BF02033704
114. Klessig, D. F., Choi, H. W., & Dempsey, D. A. (2018). Systemic Acquired Resistance and Salicylic Acid: Past, Present, and Future. *Molecular Plant-Microbe Interactions®*, *31*(9), 871–888. https://doi.org/10.1094/MPMI-03-18-0067-CR
115. Ku, Y.-S., Sintaha, M., Cheung, M.-Y., & Lam, H.-M. (2018). Plant Hormone Signaling Crosstalks between Biotic and Abiotic Stress Responses. *International Journal of Molecular Sciences*, *19*(10). https://doi.org/10.3390/ijms19103206
116. Kumar, A., Sharma, A., Vishwakarma, N., & Singh, M. (2018). Study of Cost Economics of Management of Chilli Mites through Abamectin 1.8 EC. *International Journal of Current Microbiology and Applied Sciences*, *7*(9), 1659–1663. https://doi.org/10.20546/ijcmas.2018.709.200
117. Kumar, R. R., Arora, K., Goswami, S., Sakhare, A., Singh, B., Chinnusamy, V., & Praveen, S. (2020). MAPK Enzymes: A ROS Activated Signaling Sensors Involved in Modulating Heat Stress Response, Tolerance and Grain Stability of Wheat under Heat Stress. *3 Biotech*, *10*(9), 380. https://doi.org/10.1007/s13205-020-02377-0
118. Kumar, U., Mishra, M., & Prakash, V. (2012). Assessment of antioxidant enzymes and free radical scavenging activity of selected medicinal plants. *Free Radicals and Antioxidants*, *2*(3), 58–63. https://doi.org/10.5530/ax.2012.3.8
119. Kunze, G., Zipfel, C., Robatzek, S., Niehaus, K., Boller, T., & Felix, G. (2004). The N Terminus of Bacterial Elongation Factor Tu Elicits Innate Immunity in Arabidopsis Plants. *The Plant Cell*, *16*(12), Article 12. https://doi.org/10.1105/tpc.104.026765
120. Kupferschmied, P., Maurhofer, M., & Keel, C. (2013). Promise for plant pest control: Root-associated pseudomonads with insecticidal activities. *Frontiers in Plant Science*, *4*, 287. https://doi.org/10.3389/fpls.2013.00287
121. Langens-Gerrits, M., De Klerk, G.-J., & Croes, A. (2003). Phase change in lily bulblets regenerated in vitro. *Physiologia Plantarum*, *119*(4), 590–597. https://doi.org/10.1046/j.1399-3054.2003.00214.x
122. Lara, I., Heredia, A., & Domínguez, E. (2019). Shelf Life Potential and the Fruit Cuticle: The Unexpected Player. *Frontiers in Plant Science*, *10*, 770. https://doi.org/10.3389/fpls.2019.00770

123. Larrieu, A., & Vernoux, T. (2016). Q&A: How does jasmonate signaling enable plants to adapt and survive? *BMC Biology*, *14*(1), 79. https://doi.org/10.1186/s12915-016-0308-8
124. Lecourieux, D., Ranjeva, R., & Pugin, A. (2006). Calcium in plant defence-signalling pathways. *The New Phytologist*, *171*(2), Article 2. https://doi.org/10.1111/j.1469-8137.2006.01777.x
125. Lee, Y., Kim, Y. J., Kim, M.-H., & Kwak, J. M. (2016). MAPK Cascades in Guard Cell Signal Transduction. *Frontiers in Plant Science*, *7*, 80. https://doi.org/10.3389/fpls.2016.00080
126. LeFors, J. A., Johnson, D. T., & Woodruff, T. (2017). Acaricidal Control of Broad Mites in Blackberry, 2016. *Arthropod Management Tests*, *42*(1), tsx113. https://doi.org/10.1093/amt/tsx113
127. Leus, L., Luypaert, G., Dhooghe, E., Witters, J., Pauwels, E., Van Poucke, C., Van Pamel, E., Van Huylenbroeck, J., & Audenaert, J. (2022). Jasmonic Acid and Salicylic Acid Levels in Defense Response of Azalea (*Rhododendron simsii* Hybrid) to Broad Mite (*Polyphagotarsonemus latus*). *Horticulturae*, *8*(9), Article 9. https://doi.org/10.3390/horticulturae8090840
128. Li, N., Han, X., Feng, D., Yuan, D., & Huang, L.-J. (2019). Signaling Crosstalk between Salicylic Acid and Ethylene/Jasmonate in Plant Defense: Do We Understand What They Are Whispering? *International Journal of Molecular Sciences*, *20*(3), 671. https://doi.org/10.3390/ijms20030671
129. Li, P., Liu, W., Zhang, Y., Xing, J., Li, J., Feng, J., Su, X., & Zhao, J. (2019). Fungal canker pathogens trigger carbon starvation by inhibiting carbon metabolism in poplar stems. *Scientific Reports*, *9*. https://doi.org/10.1038/s41598-019-46635-5
130. Liao, H., Wen, X., Deng, X., Wu, Y., Xu, J., Li, X., Zhou, S., Li, X., Zhu, C., Luo, F., Ma, Y., & Zheng, J. (2022). Integrated proteomic and metabolomic analyses reveal significant changes in chloroplasts and mitochondria of pepper (*Capsicum annuum* L.) during *Sclerotium rolfsii* infection. *Journal of Microbiology (Seoul, Korea)*, *60*(5), 511–525. https://doi.org/10.1007/s12275-022-1603-4
131. Liechti, R., & Farmer, E. E. (2006). Jasmonate biochemical pathway. *Science's STKE: Signal Transduction Knowledge Environment*, *2006*(322), cm3. https://doi.org/10.1126/stke.3222006cm3
132. Liu, B., Jiang, Y., Tang, H., Tong, S., Lou, S., Shao, C., Zhang, J., Song, Y., Chen, N., Bi, H., Zhang, H., Li, J., Liu, J., & Liu, H. (2021). The ubiquitin E3 ligase SR1 modulates the submergence response by degrading phosphorylated WRKY33 in Arabidopsis. *The Plant Cell*, *33*(5), 1771–1789. https://doi.org/10.1093/plcell/koab062
133. Liu, C., Yu, H., Rao, X., Li, L., & Dixon, R. A. (2021). Abscisic acid regulates secondary cell-wall formation and lignin deposition in Arabidopsis thaliana through phosphorylation of NST1. *Proceedings of the National Academy of Sciences of the United States of America*, *118*(5), e2010911118. https://doi.org/10.1073/pnas.2010911118
134. Liu, S., Hua, L., Dong, S., Chen, H., Zhu, X., Jiang, J., Zhang, F., Li, Y., Fang, X., & Chen, F. (2015). OsMAPK6, a mitogen-activated protein kinase, influences rice grain size and biomass production. *The Plant Journal*, *84*(4), 672–681. https://doi.org/10.1111/tpj.13025

135. Liu, S.-R., Zhou, J.-J., Hu, C.-G., Wei, C.-L., & Zhang, J.-Z. (2017). MicroRNA-Mediated Gene Silencing in Plant Defense and Viral Counter-Defense. *Frontiers in Microbiology*, *8*. https://doi.org/10.3389/fmicb.2017.01801
136. Liu, Y.-H., Song, Y.-H., & Ruan, Y.-L. (2022). Sugar conundrum in plant–pathogen interactions: Roles of invertase and sugar transporters depend on pathosystems. *Journal of Experimental Botany*, *73*(7), 1910–1925. https://doi.org/10.1093/jxb/erab562
137. Liu, Z., Lv, J., Liu, Y., Wang, J., Zhang, Z., Chen, W., Song, J., Yang, B., Tan, F., Zou, X., & Ou, L. (2020). Comprehensive Phosphoproteomic Analysis of Pepper Fruit Development Provides Insight into Plant Signaling Transduction. *International Journal of Molecular Sciences*, *21*(6), 1962. https://doi.org/10.3390/ijms21061962
138. Liu, Z., Song, J., Miao, W., Yang, B., Zhang, Z., Chen, W., Tan, F., Suo, H., Dai, X., Zou, X., & Ou, L. (2021). Comprehensive Proteome and Lysine Acetylome Analysis Reveals the Widespread Involvement of Acetylation in Cold Resistance of Pepper (*Capsicum annuum* L.). *Frontiers in Plant Science*, *12*, 730489. https://doi.org/10.3389/fpls.2021.730489
139. Liu, Z., Yang, B., Huang, R., Suo, H., Zhang, Z., Chen, W., Dai, X., Zou, X., & Ou, L. (2022). Transcriptome- and proteome-wide Association of Real Isogenic Line Populations Identified Twelve Core QTLs for four fruit traits in pepper (*Capsicum annuum* L.). *Horticulture Research*, *9*, uhac015. https://doi.org/10.1093/hr/uhac015
140. Lobo, L. L. B., de Andrade da Silva, M. S. R., Castellane, T. C. L., Carvalho, R. F., & Rigobelo, E. C. (2022). Effect of Indole-3-Acetic Acid on Tomato Plant Growth. *Microorganisms*, *10*(11), Article 11. https://doi.org/10.3390/microorganisms10112212
141. Love, J., Björklund, S., Vahala, J., Hertzberg, M., Kangasjärvi, J., & Sundberg, B. (2009). Ethylene is an endogenous stimulator of cell division in the cambial meristem of Populus. *Proceedings of the National Academy of Sciences of the United States of America*, *106*(14), 5984–5989. https://doi.org/10.1073/pnas.0811660106
142. Lukesh, J. C. I., Palte, M. J., & Raines, R. T. (2012). A Potent, Versatile Disulfide-Reducing Agent from Aspartic Acid. *Journal of the American Chemical Society*, *134*(9), 4057–4059. https://doi.org/10.1021/ja211931f
143. Luypaert, G., Witters, J., Van Huylenbroeck, J., Maes, M., De Riek, J., & De Clercq, P. (2014). Temperature-dependent development of the broad mite *Polyphagotarsonemus latus* (Acari: Tarsonemidae) on Rhododendron simsii. *Experimental & Applied Acarology*, *63*(3), 389–400. https://doi.org/10.1007/s10493-014-9777-z
144. Ma, K.-W., & Ma, W. (2016). Phytohormone pathways as targets of pathogens to facilitate infection. *Plant Molecular Biology*, *91*, 713–725. https://doi.org/10.1007/s11103-016-0452-0
145. Magalhaes, A. C., & Ashton, F. M. (1969). Effect of Dicamba on Oxygen Uptake and Cell Membrane Permeability in Leaf Tissue of *Cyperus Rotundus* L. *Weed Research*, *9*(1), 48–52. https://doi.org/10.1111/j.1365-3180.1969.tb01448.x
146. Maldonado-Torres, M., López-Hernández, J. F., Jiménez-Sandoval, P., & Winkler, R. (2014). "Plug and Play" assembly of a low-temperature plasma ionization mass spectrometry imaging (LTP-MSI) system. *Journal of Proteomics*, *102*, 60–65. https://doi.org/10.1016/j.jprot.2014.03.003

147. Malheiros, R. S. P., Costa, L. C., Ávila, R. T., Pimenta, T. M., Teixeira, L. S., Brito, F. A. L., Zsögön, A., Araújo, W. L., & Ribeiro, D. M. (2019). Selenium downregulates auxin and ethylene biosynthesis in rice seedlings to modify primary metabolism and root architecture. *Planta*, *250*(1), 333–345. https://doi.org/10.1007/s00425-019-03175-6
148. Mandadi, K. K., Petrillo, E., Dubrovina, A. S., & Kiselev, K. V. (2023). Editorial: Regulation of alternative splicing in plant stress responses. *Frontiers in Plant Science*, *13*. https://www.frontiersin.org/articles/10.3389/fpls.2022.1120961
149. Manivannan, A., Soundararajan, P., Muneer, S., Ko, C. H., & Jeong, B. R. (2016). Silicon Mitigates Salinity Stress by Regulating the Physiology, Antioxidant Enzyme Activities, and Protein Expression in *Capsicum annuum* "Bugwang." *BioMed Research International*, *2016*, 3076357. https://doi.org/10.1155/2016/3076357
150. Manoharan, R., Tripathi, J. N., & Tripathi, L. (2016). Plant regeneration from axillary bud derived callus in white yam (*Dioscorea rotundata*). *Plant Cell, Tissue and Organ Culture (PCTOC)*, *126*(3), 481–497. https://doi.org/10.1007/s11240-016-1017-2
151. Marullo, R., Mercati, F., & Vono, G. (2020). DNA Barcoding: A Reliable Method for the Identification of Thrips Species (Thysanoptera, Thripidae) Collected on Sticky Traps in Onion Fields. *Insects*, *11*(8), Article 8. https://doi.org/10.3390/insects11080489
152. *Matrix Science—Mascot—Peptide Mass Fingerprint*. (2015). http://www.matrixscience.com/cgi/search_form.pl?FORMVER=2&SEARCH=PMF
153. Mayzlish-Gati, E., LekKala, S. P., Resnick, N., Wininger, S., Bhattacharya, C., Lemcoff, J. H., Kapulnik, Y., & Koltai, H. (2010). Strigolactones are positive regulators of light-harvesting genes in tomato. *Journal of Experimental Botany*, *61*(11), 3129–3136. https://doi.org/10.1093/jxb/erq138
154. McAdam, S. A. M., & Brodribb, T. J. (2018). Mesophyll Cells Are the Main Site of Abscisic Acid Biosynthesis in Water-Stressed Leaves1. *Plant Physiology*, *177*(3), 911–917. https://doi.org/10.1104/pp.17.01829
155. McMurtry, J. A., Badii, M. H., & Johnson, H. G. (1984). The broad mite,*Polyphagotarsonemus* latus, as a potential prey for phytoseiid mites in California. *Entomophaga*, *29*(1), 83–86. https://doi.org/10.1007/BF02372212
156. Meng, X., & Zhang, S. (2013). MAPK Cascades in Plant Disease Resistance Signaling. *Annual Review of Phytopathology*, *51*(1), Article 1. https://doi.org/10.1146/annurev-phyto-082712-102314
157. Mertens, E., Marcellin, P., Van Schaftingen, E., & Hers, H. G. (1987). Effect of ethylene treatment on the concentration of fructose-2,6-bisphosphate and on the activity of phosphofructokinase 2/fructose-2,6-bisphosphatase in banana. *European Journal of Biochemistry*, *167*(3), 579–583. https://doi.org/10.1111/j.1432-1033.1987.tb13375.x
158. Meza, A., Rojas, P., Cely-Veloza, W., Guerrero-Perilla, C., & Coy-Barrera, E. (2020). Variation of isoflavone content and DPPH scavenging capacity of phytohormone-treated seedlings after in vitro germination of cape broom (*Genista monspessulana*). *South African Journal of Botany*, *130*, 64–74. https://doi.org/10.1016/j.sajb.2019.12.006
159. Milac, T. I., Randolph, T. W., & Wang, P. (2012). Analyzing LC-MS/MS data by spectral count and ion abundance: Two case studies. *Statistics and Its Interface*, *5*(1), 75–87. https://doi.org/10.4310/SII.2012.v5.n1.a7

160. Mizuno, T. (1998). His-Asp phosphotransfer signal transduction. *Journal of Biochemistry*, *123*(4), 555–563.
161. Moffatt, B. A., & Ashihara, H. (2002). Purine and Pyrimidine Nucleotide Synthesis and Metabolism. *The Arabidopsis Book / American Society of Plant Biologists*, *1*, e0018. https://doi.org/10.1199/tab.0018
162. Morkunas, I., & Ratajczak, L. (2014). The role of sugar signaling in plant defense responses against fungal pathogens. *Acta Physiologiae Plantarum*, *36*(7), 1607–1619. https://doi.org/10.1007/s11738-014-1559-z
163. Moura, J. C. M. S., Bonine, C. A. V., de Oliveira Fernandes Viana, J., Dornelas, M. C., & Mazzafera, P. (2010). Abiotic and biotic stresses and changes in the lignin content and composition in plants. *Journal of Integrative Plant Biology*, *52*(4), 360–376. https://doi.org/10.1111/j.1744-7909.2010.00892.x
164. Mourgues, F., Brisset, M.-N., & Chevreau, E. (1998). Strategies to improve plant resistance to bacterial diseases through genetic engineering. *Trends in Biotechnology*, *16*(5), 203–210. https://doi.org/10.1016/S0167-7799(98)01189-5
165. Muhammad Aslam, M., Waseem, M., Jakada, B. H., Okal, E. J., Lei, Z., Saqib, H. S. A., Yuan, W., Xu, W., & Zhang, Q. (2022). Mechanisms of Abscisic Acid-Mediated Drought Stress Responses in Plants. *International Journal of Molecular Sciences*, *23*(3), 1084. https://doi.org/10.3390/ijms23031084
166. Muniandi, S. K. M., Hossain, Md. A., Abdullah, Mohd. P., & Ab Shukor, N. A. (2018). Gibberellic acid (GA3) affects growth and development of some selected kenaf (*Hibiscus cannabinus* L.) cultivars. *Industrial Crops and Products*, *118*, 180–187. https://doi.org/10.1016/j.indcrop.2018.03.036
167. Na Ayudhaya, P., Kanjanawaraporn, J., Sridaphan, A., Tumtuan, N., Ritti, W., Chunthaburee, S., & Vongvanrungrueng, A. (2022). Influence of 2,4-Dichlorophenoxyacetic Acid on Callus Induction and Synthetic Cytokinins on Plant Regeneration of Three Phetchaburi Indigenous Rice Varieties. *Asian Journal of Crop Science*, *15*(1), 1–7. https://doi.org/10.3923/ajcs.2023.1.7
168. Nadiveedhi, M. R., Nuthalapati, P., Gundluru, M., Yanamula, M. R., Kallimakula, S. V., Pasupuleti, V. R., Avula, V. K. R., Vallela, S., Zyryanov, G. V., Balam, S. K., & Cirandur, S. R. (2021). Green Synthesis, Antioxidant, and Plant Growth Regulatory Activities of Novel α-Furfuryl-2-alkylaminophosphonates. *ACS Omega*, *6*(4), 2934–2948. https://doi.org/10.1021/acsomega.0c05302
169. Nakabayashi, R., Yonekura-Sakakibara, K., Urano, K., Suzuki, M., Yamada, Y., Nishizawa, T., Matsuda, F., Kojima, M., Sakakibara, H., Shinozaki, K., Michael, A. J., Tohge, T., Yamazaki, M., & Saito, K. (2014). Enhancement of oxidative and drought tolerance in Arabidopsis by overaccumulation of antioxidant flavonoids. *The Plant Journal*, *77*(3), 367–379. https://doi.org/10.1111/tpj.12388
170. Neumann, u., Brandizzi, F., & Hawes, C. (2003). Protein Transport in Plant Cells: In and Out of the Golgi†. *Annals of Botany*, *92*(2), 167–180. https://doi.org/10.1093/aob/mcg134
171. Nicaise, V., Roux, M., & Zipfel, C. (2009). Recent Advances in PAMP-Triggered Immunity against Bacteria: Pattern Recognition Receptors Watch over and Raise the Alarm. *Plant Physiology*, *150*(4), 1638–1647. https://doi.org/10.1104/pp.109.139709

172. Okada, K., Abe, H., & Arimura, G. (2015). Jasmonates Induce Both Defense Responses and Communication in Monocotyledonous and Dicotyledonous Plants. *Plant and Cell Physiology*, *56*(1), 16–27. https://doi.org/10.1093/pcp/pcu158
173. Okello, D., Yang, S., Komakech, R., Chung, Y., Rahmat, E., Gang, R., Omujal, F., Lamwaka, A. V., & Kang, Y. (2021). Indirect in vitro Regeneration of the Medicinal Plant, Aspilia africana, and Histological Assessment at Different Developmental Stages. *Frontiers in Plant Science*, *12*. https://www.frontiersin.org/articles/10.3389/fpls.2021.797721
174. Orantes-Bonilla, M., & Chen, F.-C. (2015). Effect of 6-Benzyladenine (BA) and Indole-3-Acetic Acid (IAA) on the In Vitro Regeneration of Chili Pepper (*Capsicum annuum* L.) via Node and Shoot Tip Culture. *Journal of International Cooperation*, *10*, 109–120.
175. Osorio, S., Alba, R., Nikoloski, Z., Kochevenko, A., Fernie, A. R., & Giovannoni, J. J. (2012). Integrative Comparative Analyses of Transcript and Metabolite Profiles from Pepper and Tomato Ripening and Development Stages Uncovers Species-Specific Patterns of Network Regulatory Behavior. *Plant Physiology*, *159*(4), 1713–1729. https://doi.org/10.1104/pp.112.199711
176. Pandey, P., Irulappan, V., Bagavathiannan, M. V., & Senthil-Kumar, M. (2017). Impact of Combined Abiotic and Biotic Stresses on Plant Growth and Avenues for Crop Improvement by Exploiting Physio-morphological Traits. *Frontiers in Plant Science*, *8*. https://doi.org/10.3389/fpls.2017.00537
177. Park, J.-S., Seong, Z.-K., Kim, M.-S., Ha, J.-H., Moon, K.-B., Lee, H.-J., Lee, H.-K., Jeon, J.-H., Park, S. U., & Kim, H.-S. (2020). Production of Flavonoids in Callus Cultures of Sophora flavescens Aiton. *Plants*, *9*(6), Article 6. https://doi.org/10.3390/plants9060688
178. Patavardhan, S. S., Awasthi, K., Suresh, S., Subba, P., Najar, M. A., D'Souza, L., Nivas, S. K., & Prasad, T. S. K. (2021). Proteome dataset of chili pepper plant (*Capsicum frutescens*) infested by broad mite (*Polyphagotarsonemus latus*). *Data in Brief*, *36*, 107095. https://doi.org/10.1016/j.dib.2021.107095
179. Patavardhan, S. S., Subba, P., Najar, A., Awasthi, K., D'Souza, L., Prasad, T. S. K., & Nivas, S. K. (2020). Plant-Pathogen Interactions: Broad Mite (*Polyphagotarsonemus latus*)-Induced Proteomic Changes in Chili Pepper Plant (*Capsicum frutescens*). *Omics: A Journal of Integrative Biology*, *24*(12), 714–725. https://doi.org/10.1089/omi.2020.0080
180. Paulraj, S., Lopez-Villalobos, A., & Yeung, E. C. (2015). Shoot apical meristem ontogeny in Arabidopsis embryo explants treated with abscisic acid. *Botany*, *93*(7), 445–452. https://doi.org/10.1139/cjb-2015-0043
181. Pei, H., Xie, H., Wang, X., Yan, X., Wang, B., Feng, H., Zhao, Y., Gao, J., & Gao, J. (2022). Proteomic analysis of differential anther development from sterile/fertile lines in *Capsicum annuum* L. *PeerJ*, *10*, e13168. https://doi.org/10.7717/peerj.13168
182. Peña, J. E. (1990). Relationships of Broad Mite (Acari: Tarsonemidae) Density to Lime Damage. *Journal of Economic Entomology*, *83*(5), 2008–2015. https://doi.org/10.1093/jee/83.5.2008
183. Pereira, M. F. A., & Dale, J. E. (1982). Effects of 2,4-Dichlorophenoxyacetic Acid on Shoot Apex Development of *Phaseolus vulgaris*. *Zeitschrift Für Pflanzenphysiologie*, *107*(2), 169–177. https://doi.org/10.1016/S0044-328X(82)80103-7

184. Perez, L. M., Yue, Z., Saha, S., Dean, J. F. D., Jenkins, J. N., Stelly, D. M., & Tseng, T.-M. (2022). Absorption and translocation of [14C]2,4-dichlorophenoxyacetic acid in herbicide-tolerant chromosome substitution lines of *Gossypium hirsutum* L. *Frontiers in Agronomy*, *4*. https://www.frontiersin.org/articles/10.3389/fagro.2022.936119
185. Perla, V., Nadimi, M., Reddy, R., Hankins, G. R., Nimmakayala, P., Harris, R. T., Valluri, J., Sirbu, C., & Reddy, U. K. (2018). Effect of ghost pepper on cell proliferation, apoptosis, senescence and global proteomic profile in human renal adenocarcinoma cells. *PloS One*, *13*(10), e0206183. https://doi.org/10.1371/journal.pone.0206183
186. Phillips, G. C., & Luteyn, K. J. (1983). Effects of Picloram and Other Auxins on Onion Tissue Cultures. *Journal of the American Society for Horticultural Science*, *108*(6), 948–953. https://doi.org/10.21273/JASHS.108.6.948
187. Pichardo-González, J., Guevara-Olvera, L., Couoh-Uicab, Y., González-Cruz, L., Bernardino-Nicanor, A., R. Medina, H., Chavira, M., & Acosta-Garcia, G. (2018). Effect of gibberellins on the yield of jalapeño pepper (*Capsicum annuum* L.). *9*, 925–934.
188. Pierik, R., Verkerke, W., Voesenek, R. (L). A. C. J., Blom, K. (C). W. P. M., & Visser, E. J. W. (1999). Thick Root Syndrome in Cucumber (*Cucumis sativus* L.): A Description of the Phenomenon and an Investigation of the Role of Ethylene. *Annals of Botany*, *84*(6), 755–762. https://doi.org/10.1006/anbo.1999.0980
189. Punzo, P., Grillo, S., & Batelli, G. (2020). Alternative splicing in plant abiotic stress responses. *Biochemical Society Transactions*, *48*(5), 2117–2126. https://doi.org/10.1042/BST20200281
190. Qin, F., Sakuma, Y., Tran, L.-S. P., Maruyama, K., Kidokoro, S., Fujita, Y., Fujita, M., Umezawa, T., Sawano, Y., Miyazono, K., Tanokura, M., Shinozaki, K., & Yamaguchi-Shinozaki, K. (2008). Arabidopsis DREB2A-Interacting Proteins Function as RING E3 Ligases and Negatively Regulate Plant Drought Stress–Responsive Gene Expression. *The Plant Cell*, *20*(6), 1693–1707. https://doi.org/10.1105/tpc.107.057380
191. Rajurkar, N. S., & Hande, S. M. (2011). Estimation of Phytochemical Content and Antioxidant Activity of Some Selected Traditional Indian Medicinal Plants. *Indian Journal of Pharmaceutical Sciences*, *73*(2), 146–151.
192. Ramonell, K., Berrocal-Lobo, M., Koh, S., Wan, J., Edwards, H., Stacey, G., & Somerville, S. (2005). Loss-of-Function Mutations in Chitin Responsive Genes Show Increased Susceptibility to the Powdery Mildew Pathogen E*rysiphe cichoracearum*. *Plant Physiology*, *138*(2), 1027–1036. https://doi.org/10.1104/pp.105.060947
193. Reinhardt, D., Mandel, T., & Kuhlemeier, C. (2000). Auxin Regulates the Initiation and Radial Position of Plant Lateral Organs. *The Plant Cell*, *12*(4), 507–518.
194. Ren, J., Wang, X., & Yin, J. (2010). Dicamba and Sugar Effects on Callus Induction and Plant Regeneration from Mature Embryo Culture of Wheat. *Agricultural Sciences in China*, *9*(1), 31–37. https://doi.org/10.1016/S1671-2927(09)60064-X
195. Ribeiro, D. M., Araújo, W. L., Fernie, A. R., Schippers, J. H. M., & Mueller-Roeber, B. (2012). Translatome and metabolome effects triggered by gibberellins during rosette growth in Arabidopsis. *Journal of Experimental Botany*, *63*(7), 2769–2786. https://doi.org/10.1093/jxb/err463
196. Rödiger, A., Agne, B., Dobritzsch, D., Helm, S., Müller, F., Pötzsch, N., & Baginsky, S. (2021). Chromoplast differentiation in bell pepper (*Capsicum annuum*) fruits. *The Plant*

Journal: For Cell and Molecular Biology, *105*(5), 1431–1442. https://doi.org/10.1111/tpj.15104

197. Rodrigues, M. A., Bianchetti, R. E., & Freschi, L. (2014). Shedding light on ethylene metabolism in higher plants. *Frontiers in Plant Science*, *5*. https://www.frontiersin.org/articles/10.3389/fpls.2014.00665
198. Rojas, C. M., Senthil-Kumar, M., Tzin, V., & Mysore, K. S. (2014). Regulation of primary plant metabolism during plant-pathogen interactions and its contribution to plant defense. *Frontiers in Plant Science*, *5*, 17. https://doi.org/10.3389/fpls.2014.00017
199. Russell, S. A., Old, W., Resing, K. A., & Hunter, L. (2004). Proteomic Informatics. In *International Review of Neurobiology* (Vol. 61, pp. 127–157). Academic Press. https://doi.org/10.1016/S0074-7742(04)61006-3
200. Sacco Botto, C., Matić, S., Moine, A., Chitarra, W., Nerva, L., D'Errico, C., Pagliarani, C., & Noris, E. (2023). Tomato Yellow Leaf Curl Sardinia Virus Increases Drought Tolerance of Tomato. *International Journal of Molecular Sciences*, *24*(3), Article 3. https://doi.org/10.3390/ijms24032893
201. Saini, S., Sharma, I., & Pati, P. K. (2015). Versatile roles of brassinosteroid in plants in the context of its homoeostasis, signaling and crosstalks. *Frontiers in Plant Science*, *6*. https://doi.org/10.3389/fpls.2015.00950
202. Sajedi, N., Madani, H., & Naderi, A. (2011). Effect of Microelements and Selenium on Superoxide Dismutase Enzyme, Malondialdehyde Activity and Grain Yield Maize (Z*ea mays* L.) under Water Deficit Stress. *Notulae Botanicae Horti Agrobotanici Cluj-Napoca*, *39*(2), Article 2. https://doi.org/10.15835/nbha3925500
203. Salazar-Iribe, A., & De-la-Peña, C. (2020). Auxins, the hidden player in chloroplast development. *Plant Cell Reports*, *39*(12), 1595–1608. https://doi.org/10.1007/s00299-020-02596-y
204. Sánchez-Bel, P., Egea, I., Sánchez-Ballesta, M. T., Martinez-Madrid, C., Fernandez-Garcia, N., Romojaro, F., Olmos, E., Estrella, E., Bolarín, M. C., & Flores, F. B. (2012). Understanding the mechanisms of chilling injury in bell pepper fruits using the proteomic approach. *Journal of Proteomics*, *75*(17), 5463–5478. https://doi.org/10.1016/j.jprot.2012.06.029
205. Santos, M. O., & Aragão, F. J. L. (2009). Role of SERK genes in plant environmental response. *Plant Signaling & Behavior*, *4*(12), Article 12.
206. Schilmiller, A. L., Koo, A. J. K., & Howe, G. A. (2007). Functional diversification of acyl-coenzyme A oxidases in jasmonic acid biosynthesis and action. *Plant Physiology*, *143*(2), 812–824. https://doi.org/10.1104/pp.106.092916
207. Schnurr, J. A., Shockey, J. M., de Boer, G.-J., & Browse, J. A. (2002). Fatty Acid Export from the Chloroplast. Molecular Characterization of a Major Plastidial Acyl-Coenzyme A Synthetase from Arabidopsis. *Plant Physiology*, *129*(4), 1700–1709. https://doi.org/10.1104/pp.003251
208. Shao, R., Wang, K., & Shangguan, Z. (2010). Cytokinin-induced photosynthetic adaptability of Zea mays L. to drought stress associated with nitric oxide signal: Probed by ESR spectroscopy and fast OJIP fluorescence rise. *Journal of Plant Physiology*, *167*(6), 472–479. https://doi.org/10.1016/j.jplph.2009.10.020

209. Shi, J., He, H., Hu, D., & Song, B. (2022). Defense Mechanism of *Capsicum annuum* L. Infected with Pepper Mild Mottle Virus Induced by Vanisulfane. *Journal of Agricultural and Food Chemistry*, *70*(12), 3618–3632. https://doi.org/10.1021/acs.jafc.2c00659
210. Shi, J., Yu, L., & Song, B. (2018). Proteomics analysis of Xiangcaoliusuobingmi-treated *Capsicum annuum* L. infected with Cucumber mosaic virus. *Pesticide Biochemistry and Physiology*, *149*, 113–122. https://doi.org/10.1016/j.pestbp.2018.06.008
211. Sinha, A. K., Jaggi, M., Raghuram, B., & Tuteja, N. (2011). Mitogen-activated protein kinase signaling in plants under abiotic stress. *Plant Signaling & Behavior*, *6*(2), 196–203. https://doi.org/10.4161/psb.6.2.14701
212. Skalák, J., Vercruyssen, L., Claeys, H., Hradilová, J., Černý, M., Novák, O., Plačková, L., Saiz-Fernández, I., Skaláková, P., Coppens, F., Dhondt, S., Koukalová, Š., Zouhar, J., Inzé, D., & Brzobohatý, B. (2019). Multifaceted activity of cytokinin in leaf development shapes its size and structure in Arabidopsis. *The Plant Journal*, *97*(5), 805–824. https://doi.org/10.1111/tpj.14285
213. Smith, T. C., Weathers, P. J., & Cheetham, R. D. (1997). Effects of gibberellic acid on hairy root cultures of *Artemisia annua*: Growth and artemisinin production. *In Vitro Cellular & Developmental Biology - Plant*, *33*(1), 75–79. https://doi.org/10.1007/s11627-997-0044-4
214. Solomos, T., & Laties, G. G. (1976). Effects of Cyanide and Ethylene on the Respiration of Cyanide-sensitive and Cyanide-resistant Plant Tissues 1. *Plant Physiology*, *58*(1), 47–50.
215. Son, Y., Cheong, Y.-K., Kim, N.-H., Chung, H.-T., Kang, D. G., & Pae, H.-O. (2011). Mitogen-Activated Protein Kinases and Reactive Oxygen Species: How Can ROS Activate MAPK Pathways?. *Journal of Signal Transduction*. https://doi.org/10.1155/2011/792639
216. Spoel, S. H., & Dong, X. (2008). Making Sense of Hormone Crosstalk during Plant Immune Responses. *Cell Host & Microbe*, *3*(6), 348–351. https://doi.org/10.1016/j.chom.2008.05.009
217. Sumaryono, Muslihatin, W., & Ratnadewi, D. (2012). Effect of Carbohydrate Source on Growth and Performance of In Vitro Sago Palm (*Metroxylon sagu* Rottb.) Plantlets. *HAYATI Journal of Biosciences*, *19*(2), 88–92. https://doi.org/10.4308/hjb.19.2.88
218. Sun, Q., Xu, Z., Huang, W., Li, D., Zeng, Q., Chen, L., Li, B., & Zhang, E. (2022). Integrated metabolome and transcriptome analysis reveals salicylic acid and flavonoid pathways' key roles in cabbage's defense responses to X*anthomonas campestris* pv. Campestris. *Frontiers in Plant Science*, *13*. https://www.frontiersin.org/articles/10.3389/fpls.2022.1005764
219. Suzuki, N., Miller, G., Morales, J., Shulaev, V., Torres, M. A., & Mittler, R. (2011). Respiratory burst oxidases: The engines of ROS signaling. *Current Opinion in Plant Biology*, *14*(6), Article 6. https://doi.org/10.1016/j.pbi.2011.07.014
220. Suzuki, T., Ishikawa, K., Yamashino, T., & Mizuno, T. (2002). An Arabidopsis Histidine-Containing Phosphotransfer (HPt) Factor Implicated in Phosphorelay Signal Transduction: Overexpression of AHP2 in Plants Results in Hypersensitiveness to Cytokinin. *Plant and Cell Physiology*, *43*(1), 123–129. https://doi.org/10.1093/pcp/pcf007

221. Taj, G., Agarwal, P., Grant, M., & Kumar, A. (2010). MAPK machinery in plants. *Plant Signaling & Behavior*, *5*(11), 1370–1378. https://doi.org/10.4161/psb.5.11.13020
222. Tanaka, Y., Suzuki, T., Yamashino, T., & Mizuno, T. (2004). Comparative studies of the AHP histidine-containing phosphotransmitters implicated in His-to-Asp phosphorelay in *Arabidopsis thaliana*. *Bioscience, Biotechnology, and Biochemistry*, *68*(2), 462–465. https://doi.org/10.1271/bbb.68.462
223. Tjong, E., Dimri, M., & Mohiuddin, S. S. (2023). Biochemistry, Tetrahydrofolate. In *StatPearls*. StatPearls Publishing. http://www.ncbi.nlm.nih.gov/books/NBK539712/
224. Tonini, P. P., Purgatto, E., & Buckeridge, M. S. (2010). Effects of abscisic acid, ethylene and sugars on the mobilization of storage proteins and carbohydrates in seeds of the tropical tree *Sesbania virgata* (Leguminosae). *Annals of Botany*, *106*(4), 607–616. https://doi.org/10.1093/aob/mcq159
225. Trobacher, C. P. (2009). Ethylene and programmed cell death in plants. *Botany*, *87*(8), 757–769. https://doi.org/10.1139/B09-041
226. Tsiatsiani, L., & Heck, A. J. R. (2015). Proteomics beyond trypsin. *The FEBS Journal*, *282*(14), 2612–2626. https://doi.org/10.1111/febs.13287
227. Tubaon, R. M., Haddad, P. R., & Quirino, J. P. (2017). Sample Clean-up Strategies for ESI Mass Spectrometry Applications in Bottom-up Proteomics: Trends from 2012 to 2016. *Proteomics*, *17*(20). https://doi.org/10.1002/pmic.201700011
228. Vaseva, I. I., Qudeimat, E., Potuschak, T., Du, Y., Genschik, P., Vandenbussche, F., & Van Der Straeten, D. (2018). The plant hormone ethylene restricts Arabidopsis growth via the epidermis. *Proceedings of the National Academy of Sciences*, *115*(17), E4130–E4139. https://doi.org/10.1073/pnas.1717649115
229. Wang, C. H., Persyn, A., & Krackov, J. (1962). Role of the Krebs Cycle in Ethylene Biosynthesis. *Nature*, *195*(4848), Article 4848. https://doi.org/10.1038/1951306a0
230. Wang, J., Wu, D., Wang, Y., & Xie, D. (2019). Jasmonate action in plant defense against insects. *Journal of Experimental Botany*, *70*(13), 3391–3400. https://doi.org/10.1093/jxb/erz174
231. Wang, M., Zang, L., Jiao, F., Perez-Garcia, M.-D., Ogé, L., Hamama, L., Le Gourrierec, J., Sakr, S., & Chen, J. (2020). Sugar Signaling and Post-transcriptional Regulation in Plants: An Overlooked or an Emerging Topic? *Frontiers in Plant Science*, *11*. https://www.frontiersin.org/articles/10.3389/fpls.2020.578096
232. Wang, Y., Zhang, X., Huang, G., Feng, F., Liu, X., Guo, R., Gu, F., Zhong, X., & Mei, X. (2020). Dynamic changes in membrane lipid composition of leaves of winter wheat seedlings in response to PEG-induced water stress. *BMC Plant Biology*, *20*(1), 84. https://doi.org/10.1186/s12870-020-2257-1
233. Wasternack, C., & Hause, B. (2013). Jasmonates: Biosynthesis, perception, signal transduction and action in plant stress response, growth and development. An update to the 2007 review in Annals of Botany. *Annals of Botany*, *111*(6), 1021–1058. https://doi.org/10.1093/aob/mct067
234. William Allwood, J., Clarke, A., Goodacre, R., & Mur, L. A. J. (2010). Dual metabolomics: A novel approach to understanding plant–pathogen interactions. *Phytochemistry*, *71*(5), 590–597. https://doi.org/10.1016/j.phytochem.2010.01.006

235. Wilson, R. G., & Michiels, A. (2003). Fall Herbicide Treatments Affect Carbohydrate Content in Roots of Canada Thistle (*Cirsium arvense*) and Dandelion (T*araxacum officinale*). *Weed Science*, *51*(3), 299–304.
236. Wilson, S. R., Vehus, T., Berg, H. S., & Lundanes, E. (2015). Nano-LC in proteomics: Recent advances and approaches. *Bioanalysis*, *7*(14), 1799–1815. https://doi.org/10.4155/bio.15.92
237. Wu, J., & Baldwin, I. T. (2009). Herbivory-induced signalling in plants: Perception and action. *Plant, Cell & Environment*, *32*(9), Article 9. https://doi.org/10.1111/j.1365-3040.2009.01943.x
238. Wu, S., Wang, H., Yang, Z., & Kong, L. (2014). Expression Comparisons of Pathogenesis-Related (PR) Genes in Wheat in Response to Infection/Infestation by Fusarium, Yellow dwarf virus (YDV) Aphid-Transmitted and Hessian Fly. *Journal of Integrative Agriculture*, *13*(5), 926–936. https://doi.org/10.1016/S2095-3119(13)60570-5
239. Wu, Z., Cheng, J., Qin, C., Hu, Z., Yin, C., & Hu, K. (2013). Differential proteomic analysis of anthers between cytoplasmic male sterile and maintainer lines in *Capsicum annuum* L. *International Journal of Molecular Sciences*, *14*(11), 22982–22996. https://doi.org/10.3390/ijms141122982
240. Wurzinger, B., Mair, A., Pfister, B., & Teige, M. (2011). Cross-talk of calcium-dependent protein kinase and MAP kinase signaling. *Plant Signaling & Behavior*, *6*(1), 8–12. https://doi.org/10.4161/psb.6.1.14012
241. Xia, Y., Chiu, C.-H., Do, Y.-Y., & Huang, P.-L. (2020). Expression Fluctuations of Genes Involved in Carbohydrate Metabolism Affected by Alterations of Ethylene Biosynthesis Associated with Ripening in Banana Fruit. *Plants*, *9*(9), Article 9. https://doi.org/10.3390/plants9091120
242. Yan, C., & Xie, D. (2015). Jasmonate in plant defence: Sentinel or double agent? *Plant Biotechnology Journal*, *13*(9), 1233–1240. https://doi.org/10.1111/pbi.12417
243. Yang, H., Li, P., Jin, G., Gui, D., Liu, L., & Zhang, C. (2022). Temporal regulation of alternative splicing events in rice memory under drought stress. *Plant Diversity*, *44*(1), 116–125. https://doi.org/10.1016/j.pld.2020.11.004
244. Yemm, E. W., & Willis, A. J. (1954). The estimation of carbohydrates in plant extracts by anthrone. *Biochemical Journal*, *57*(3), 508–514.
245. Yip Delormel, T., & Boudsocq, M. (2019). Properties and functions of calcium-dependent protein kinases and their relatives in *Arabidopsis thaliana*. *New Phytologist*, *224*(2), 585–604. https://doi.org/10.1111/nph.16088
246. Yu, F., Wu, Y., & Xie, Q. (2016). Ubiquitin–Proteasome System in ABA Signaling: From Perception to Action. *Molecular Plant*, *9*(1), 21–33. https://doi.org/10.1016/j.molp.2015.09.015
247. Yu, Y., Smith, M., & Pieper, R. (2014). *A spinnable and automatable StageTip for high throughput peptide desalting and proteomics*. https://www.nature.com/protocolexchange/protocols/3421
248. Yuan, N., Yuan, S., Li, Z., Zhou, M., Wu, P., Hu, Q., Mendu, V., Wang, L., & Luo, H. (2018). STRESS INDUCED FACTOR 2, a Leucine-Rich Repeat Kinase Regulates Basal Plant Pathogen Defense. *Plant Physiology*, *176*(4), Article 4. https://doi.org/10.1104/pp.17.01266

249. Yuasa, T., Ichimura, K., Mizoguchi, T., & Shinozaki, K. (2001). Oxidative stress activates ATMPK6, an Arabidopsis homologue of MAP kinase. *Plant & Cell Physiology*, *42*(9), 1012–1016. https://doi.org/10.1093/pcp/pce123
250. Yunita, R., Bagus, F. R. M., Nova, B., Rosadi, F. N., & Jamsari, J. (2021). Optimization of growth regulators to induce callus in chili (*Capsicum annuum*) cv. Berangkai. *IOP Conference Series: Earth and Environmental Science*, *741*(1), 012047. https://doi.org/10.1088/1755-1315/741/1/012047
251. Zarzecka, K., Gugała, M., Sikorska, A., Mystkowska, I., Baranowska, A., Niewęgłowski, M., & Dołęga, H. (2019). The effect of herbicides and biostimulants on polyphenol content of potato (*Solanum tuberosum* L.) tubers and leaves. *Journal of the Saudi Society of Agricultural Sciences*, *18*(1), 102–106. https://doi.org/10.1016/j.jssas.2017.02.004
252. Zhang, C., Xu, B., Geng, W., Shen, Y., Xuan, D., Lai, Q., Shen, C., Jin, C., & Yu, C. (2019). Comparative proteomic analysis of pepper (*Capsicum annuum* L.) seedlings under selenium stress. *PeerJ*, *7*, e8020. https://doi.org/10.7717/peerj.8020
253. Zhang, J., Zhang, Y.-Z., Jiang, J., & Duan, C.-G. (2020). The Crosstalk Between Epigenetic Mechanisms and Alternative RNA Processing Regulation. *Frontiers in Genetics*, *11*, 998. https://doi.org/10.3389/fgene.2020.00998
254. Zhang, L., Zhang, F., Melotto, M., Yao, J., & He, S. Y. (2017). Jasmonate signaling and manipulation by pathogens and insects. *Journal of Experimental Botany*, *68*(6), 1371–1385. https://doi.org/10.1093/jxb/erw478
255. Zhang, Q., & Xiao, S. (2015). Lipids in salicylic acid-mediated defense in plants: Focusing on the roles of phosphatidic acid and phosphatidylinositol 4-phosphate. *Frontiers in Plant Science*, *6*. https://www.frontiersin.org/articles/10.3389/fpls.2015.00387
256. Zhang, Z., Zhou, W., & Li, H. (2005). The role of GA, IAA and BAP in the regulation of in vitro shoot growth and microtuberization in potato. *Acta Physiologiae Plantarum*, *27*(3), 363–369. https://doi.org/10.1007/s11738-005-0013-7
257. Zhao, Y., Chan, Z., Gao, J., Xing, L., Cao, M., Yu, C., Hu, Y., You, J., Shi, H., Zhu, Y., Gong, Y., Mu, Z., Wang, H., Deng, X., Wang, P., Bressan, R. A., & Zhu, J.-K. (2016). ABA receptor PYL9 promotes drought resistance and leaf senescence. *Proceedings of the National Academy of Sciences*, *113*(7), 1949–1954. https://doi.org/10.1073/pnas.1522840113
258. Zhu, Y., Guo, M.-J., Song, J.-B., Zhang, S.-Y., Guo, R., Hou, D.-R., Hao, C.-Y., An, H.-L., & Huang, X. (2021). Roles of Endogenous Melatonin in Resistance to Botrytis cinerea Infection in an Arabidopsis Model. *Frontiers in Plant Science*, *12*. https://www.frontiersin.org/articles/10.3389/fpls.2021.683228
259. Zimny, J., & Lörz, H. (1986). Plant regeneration and initiation of cell suspensions from root-tip derived callus of *Oryza sativa* L. (rice). *Plant Cell Reports*, *5*(2), 89–92. https://doi.org/10.1007/BF00269241
260. Zipfel, C., Kunze, G., Chinchilla, D., Caniard, A., Jones, J. D. G., Boller, T., & Felix, G. (2006). Perception of the bacterial PAMP EF-Tu by the receptor EFR restricts Agrobacterium-mediated transformation. *Cell*, *125*(4), Article 4. https://doi.org/10.1016/j.cell.2006.03.037

261. Zubo, Y. O., Yamburenko, M. V., Selivankina, S. Y., Shakirova, F. M., Avalbaev, A. M., Kudryakova, N. V., Zubkova, N. K., Liere, K., Kulaeva, O. N., Kusnetsov, V. V., & Börner, T. (2008). Cytokinin Stimulates Chloroplast Transcription in Detached Barley Leaves. *Plant Physiology*, *148*(2), 1082–1093. https://doi.org/10.1104/pp.108.122275
262. Zuin, A., Isasa, M., & Crosas, B. (2014). Ubiquitin Signaling: Extreme Conservation as a Source of Diversity. *Cells*, *3*(3), 690–701. https://doi.org/10.3390/cells3030690

9 Publications

9.1 Publications in journals

1. Patavardhan, S.S., Subba, P., Najar, A., Awasthi, K., D'Souza, L., Prasad, T.S.K. and Nivas, S.K., 2020. Plant–pathogen interactions: broad mite (*Polyphagotarsonemus latus*)-induced proteomic changes in chilli Pepper Plant (*Capsicum frutescens*). OMICS: A Journal of Integrative Biology, 24(12), pp.714-725.
   Listed in UGC-CARE List Group II

   Scopus link: https://www.scopus.com/sourceid/19001
2. Patavardhan, S.S., Awasthi, K., Suresh, S., Subba, P., Najar, M.A., D'Souza, L., Nivas, S.K. and Prasad, T.S.K., 2021. Proteome dataset of chilli pepper plant (*Capsicum frutescens*) infested by broad mite (*Polyphagotarsonemus latus*). Data in brief, 36, p.107095.
   Listed in UGC-CARE List Group II

   Scopus link: https://www.scopus.com/sourceid/21100372856

9.2 Scientific presentations in conferences:

1. "Unravelling ubiquitination in plant-pathogen interaction through proteomic analysis of broad mite infestation in birds eye chilli" presented at "42nd Annual Meeting of Plant Tissue Culture Association – India (PTCA-I)" and International Symposium on "Advances in Plant Biotechnology and Genome Editing" 8 th to 10 th April 2021.
2. "Proteomic analysis of broad mite (*Polyphagotarsonemus latus*) infestation in Chilli (*Capsicum frutescens*)" presented at National Conference "Recent Advances in Biochemistry-2019 February 23, 2019.

10 Attachments

10.1 Paper 1: Plant-Pathogen Interactions: Broad Mite (*Polyphagotarsonemus latus*)-Induced Proteomic Changes in Chilli Pepper Plant (*Capsicum frutescens*)

10.2 **Paper 2:** Proteome dataset of chilli pepper plant (*Capsicum frutescens*) infested by broad mite (*Polyphagotarsonemus latus*)